F 1503/2.
FF
8 000000 683120

BULETINUL INSTITUTULUI POLITEHNIC DIN IAŞI

Editat de
UNIVERSITATEA TEHNICĂ „GH. ASACHI", IAŞI

Tomul XLIV (XLVIII)

Fasc. 1 - 2

Secţia II

CHIMIE ŞI INGINERIE CHIMICĂ

1998

MŰSZAKI INFORMÁCIÓS KÖZPONTI KÖNYVTÁR

BULETINUL INSTITUTULUI POLITEHNIC DIN IAŞI

Tomul XLIV (XLVIII)
Fasc. 1–2

Secţia II

CHIMIE şi INGINERIE CHIMICĂ

1998

EDITORIAL STAFF

Prof. Dr. Eng. **MIHAI GAFIŢANU** (President)
Prof. Dr. Eng. **VICTOR BULACOVSCHI** (Vice-President)
Prof. Dr. Eng. **LIVIU GROLL** (Vice-President)
Prof. Dr. Eng. **GHEORGHE ZET** (Secretary)
Prof. Dr. Doc. Eng. **ALFRED BRAIER** (Editor)
Prof. Dr. Eng. **HUGO ROSMAN** (Editor)
Prof. Dr. Eng. **MIHAIL VOICU** (Head of the Exchange Service)
Prof. Dr. Eng. **DIMITRIE ALEXA**
Prof. Dr. Eng. **ION BALASANIAN**
Prof. Dr. **AUREL BEJANCU**
Prof. Dr. Eng. **MIRCEA COZMÎNCĂ**
Prof. Dr. Eng. **SPIRIDON CREŢU**
Prof. Dr. Eng. **ION GIURMA**
Prof. Dr. Eng. **AURELIA GRIGORIU**
Prof. Dr. Eng. **CONSTANTIN PREDA**
Prof. Dr. Eng. **PAULICĂ RĂILEANU**

The **Bulletin of the Polytechnic Institute of Jassy** is edited by
the **Technical University "Gh.Asachi"** (the former Polytechnic Institute), Jassy.

TEXredaction:
B. Grigoriu, A. Rotaru
Technical University of Jassy

BULETINUL INSTITUTULUI POLITEHNIC DIN IAŞI
BULLETIN OF THE POLYTECHNIC INSTITUTE OF JASSY
Tomul XLIV (XLVIII), Fasc. 1–2 1998

ORSZÁGOS MŰSZAKI INFORMÁCIÓS KÖZPONT ÉS KÖNYVTÁR 1983

Secţia II

CHIMIE ŞI INGINERIE CHIMICĂ

SUMAR

Pag.

N. FOCA şi N. CALU, Studiul reacţiei dintre hexanitrocobaltiatul trisodic şi 1,1-dietil-1,3,4-triazolil-2-azo-4(N,N-dietilanilină) (I) (engl., rez. rom.) 7

DOINA BEJAN şi ALINA BEJAN, Programarea în limbajul C a unor probleme de chimie analitică (II) (engl., rez. rom.) 17

DANIEL SUTIMAN, MIHAELA VIZITIU, TRAIAN CIOROIANU şi OVIDIU GEORGESCU, Coroziunea oţelurilor slab aliate în sistemul metanol–acid malonic–apă (engl., rez. rom.) 25

N. AELENEI, MARCEL-IONEL POPA şi GABRIEL PĂDURARU, Compatibilitatea polistirenului cu copolimerul poli(etilen-s-vinil acetat) (engl., rez. rom.) 31

ŞT. IVĂŞCAN, MARIA APOSTOLESCU, N. APOSTOLESCU, EDUARD-EMIL IOJOIU şi FLORIN BANDRABUR, Consideraţii asupra coroziunii electrofiltrelor (engl., rez. rom.) 41

FLORIN BANDRABUR, ŞT. IVĂŞCAN şi N. APOSTOLESCU, Cercetări privind depunerea galvanică a cuprului din soluţii acide, pe cilindri din oţel (engl., rez. rom.) 47

DANIELA ŞUTEU şi AL. NACU, Recuperarea coloranţilor trifenilmetanici din ape reziduale folosind schimbători de ioni (engl., rez. rom.) 53

I. SIMINICEANU şi MARIANA NEAMŢU, Fotodegradarea bisfenolului-A din apă cu peroxid de hidrogen activat cu radiaţii ultraviolete (engl., rez. rom.) 61

DAN CAŞCAVAL, CORNELIU ONISCU, LILIANA MARIN şi VLAD ROŞCA, Extracţia lichid–lichid a produselor de biosinteză direct din lichidele de fermentaţie. I. Transferul de masă către picături (engl., rez. rom.) 69

EMIL DUMITRIU şi V. HULEA, Condensarea aldolică a formaldehidei şi acetaldehidei pe tufuri vulcanice tratate alcalin (engl., rez. rom.) 75

SILVIA CURTEANU şi VICTOR BULACOVSCHI, Influenţa unor parametri în polimerizarea radicalică discontinuă în masă a metacrilatului de metil (engl., rez. rom.) 83

	Pag.
M. RUSU şi VERONICA MUNTEANU, Obţinerea şi caracterizarea unor poliacetali vinilici. II. Sinteza polivinil formalului în mediu de amestec apă–acid acetic şi în acid acetic (engl., rez. rom.)	97
M. NICU, CARMEN ZAHARIA, FLORIN MOŢOC, MAGDALENA-DUMITRIŢA VICOL, CONSTANŢA IBĂNESCU şi MARIA LUNGU, Comportarea reologică a soluţiilor de copolimer ternar acrilonitril–acetat de vinil–α-metilstiren (engl., rez. rom.)	103
IULIANA SPIRIDON şi VALENTIN I. POPA, Contribuţii la studiul transformărilor enzimatice ale pastelor de mare randament (engl., rez. rom.)	115
RECENZII	123

BULETINUL INSTITUTULUI POLITEHNIC DIN IAŞI
BULLETIN OF THE POLYTECHNIC INSTITUTE OF JASSY
Tome XLIV (XLVIII), Fasc. 1-2 1998

MŰSZAKI INFORMÁCIÓS KÖNYVTÁR 1993

Section II

CHEMISTRY and CHEMICAL ENGINEERING

CONTENTS

Pp.

N. FOCA and N. CALU, The Study of the Reaction between $Na_3[Co(NO_2)_6]$ and 1-Methyl-1,3,4-Triazolil-2-Azo-4(N,N-Diethylaniline) (I) (English, Romanian summary) 7

DOINA BEJAN and ALINA BEJAN, Programming of Some Problems of Analytical Chemistry in C Language (II) (English, Romanian summary) 17

DANIEL SUTIMAN, MIHAELA VIZITIU, TRAIAN CIOROIANU and OVIDIU GEORGESCU, The Corrosion of Low Alloy Steels in the System Methanol–Malonic Acid–Water (English, Romanian summary) 25

N. AELENEI, MARCEL-IONEL POPA and GABRIEL PĂDURARU, On the Compatibility of Polystyrene with Poly(Ethylene-s-Vinyl Acetate) Copolymer (English, Romanian summary) 31

ŞT. IVĂŞCAN, MARIA APOSTOLESCU, N. APOSTOLESCU, EDUARD-EMIL IOJOIU and FLORIN BANDRABUR, Considerations on Corrosion of Pipe Precipitators (English, Romanian summary) 41

FLORIN BANDRABUR, ŞT. IVĂŞCAN and N. APOSTOLESCU, Studies on Copper Deposition from Acid Solutions on Steel Cylinders (English, Romanian summary) 47

DANIELA ŞUTEU and AL. NACU, Removal the Triphenylmethanic Dyes from Waste Waters Using Ion Exchangers (I) (English, Romanian summary) 53

I. SIMINICEANU and MARIANA NEAMŢU, Photodegradation of Bisphenol-A in Water by Ultraviolet-Activated Hydrogen Peroxide (English, Romanian summary) 61

DAN CAŞCAVAL, CORNELIU ONISCU, LILIANA MARIN and VLAD ROŞCA, Liquid–Liquid Extraction of Biosynthesis Products Directly from Fermentation Broths. I. Mass Transfer to Drops (English, Romanian summary) 69

EMIL DUMITRIU and V. HULEA, Aldol Condensation of Formaldehyde and Acetaldehyde over the Alkali Treated Volcanic Tuffs (English, Romanian summary) 75

SILVIA CURTEANU and VICTOR BULACOVSCHI, The Influence of Some Parameters on Free Radical Polymerization of Methyl Methacrylate (English, Romanian summary) 83

	Pp.
M. RUSU and VERONICA MUNTEANU, Obtention and Characterization of Some Poly(Vinyl Acetals). II. Synthesis of Poly(Vinyl Formal) in a Mixture of Water–Acetic Acid and in Acetic Acid (English, Romanian summary)	97
M. NICU, CARMEN ZAHARIA, FLORIN MOŢOC, MAGDALENA-DUMITRIŢA VICOL, CONSTANŢA IBĂNESCU and MARIA LUNGU, Rheological Behaviour of Some Solutions of Ternary Copolymer Acrylonitrile–Vinylacetate–α-Methylstyrene (English, Romanian summary)	103
IULIANA SPIRIDON and VALENTIN I. POPA, Contributions to the Study of Enzymatic Transformations of High-Yield Pulps (English, Romanian summary)	115
BOOK REVIEWS	123

BULETINUL INSTITUTULUI POLITEHNIC DIN IAŞI
Tomul XLIV (XLVIII), Fasc. 1–2, 1998
Secţia II
CHIMIE şi INGINERIE CHIMICĂ

D.C. 547.257.3

THE STUDY OF THE REACTION BETWEEN $Na_3[Co(NO_2)_6]$ AND 1-METHYL-1,3,4-TRIAZOLIL-2-AZO-4(N,N-DIETHYLANILINE) (I)

BY

N. FOCA and N. CALU

A series of data from a large study over the interaction between $Na_3[Co(NO_2)_6]$ and some organic ligands is presented.

The study is made starting with an aqueous solution of $Na_3[Co(NO_2)_6]$ or with the solution containing the aqueous-complex $[Co(H_2O)_6]^{3+}$ resulted from decomposition reaction of $Na_3[Co(NO_2)_6]$.

The interaction between the complex ion $[Co(NO_2)_6]^{3-}$ and some organic ligands follows a certain kinetics.

At the beginning, the reaction between the complex ion $[Co(NO_2)_6]^{3-}$ and the ligand 1-methyl-1,3,4-triazolyl-2-ozo-4(N,N-diethyl)-aniline is studied. Spectrophotometrically, the decomposition of $[Na_3Co(NO_2)_6]$ and the combination ratio metal–ligand are established and also the values of the stability constants of the obtained complex compounds are determined.

1. Introduction

The complex ion $[Co(NO_2)_6]^{3-}$ is not stable in aqueous medium and it develops a decomposition reaction in which the ions NO_2^-, from the coordination sphere, are replaced one by one by water molecules, finally resulting an aquo-compound $\left[Co^{III}(H_2O)_6\right]^{3+}$.

The composition reaction of $[Co(NO_2)_6]^{3-}$ occurs in time and presents a certain kinetic mechanism depending on the replacement of NO_2^- ions with water molecules [1], [2].

The decomposition process of the nitrocomplex and the formation of the aquo-complex occurs gradually and can be written as it follows:

$$\begin{aligned}
&[Co^{III}(NO_2)_6]^{3-} + H_2O \longrightarrow [Co^{III}(NO_2)_5(H_2O)]^{2-} + NO_2^- \\
&[Co^{III}(NO_2)_5(H_2O)]^{2-} + H_2O \longrightarrow [Co(NO_2)_4(H_2O)_2]^{-} + NO_2^- \\
&\vdots \\
&[Co(NO_2)(H_2O)_5]^{2+} + H_2O \longrightarrow [Co(H_2O)_6]^{3+} + NO_2^-
\end{aligned}$$

The NO_2^- ions that are replaced in the coordination sphere are submitted to a series of transformations, some of them react wich Na^+ ions derived from the

dissociation ones, react with water or are oxidized and participate in other chemical reactions.

The decomposition of the complex compound $Na_3[Co(H_2O)_6]$ occurs in a mechanism that involves more chemical processes [3], [4]:

$$Na^+ + NO_2^- \longrightarrow NaNO_2; \quad NO_2^- \longrightarrow NO_2 + 1e^-$$
$$2NO_2 + H_2O \longrightarrow HNO_3 + HNO_2; \quad 3HNO_2 \longrightarrow HNO_3 + NO_2 + H_2O$$
$$HNO_3 + H_2O \rightleftharpoons H_3O^+ + NO_3^-; \quad NO_2^- + H_3O^+ \longrightarrow HNO_2 + H_2O$$

The $\left[Co^{III}(H_2O)_6\right]^{3+}$ ions present a higher reactivity in comparison with the ions $\left[Co^{II}(H_2O)_6\right]^{2+}$.

For example, ions $\left[Co^{III}(H_2O)_6\right]^{3+}$ react with 1-methyl-1,3,4-triazolyl-2-ozo-4(N, N-diethylaniline) (noted L), while the $\left[Co^{II}(H_2O)_6\right]^{2+}$ ions do not react with this dye.

The structure of the dye L is the following:

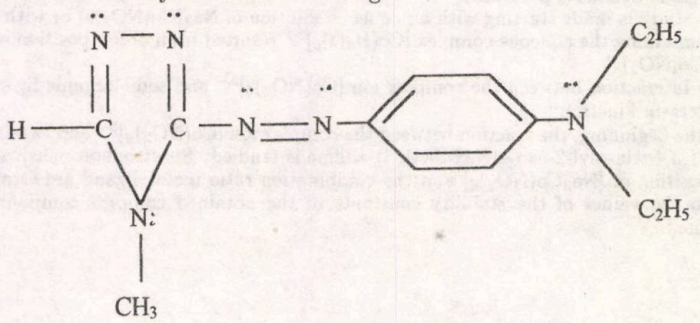

The reaction between $\left[Co^{III}(H_2O)_6\right]^{3+}$ and the dye L occurs different from the reactions of the some dye and the following cations: Pd(II), Cu(II), Hg(I) and Hg(II) [5].

In the system $\left[Co^{III}(NO_2)_6\right]^{3-}$–$L$ the following parallel reactions take place simultaneously: the decomposition of $Na_3[Co(NO_2)_6]$, the hydration of the ion Co(III) and also the reaction of the $\left[Co^{III}(H_2O)_6\right]^{3+}$ with the ligand L.

2. Experimental

The ligand (L) 1-methyl-1,3,4-triazolil-2-azo-4′-(N,N-diethylaniline) is rather sparingly soluble in water due to the lace of solubilizing groups. It is instead soluble in strong mineral acids (HCl, H_2SO_4), low organic acids (formic and acetic acids) as well as in dimethylformamide (D.M.F.).

For the present study the ligand (L) was taken as an acetic solution of an initial concentration of 1×10^{-3} mol.l^{-1} and the hexanitrocobaltiat ion, $\left[Co^{III}(NO_2)_6\right]^{3-}$, as a freshly prepared aqueous solution of 1×10^{-3} mol.l^{-1} initial concentration.

The reaction of this metal–ligand system was studied in aqueous solution at pH=4.5.

3. Results and Discussion

The decomposition of the complex ion $[Co(NO_2)_6]^{3-}$ in aqueous solution was followed in time by recording the UV absorption spectra at different temperatures (Fig. 1).

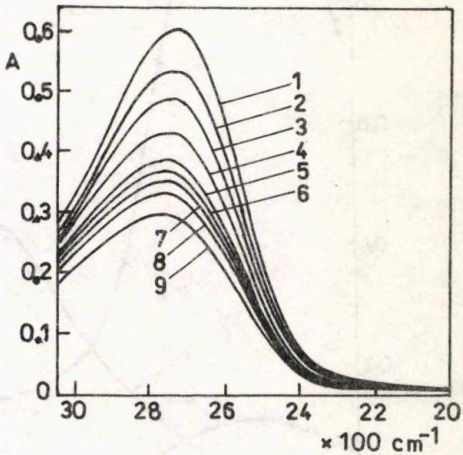

Fig. 1.– Evolution in time of $Na_3[Co(NO_2)_6]$ complex: $c = 2 \times 10^{-4}$ moles.l^{-1}; solvent H_2O; t = 14°C; Cell = 0.2 cm; standard sample–distilled water.

The complex ion $\left[Co^{III}(NO_2)_6\right]^{3-}$ is noticed to show in solution a maximum absorption at 360 nm, where the absorbance decreases in time (Fig. 1), which confirms the hydration process in this system.

By adding the ligand, the $\left[Co^{III}(H_2O)_6\right]^{3+}$ ions react with 1-methyl-1,3,4- triazolil-2-azo-4′-(N,N-diethylaniline) giving complex combinations with characteristic absorption spectrum.

The absorption spectra recorded at different times are indicative of a certain development of the reaction between $[Co(H_2O)_6]^{3+}$ and ligand. In Fig. 2 the absorption spectra of the ligand (L), the complex ion $[Co(NO_2)_6]^{3-}$, as well as the $\left[Co^{III}(H_2O)_6\right]^{3+}$–$L$ system recorded an hour after the reagents mixing are given.

By examining the absorption electric spectra (Fig. 2) would can be noticed that shortly after the reagents mixing a new band appears at λ_{max} = 560 nm apart from that at λ_{max} = 360 nm. The new band which would apparently be specific for the complexes in the system under study can be noticed at high reactant concentrations only.

At the beginning of the $[Co(NO_2)_6]^{3-}$–L reaction the band at 360 nm, characteristic for the nitrocomplex, remains completely unchanged. Then significant modifications are the optical properties of the reaction system solution which appear during the reaction development.

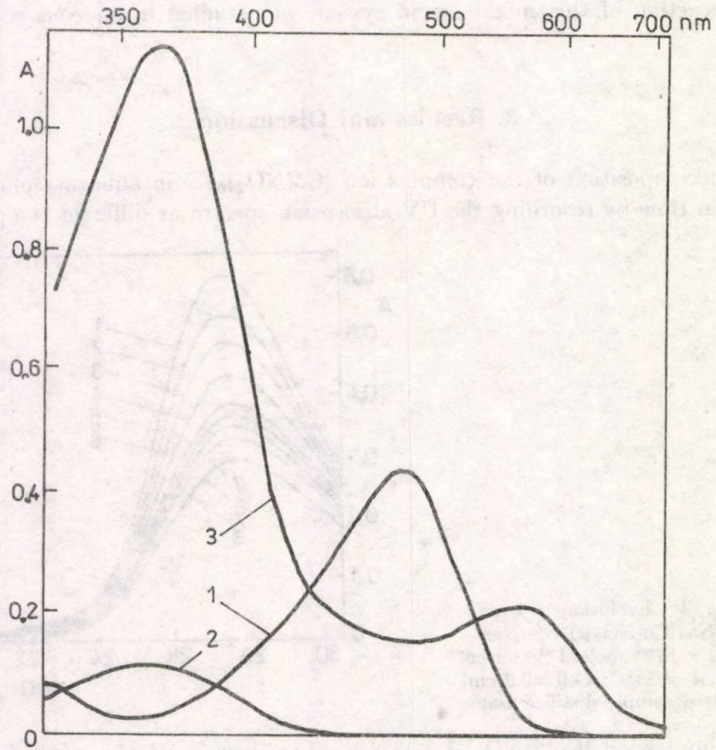

Fig. 2.– Absorption spectra of the $Na_3[Co(NO_2)_6]$–L system: *1* – L, $c = 1 \times 10^{-4}$ moles.l^{-1}; *2* – $Na_3[Co(NO_2)_6]$, $c = 1 \times 10^{-4}$ moles.l^{-1}; *3* – $Na_3[Co(NO_2)_6]$–L, $1M : 2L$, $V = 3$ cm^3, solvent – H_2O; cell = 0.2 cm; standard sample–distilled water.

After 24 hours the reactions are completed and the absorption bands at $\lambda_{max} =$ = 480 nm, characteristic for the ligand (360 nm) characteristic for the complex ion $[Co(NO_2)_6]^{3-}$ and 560 nm occured by the reactants, disappear.

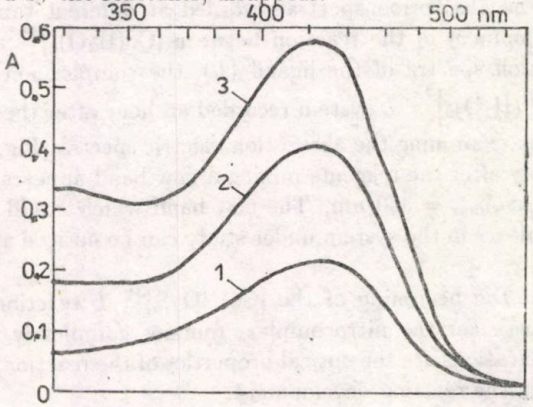

Fig. 3.– Absorption electronic spectra recorded on stabilized Co(III)–L systems: *1* – M–L (1:1); *2* – M–L (1:2); *3* – M–L (1:3); *4* – $V_{final} = 15$ cm^3; solvent – H_2O; cell = 0.2 cm; standard sample – distilled water.

Instead new bands quite different from the above mentioned ones are made evident for the M–L stabilized systems.

At this concentration the absorbtion spectra were recorded for the combination ratios: $1M : 1L$; $1M : 2L$ and $1M : 3L$, with the same final volume ($V_f = 15$ ml) and Co(III) concentration – 6.660×10^{-5} mol.l^{-1} (Fig. 3).

As can be seen in Fig. 3, all the metal–ligand systems show the same absorption spectrum regardles the combination ratio, namely $\lambda_{max} = 425$ nm and different λ_{max} values as follows: $1M : 1L$, $\varepsilon_{max} = 16,540$ moles^{-1}cm^{-1}; $1M : 2L$, $\varepsilon_{max} = 30,830$ moles^{-1}cm^{-1}; $1M : 3L$, $\varepsilon_{max} = 43,609$ moles^{-1}cm^{-1} [6].

The differences in the ε_{max} values for different metal–ligand combination ratios are influenced by the fact that the absorption bands of the ligand and of the $1M : 1L$; $1M : 2L$ and $1M : 3L$ systems are partially supercomposed at $\lambda_{max} = 425$ nm (s. Figs. 2 and 3) [6], [7].

3.1. Composition of Complexes in the System $Na_3[Co(NO_2)_6]$–L

Studying the evolution in time of the system $[Co(NO_2)_6]^{3-}$–L, and also the modifications that appear in the absorption spectra a lot of determinations of the composition metal–ligand at different moments were made from hour to hour after 24 hours and also after 48 hours from the moment the reagents were mixed.

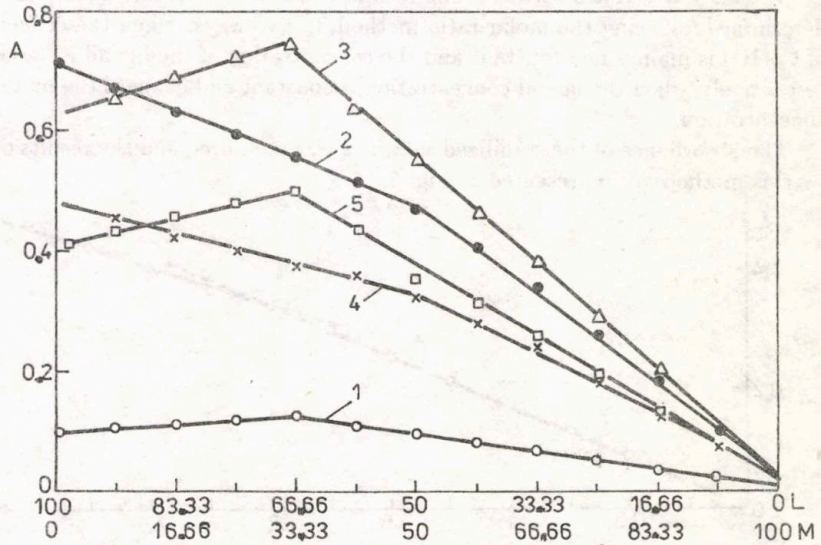

Fig. 4.– Obtained results from the study of the $[Co(NO_2)_6]^{3-}$–L system by the Job method: *1* – the absorbance readings were performed after one hour at $\lambda = 560$ nm; *2* – the absorbance readings were performed after one hour at $\lambda = 425$ nm; *3* – the absorbance readings were performed after 24 hours at 425 nm; *4* – the absorbance was measured one hour after the reactions mixing, at 560 nm, $V = 15$ cm^3; layer thickness – 0.2 cm; solvent – distilled water.

The determinations were made at two different wave lenghts: 560 nm and 425 nm respectively.

In order to determine the metal–ligand composition two spectrophotometric methods were used: the continuous variations method [8] and the molar ratio one [9].

a) *The Continuous Variations Method.* The experimental data obtained by this method are presented in Fig. 4. Studying this figure the following conclusions regarding the reaction between $Na_3[Co(NO_2)_6]$–L are assigned:

i) by measuring the absorbance of the mixture M–L after one hour, at 425 nm and 560 nm wave lenghts, it is shown that in the studied system two complex compounds are obtained namely, $1M : 1L$ (curve *2*) and $1M : 2L$ (curve *1*);

ii) also it is shown that at the beginning after one hour from the moment the reagents were mixed, in the M–L, the complex compound in which the combination ratio is $1M : 1L$ is predominant (curves *2* and *4*). In time, other reactions take place and the system finally contains only the complex compound in which the combination ratio is $1M : 2L$ (curves *3* and *5*).

The composition determinations were made for two different values of the concentration of the solutions of $[Co(NO_2)_6]^{3-}$; curves *2* and *3* correspond to the concentration value $c = 1 \times 10^{-5}$ moles.l^{-1} and curves *3* and *5* to the value $c = 6.66 \times 10^{-5}$ moles.l^{-1}.

b) *The Molar Rates Method.* The composition of the system Co(III)–L was also determined following the molar ratio method, in two ways: when the concentration of Co(III) is maintained constant and the concentration of the ligand is variable and respectively, when the ligand concentration is constant and changes the metallic ions concentration.

The absorbance of the stabilized solutions was measured and the results obtained by this method are represented in Fig. 5.

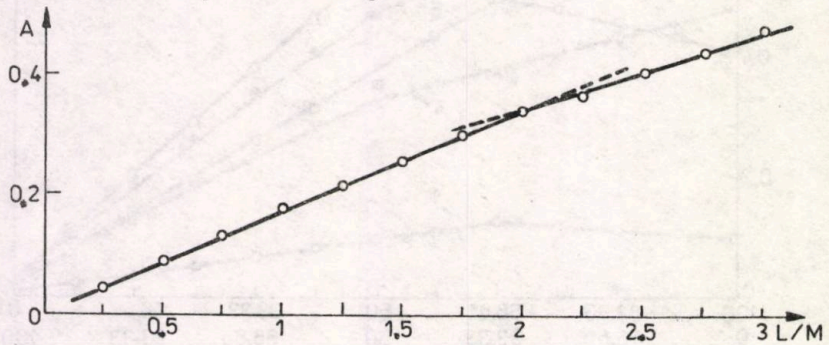

Fig. 5.– Obtained results from the study of the $[Co(NO_2)_6]^{3-}$ – azo dye system by the ratio method: c_M = const.; c_L = variable; V_{final} = 15 cm^3; the absorbance was measured on stabilized solutions; λ = 560 nm; layer thickness = 0.2 cm; solvent – distilled water.

Applying the molar ratio method and maintaining constant the ligand concentration, the value of the absorbance of the system Co(III)–L, measured after one hour and, respectively, 24 hours after mixing the reagents, are presented in the Figs. 6 *a* and 6 *b*.

Studying the system $Na_3[Co(NO_2)_6]$–1-methyl-1,3,4-triazolyl-2-azo-4(N,N-diethylazoaniline) it is shown an evolution in time of the reaction, in order to obtain the complex compound with a combination rate of $1M : 2L$; this fact also shows that this compound is the most stable one from all the complexes formed between the Co(III) ions and the mentioned ligand [11].

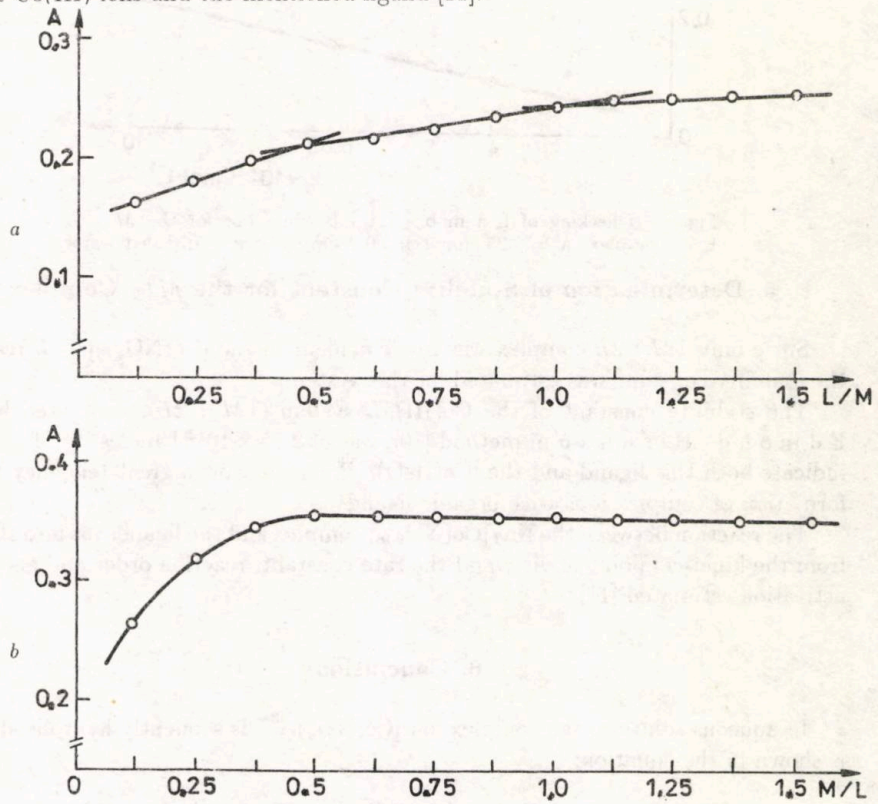

Fig. 6.– Obtained results from the study of $Na_3[Co(NO_2)_6]$ by the mole ratio method: *a* – the absorbance readings were performed one hour after the reactants mixing; *b* – the absorbance was measured on stabilized solutions after 24 hours; $V_f = 15$ cm^3 at $\lambda = 425$ nm; cell = 0.2 cm; solvent – distilled water.

4. Checking of the Lambert-Beer Law

Because of the evolution in time of the system Co(III)–L, the L a m b e r t - B e e r law was checked on stabilized solutions containing only the complex ML_2, because the complex $1M : 1L$ is not stable in time (Fig. 7).

Also, it has to be added that till the stabilization of the system Co(III)–L, the two complex compounds: $1M : 1L$ and respectively $1M : 2L$ are present in the solution.

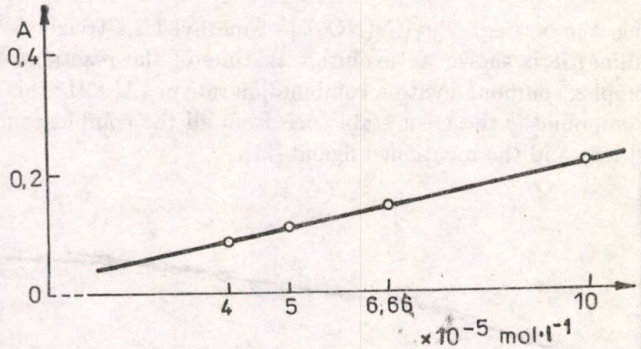

Fig. 7.– Checking of L a m b e r t - B e e r law for the $M : L$ (1 : 2) complex; $\lambda = 425$ nm; cell = 0.2 cm; solvent – distilled water.

5. Determination of Stability Constant for the ML_2 Complex

Since only $1M : 2L$ complex was made evident in the $[Co(NO_2)_6]^{3-}$–L reaction the stability constant was estimated for this system.

The stability constant of the Co(III)–L system ($1M : 2L$), estimated by the E d m o n d - B i r n h a u m method [10], was of 2.75×10^{12} l²moles^{-2}. This would indicate both this ligand and the $[Co(H_2O)_6]^{3+}$ ion to show a great tendency to the formation of complex ions with organic ligands.

The reaction between the $Na_3[Co(NO_2)_6]$ complex and the ligand was also studied from the kinetical point of view and the rate constant, reaction order and energy of activation estimated [11].

6. Conclusions

In aqueous solution, the complex ion $[Co(NO_2)_6]^{3-}$ is sequently hydrolized, as it is shown in the equation:

$$[Co(NO_2)_6]^{3-} + xH_2O \rightleftharpoons [Co(NO_2)_{6-x}(H_2O)_x]^{q-(+)x} + xNO_2^-,$$

where $q = -2$, if $x = 1$.

The substitution reaction of the ions NO_2^- with water molecules takes place step by step, the aquo-complex compounds being obtained as intermediate ones; the final compound is the ion $[Co(H_2O)_6]^{3+}$.

The resulted aquo-complexes are submitted more easily to a substitution reaction with effects in *trans* position, and in the same time, a lot of changes take place.

The kinetics of the substitution reaction is studied by a spectrophotometrical method, in the system $\left[Co(NO_2)_{6-x}(H_2O)_x\right]^{q-(+)x}$–$L$, where L is 1-methyl-1,3,4-triazolyl-2-azo-4(N,N-dimethyl-aniline).

Based on these data the combination ratios metal:ligand are established ($1M : 1L$ and $1M : 2L$) and the stability constant of the complex $1M : 2L$ is calculated, this

complex compound being the most stable from this system.

Received, November 28, 1997

Technical University "Gh.Asachi", Jassy,
Department of Inorganic Chemistry

REFERENCES

1. Basolo F., Pearson G.R., *Mechanism of Inorganic Reactions.* John Wiley, New York, 1967.
2. Pearson G.R., Boston R.C., Basolo F., J. Phys. Chem., **59**, 304 (1955).
3. Ablov V.A., Sukhov A., Zhur. Anorg. Khim., **4**, 2485 (1959).
4. Moh S.K., Poon K.C., Inorg. Chem., **10**, 225 (1971); Chem. Comm., 1358 (1971).
5. Mc.Cluve D.S., *Advanced in the Chemistry of the Coordination Compounds.* Edited by S. Kirshner, 498 (1961).
6. Lepădatu C.I., Rev. Roum. Chem., **11**, 1175 (1966).
7. Lever A.B.P., *Inorganic Electronic Spectroscopy.* Elsevier Publ. Co., Amsterdam-London-New York, 1968.
8. Job P., Ann. Chem., 113 (1928).
9. Jae, Jones A., Ind. Eng. Chem. Anal., **16**, 111 (1944).
10. Edmonds S., Birnsbaum N., J. Amer. Chem. Soc., **63**, 1471 (1941).
11. Foca N., Calu N., *Kinetic Data about Co(III)-1-Ethyl-1,3,4-Triazolil-2-Azo-4(N,N-Diethylaniline) System* (in print).

STUDIUL REACŢIEI DINTRE HEXANITROCOBALTIATUL TRISODIC ŞI 1,1-DIETIL-1,3,4-TRIAZOLIL-2-AZO-4(N,N-DIETILANILINĂ) (I)

(Rezumat)

S-a studiat reacţia ce are loc, în soluţie apoasă, între $Na_3[Co(NO_2)_6]$ şi 1,1-dietil-1,3,4-triazolil-2-azo-4(N,N-dietilazoanilină).

A fost urmărită spectrofotometric descompunerea în timp a soluţiei apoase de $Na_3[Co(NO_2)_6]$.

De asemenea, prin metode spectrofotometrice, s-a stabilit raportul de combinare Co(III)–colorant azoic (L), la diferite intervale de timp.

Pe baza datelor experimentale obţinute prin metode spectrofotometrice s-a calculat constanta de stabilitate a complecşilor $1M : 1L$ şi $1M : 2L$ care se formează în acest sistem.

BULETINUL INSTITUTULUI POLITEHNIC DIN IAŞI
Tomul XLIV (XLVIII), Fasc. 1–2, 1998
Secţia II
CHIMIE şi INGINERIE CHIMICĂ

D.C. 544.19

PROGRAMMING OF SOME PROBLEMS OF ANALYTICAL CHEMISTRY IN C LANGUAGE (II)

BY

DOINA BEJAN and ALINA BEJAN

In the first part of the paper [1] some programmes in C language are presented by means of which some analytical chemistry problems referring to acido-basic systems can be solved.

By extending the preoccupation area in this field, the present paper includes the solutions on computer in C language of some analytical aspects in different domains such as: complexing equilibria, estimation of accuracy of the analytical determinations by means of the statistical-mathematical calculation, drawing and interpretation of the polarographic curves.

1. Introduction

The simulation on computer of numerous chemical processes and phenomena [2],...,[6], among which those of analytical chemistry deserve mention [7], permitted their evaluation, interpretation and anticipation on scientific criteria as well as the design of new materials of desired properties [8].

The C language is considered as standard among the actual programming languages due to its superior technical and operational characteristics [9],...,[12].

2. Experimental

The programming of above mentionated problems in the C language was carried out on a 386 SX Packard Bell PC (IBM compatible). Source programmes are similar to those presented in [1].

3. Results and Discussions

3.1. Competitive Complexing Equilibria Studied on Computer in C Programming Language

From the analytical point of view the obtaining of complexes of a high stability degree is particularly important.

The stability of complex combinations is much influenced by the presence of competitive equilibria.

The study on computer makes possible the finding of the optimum experimental conditions, especially for the complex systems, when several components which may interfere are present within the solution, such as several ligands reacting with the metallic ions and several metallic ions which could react with a certain ligand [7], [13].

A series of complex ions of known standard stability constants as well as the known concentrations of some interfering ligands are considered. The stability of the initial complexes is to be calculated by varying the stability constants of the secondary complexes as well as the ligand concentration and coordination number.

a) *Mathematical Model* [7]

$$\alpha_M = 1 + K_{s_1}[L] + K_{s_1}K_{s_2}[L]^2 + \cdots + K_{s_1}K_{s_2}...K_{s_l}[L]^l,$$

$$\beta_{s_M} = \frac{\beta_s}{\alpha_M}.$$

I n p u t: $\beta_s = 10^{10}$; $l = 2, 4, 6$; $[L] = 10^{-4}...4$ (10 values); $K_{s_1}, ..., K_{s_6} = 10^3...10^2$ (3 sets of values).

O u t p u t: β_{s_M} for each combination of the above parameters.

b) *Algorithm and Codification.* The relations in the mathematical model are to be calculated as part of the programme.

For calculating α_M, the sums (SUM) composed of $K_{s_1}[L]$ were calculated successively and then one term after each iteration after j. When the iteration were over, the unity was added to this sum and the α_M, denoted as ALFB, is obtained.

This cycle was repeated for different values of $[L]$, denoted as AL[k], and different values of the constants $K_{s_1}, ..., K_{s_6}$, denoted as AKS[i][j].

For each cycle in j the β_{s_M} is printed and also the values l, k, i to know the values given to the amounts $l, [L]$ and to the set of the constants $K_{s_1}, ..., K_{s_6}$, respectively (l has the meaning as in the mathematical model; k – order number in the set of values chosen for $[L]$; i – order number of the set of values for the constants $K_{s_1}, ..., K_{s_6}$).

The obtained results are given partially in Table 1.

Table 1

Beta s value is: 1e+11
Values for $[L]$ are:
0.0001 0.001 0.01 0.1 0 1 1.5 2 3 4
The values for $K_{s_1}, ..., K_{s_6}$ are:
1000 800 600 400 200 100
1000 900 700 500 300 100
950 750 550 350 150 100

```
l=2  k=1  i=1  BetaSm=   90252705792.000000
l=2  k=1  i=2  BetaSm=   90171326464.000000
l=2  k=1  i=3  BetaSm=   90733805568.000000
l=2  k=2  i=1  BetaSm=   35714285568.000000
l=2  k=2  i=2  BetaSm=   34482757632.000000
l=2  k=2  i=3  BetaSm=   37558681600.000000
l=2  k=3  i=1  BetaSm=    1098901120.000000
l=2  k=3  i=2  BetaSm=     990099008.000000
l=2  k=3  i=3  BetaSm=    1223241600.000000
l=2  k=4  i=1  BetaSm=      12344155.000000
l=2  k=4  i=2  BetaSm=      10987803.000000
l=2  k=4  i=3  BetaSm=      13848497.000000
l=2  k=5  i=1  BetaSm=   99999997952.000000
l=2  k=5  i=2  BetaSm=   99999997952.000000
l=2  k=5  i=3  BetaSm=   99999997952.000000
l=2  k=6  i=1  BetaSm=        124843.789062
l=2  k=6  i=2  BetaSm=        110987.664062
l=2  k=6  i=3  BetaSm=        140163.796875
l=2  k=7  i=1  BetaSm=         55509.265625
l=2  k=7  i=2  BetaSm=         49346.136719
l=2  k=7  i=3  BetaSm=         62322.730469
l=2  k=8  i=1  BetaSm=         31230.470703
l=2  k=8  i=2  BetaSm=         27762.345703
l=2  k=8  i=3  BetaSm=         35064.328125
l=2  k=9  i=1  BetaSm=         13883.101562
l=2  k=9  i=2  BetaSm=         12341.106445
l=2  k=9  i=3  BetaSm=         15587.611328
l=2  k=10 i=1  BetaSm=          7810.058594
l=2  k=10 i=2  BetaSm=          6942.515137
l=2  k=10 i=3  BetaSm=          8769.005859
```

3.2. Elaboration of the Programme for Estimating the Accuracy of Analytical Determinations

The analytical determinations are significant only when their certainty degree is known since the obtained results must offer an image as truthful as possible on the values of the determined amounts.

The essential problem of the analytical determination consists in the choice of the best value among the obtained data, that means the value which is closest to the true value. In this purpose the errors must be estimated [7].

The programming on computer of the accuracy estimation of the analytical determinations is particularly important for saving a great deal of effort since number of experiments are rather numerous.

a) *Mathematical Model* [7].

$$X = \frac{1}{n}\sum_{i=1}^{n} X_i; \quad s = \sqrt{\frac{\sum_{i=1}^{n} |X_i - \overline{X}|^2}{n-1}}; \quad s_m = \sqrt{\frac{\sum_{i=1}^{n} |X_i - \overline{X}|^2}{n(n-1)}};$$

$$d = \frac{\sum_{i=1}^{n} |X_i - X|}{n};$$

$$\overline{X} - ts_m < \mu < \overline{X} + ts_m,$$

where: t is the Student coefficient; μ - certainty interval.

I n p u t: X_i, with $i = 1, ..., n$; $n = 7, 11, 21$; t_{95}, t_{99} for each value of n.

O u t p u t: $\overline{X}, d, s, s_m, T_1$ and T_2, where with T_1 and T_2 stand for the algebraic sums $\overline{X} + ts_m$ and $\overline{X} - ts_m$, respectively.

b) *Algorithm.* The algorithm calculates the above relations for each value of n with a total cycle having also two cycles for calculation of $\overline{X}$ and $\sum_{i=1}^{n} |X_i - \overline{X}|^2$, respectively.

c) *Codification.* The following notation have been used:

XM1 for Σ; SM for s_m; D1 for $\sum_{i=1}^{n} |X_i - \overline{X}|$; D2 for d;
T1[j][k] for t (j $= 1, 2, 3$; k $= 1, 2$); T2 for $T2$;
D[k] for probabilities (k $= 1, 2$).

The results for the three values of n are given in Table 2.

Table 2

N values: 21 11 7
$T1$ values: 2.09 2.85 2.23 3.17 2.45 3.71
X values: 10.1 10.3 10.2 9.7 9.8 9.9 9.92 10.4 9.76 10 9.78
10.15 10.25 10.18 10.32 10.04 10.21 10.08 9.84 9.88 9.81
Probabilities' values: 0.95 0.99
AVG.=10.030 ERR.AVG.=0.181 SQ.ERR.AVG.=0.210
SQ.AVG OF AVGS.=4.583E-02
MIU BELONGS TO [9.93E+00, 1.01E+01], PROB.=0.95
MIU BELONGS TO [9.90E+00, 1.02E+01], PROB.=0.99
AVG.=9.987 ERR.AVG.=0.193 SQ.ERR.AVG.=0.235
SQ.AVG OF AVGS.=7.075E-02
MIU BELONGS TO [9.83E+00, 1.01E+01], PROB.=0.95
MIU BELONGS TO [9.76E+00, 1.02E+01], PROB.=0.99
AVG.=9.989 ERR.AVG.=0.181 SQ.ERR.AVG.=0.218
SQ.AVG OF AVGS.=8.245E-02
MIU BELONGS TO [9.79E+00, 1.02E+01], PROB.=0.95
MIU BELONGS TO [9.68E+00, 1.03E+01], PROB.=0.99

3.3. Programme in C Language for Drawing and Interpreting the Cathodic Wave $i = f(E)$ and of the Logarithmic Function $\log[\bar{i}/(\bar{i}_d - \bar{i})] = z(E^0 - E)/0.059$

The reduction of a metallic ion on the dropping mercury is considered according to the general equilibrium:

$$ox + ze^- \rightleftharpoons \text{red}.$$

The equation of the cathodic wave or this process is considered [7],[14]:

$$\log \frac{\bar{i}}{\bar{i}_d - \bar{i}} = \frac{z(E^0 - E)}{0.059}.$$

The inflexion point of the curve corresponds to the half-wave potential $E_{1/2}$ ($E^0 = E_{1/2}$) and $\bar{i} = \bar{i}_d/2$ ($\bar{i}_d$ – intensity of the limit diffusion current; $\bar{i}$ – value of the diffusion current intensity in different potential stages on the polarographic curve $i = f(E)$).

The equation reveals that the $\log[\bar{i}/(\bar{i}_d - \bar{i})]$ versus potential (E) dependence is a straight line with slope $z/0.059$ and $E_{1/2}$ can be found at the value for which $\log[\bar{i}/(\bar{i}_d - \bar{i})] = 0$ (z is the number of electrons participating to the electrod process).

Hence, the interpretation of the logarithmical function of the polarogramme of the cathodic wave affords important information about the analysed chemical system $(z, E_{1/2})$.

a) *Mathematical Model* [7]

$$E = E^0 + \frac{0.059}{z} \log \frac{\bar{i}_d - \bar{i}}{\bar{i}}.$$

I n p u t: $E^0 = -1, ..., 1.5$ (15 values); $E = -1, ..., 1.5$ (15 values); $\bar{i}_d = 10, ..., 150$ (30 values); $z = 1, ..., 5$ (5 values).

O u t p u t: a) graph and listing of the values $i = f(E)$; b) graph of the function $\log[\bar{i}/(\bar{i}_d - \bar{i}] = f(E)$ and the slope of this function.

b) *Algorithm*

$$\bar{i} = \frac{\bar{i}_d}{10^{(E-E^0)z/0.059} + 1}; \quad \log \frac{\bar{i}}{\bar{i}_d - \bar{i}} = \frac{z(E^0 - E)}{0.059} = F(E); \quad \frac{dF}{dE} = -\frac{z}{0.059}.$$

The relation for calculating the values of the required functions as well as the slope of the second function, which will be taken as an absolute value, were obtained.

c) *Codification.* The amounts in the mathematical model were denoted as follows:

EO[i] for E^0, (i = 1, ..., 4); FFI[i] for i, (i = 1, ..., 33);
ID[i] for $\bar{i}_d$, (i = 1, ..., 4); FFLOG[i] for $\log[\bar{i}/(\bar{i}_d - \bar{i})]$, (i = 1, ..., 33);
Z[i] for z, (i = 1, ..., 3); P[i] for dF/dE, (i = 1, ..., 3).

For illustration certain values for $E^0, \bar{i}_d, z$ were arbitrary chosen, in the definition domain, for the variation of E over its entire interval of definition ($E^0 = -1.0; \bar{i}_d = 10; z = 1$).

For these values the graphs were made and the slope of the logarithmic function estimated. The graph slopes can be modified by varying the value of the drawing steps of the points so that to represent exactly, at a convenient scale, the usual graphs in the analytical chemistry (Fig. 1).

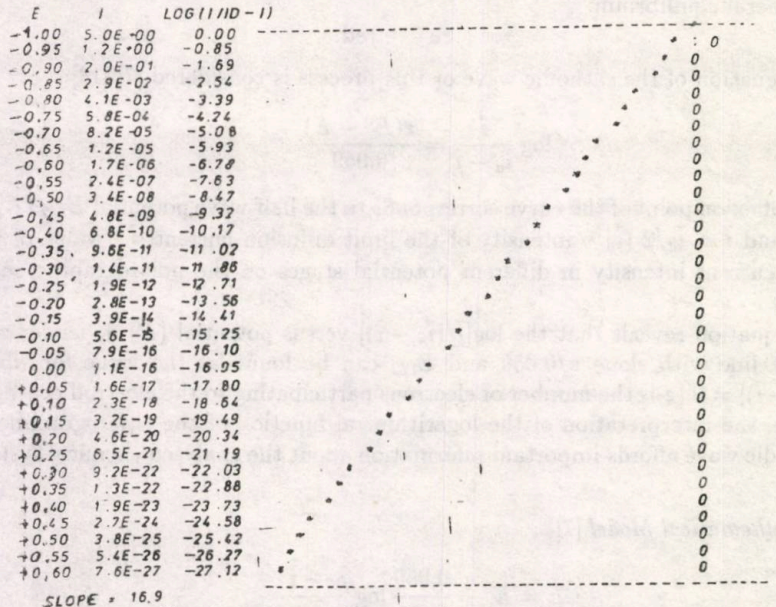

Fig. 1.– Polarographic cathodic wave plotting.

4. Conclusions

The programmes elaborated in C language offer to the analytical chemists a superior, efficient and rapid alternative for studying and interpreting some chemical equilibria and processes. The statistical-mathematical processing of the results affords the scientific evaluation of the accuracy of analytical determinations.

Received, April 14, 1996
Revised, September 27, 1997

Technical University "Gh. Asachi", Jassy,
Department of Analytical Chemistry
and
"Al. I. Cuza" University, Jassy,
Computer Science Faculty

REFERENCES

1. Bejan D., Bejan A., Bul. Inst. polit., Iaşi, **XLIII (XLVII)**, *1-2*, s. II (1997).
2. Mărculeţiu V., Stoica L., Constantinescu I., *Aplicaţii de calcul în Chimia Generală şi Anorganică*. Ed. Tehnică, Bucureşti, 1972.
3. Babic D., Trinajistic N., Klein J.D., Croat. Chem. Acta, **67**, *1*, 37-44 (1994).

4. Belen R., Fernandez-Serra P., Smeyers Y.G., Croat. Chem. Acta, **67**, *1*, 73-83 (1994).
5. Randic M., Trinajistic N., Croat. Chem. Acta, **67**, *1*, 1-30 (1994).
6. Trinajistic N., Nicolic S., Knops J.V., Muller V.R., Szymanski K., *Computational Chemical Graph Theory - Characterization Enumeration and Generation of Computer Methods.* Harwood, Simon & Schuster, New York, 1991.
7. Croitoru V., Constantinescu D.A., *Aplicaţii şi probleme de chimie analitică.* Ed. Tehnică, Bucureşti, 1979, 160, 309, 338, 360.
8. Otto P., Croat. Chem. Acta, **67**, *1*, 85-94 (1994).
9. Petrovici V., Goicea F., *Programarea în limbajul C.* Ed. Tehnică, Bucureşti, 1993, 9.
10. Marinescu D., Trandafirescu M., *PC pentru începători, pornind de la zero.* Ed. Teora, Bucureşti, 1993, 185.
11. Negrescu L., *Limbajul C şi C++ pentru începători.* Ed. MicroInformatica, Cluj-Napoca, 1994, 13.
12. Spircu T., *Introducere în informatică.* Ed. Teora, Bucureşti, 1993, 47.
13. Kekedy L., *Chimie analitică calitativă.* Ed. Scrisul Românesc, Craiova, 1982, 170.
14. Duca Al., Nacu Al., Calu C., *Chimie analitică şi analiză instrumentală.* Vol. **III**, Inst. polit., Iaşi, 1980, 339.

PROGRAMAREA ÎN LIMBAJUL C A UNOR PROBLEME DE CHIMIE ANALITICĂ (II)

(Rezumat)

În prima parte a lucrării s-au prezentat programe în limbaj C care permit rezolvarea unor probleme de chimie analitică referitoare la sistemele acido-bazice.

Extinzând sfera preocupărilor în aceeaşi direcţie, se prezintă soluţiile pe calculator, în limbaj de programare C, ale unor aspecte analitice din domenii diferite, cum ar fi: echilibrele de complexare, evaluarea preciziei determinărilor analitice cu ajutorul calculului statistico-matematic, trasarea şi interpretarea curbelor polarografice.

BULETINUL INSTITUTULUI POLITEHNIC DIN IAŞI
Tomul XLIV (XLVIII), Fasc. 1–2, 1998
Secţia II
CHIMIE şi INGINERIE CHIMICĂ

D.C. 620.193; 547.461.3

THE CORROSION OF LOW ALLOY STEELS IN THE SYSTEM METHANOL–MALONIC ACID–WATER

BY

DANIEL SUTIMAN, MIHAELA VIZITIU,
*TRAIAN CIOROIANU and **OVIDIU GEORGESCU

The behavior of three types of low alloy steels with 0.2...0.4% C, in the system methanol–5% malonic acid–(1...5)% water is studied, and the polarization curves for the concentration of 5% water are obtained. Analyzing the metallic surface and the corrosion degree, a corrosion mechanism is assigned.

1. Introduction

The corrosion process of steels in organic solutions, with low concentration of water, takes place in a different mechanism than the corrosion in aqueous solutions. It is known that in aqueous solutions water is the main source of oxygen for the formation of the oxihydroxylic film [1],...,[5].

In organic solutions of electrolytes, metals cannot form oxides layers on the surface, unless the solutions contain a certain water concentration [6]. The optimal water concentration for obtaining the oxides films depends mainly on the nature of aggresive reagent [7],...,[9]. The present paper studies the behavior of three types of low alloy steels in a system formed by methanol – 5% malonic acid with a low and different water concentration. The study is very important for the industry of synthetic fibers where the malonic acid is a significant corrosion agent in the installation for etyleneglycol recuperation.

2. Experimental Part

Three types of steels with the composition presented in Table 1 were tested.

The metallic samples had a cylinder form with a circular surface of 5 cm^2. The metallic surface submitted to corrosion was polished, and the other surface, that was not corroded, was protected by dyeing. The samples were totally immersed in the corrosive solution, and the process took place without stirring and in direct contact with oxygen from the atmosphere.

Table 1
The Composition of the Steels Submitted to the Corrosion Process

Type of steel	C, [%]	Mn, [%]	S, [%]	Si, [%]	P, [%]
OL 37	0.20	0.80	0.06	0.40	0.06
OL 50	0.30	0.80	0.05	0.40	0.05
OL 60	0.40	0.80	0.05	0.40	0.05

After 60 days the samples were removed from the corrosive solutions, washed up in an hydrochloric acid 3% for 15 sec., then dried in vacuum for 5 min. and weighted.

The composition of the corrosive solutions was: methanol as solvent, malonic acid as corrosive reagent with a concentration of 5% (using Merck product) and bidistilled water with a variable concentration between 1% and 5%. The weight losses determined after 60 days of immersion in the corrosive solutions were processed to figures K, [g/m^{2}hour] and P, [mm/year].

The metallic surfaces were analyzed by SEM with TESLA B300 microscope. Also the anodic and cathodic polarization curves were plotted on a potentiometer TACUSEL S8R. The corrosion compounds were analyzed by X-ray diffraction on a diffractometer HZG 4A with Co(K_α) radiation and by IR spectrometry using a SPECORD M82 apparatus.

3. Results and Discussions

The values of the figures K and P, calculated from weight losses, are presented in Table 2.

Table 2
The Values of K and P Figures

H_2O %	OL 37 K/P	OL 50 K/P	Ol 60 K/P
1	0.233/0.21	0.218/0.20	0.196/0.18
2	0.237/0.21	0.222/0.20	0.208/0.19
3	0.242/0.22	0.226/0.20	0.216/0.19
4	0.249/0.22	0.231/0.21	0.221/0.20
5	0.255/0.23	0.239/0.22	0.237/0.20

Studying the values of these figures it is observed that the corrosion rate increases with the increasing of water concentration.

The metallic surface is totally corroded in pitting for all types of steels. In Fig. 1 the metallic surface of OL 37 is presented.

The polarization curves plotted for 5% water concentration (Fig. 2) show that all three types of steel do not present passive ranges in the studied potential field. The corrosion parameters are shown in Table 3.

The X-ray diffraction and IR spectrum of the corrosion compounds from all types of steel are identical. The X-ray spectrum is characteristic for the amorphous compounds. In IR spectrum (Fig. 3) is observed a shoulder at 3,200 cm^{-1} that corresponds to a different bonding of OH groups; the existence of a shoulder between

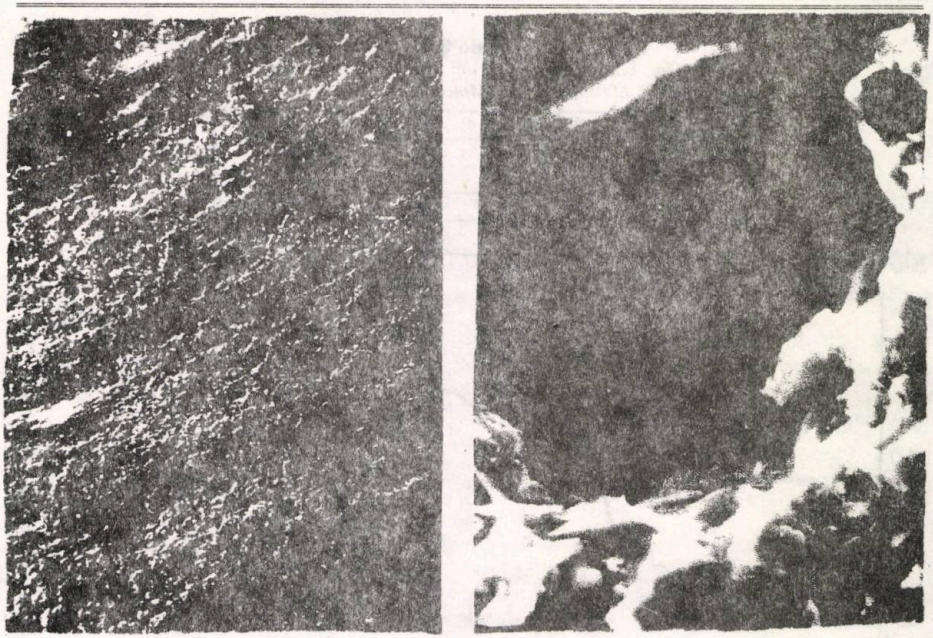

a *b*

Fig. 1.– The metallic surface of OL 37 in the system methanol – 5% malonic acid – 5% water (*a* – ×60; *b* – ×1,200).

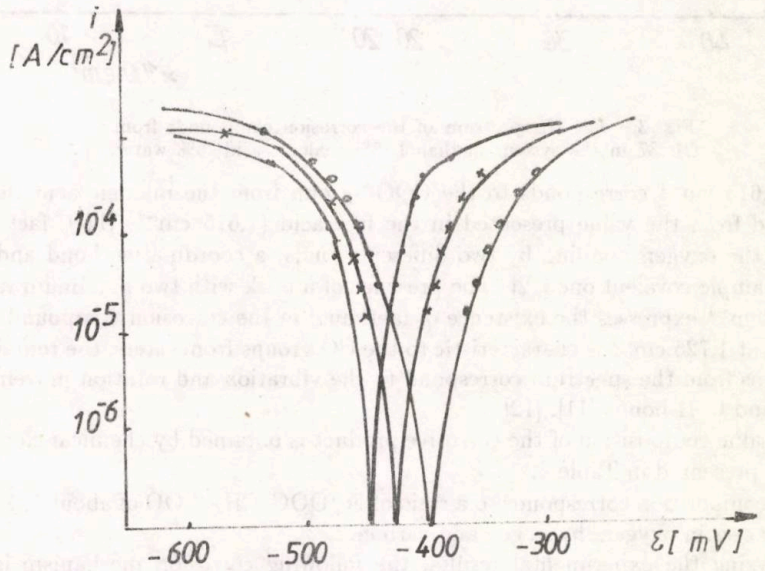

Fig. 2.– The polarization curves in the system methanol – 5% malonic acid – 5% water: • OL 37; × OL 50; ○ OL 60.

Table 3

The Values of Corrosion Parameters in the System Methanol – 5% Malonic Acid – 5% Water

Type of steel	ε_{st}, [mV]	ε_{cor}, [mV]	i_{cor}, [μA/cm^2]
OL 37	–450	–465	22.18
OL 50	–430	–455	21.03
OL 60	–400	–435	20.28

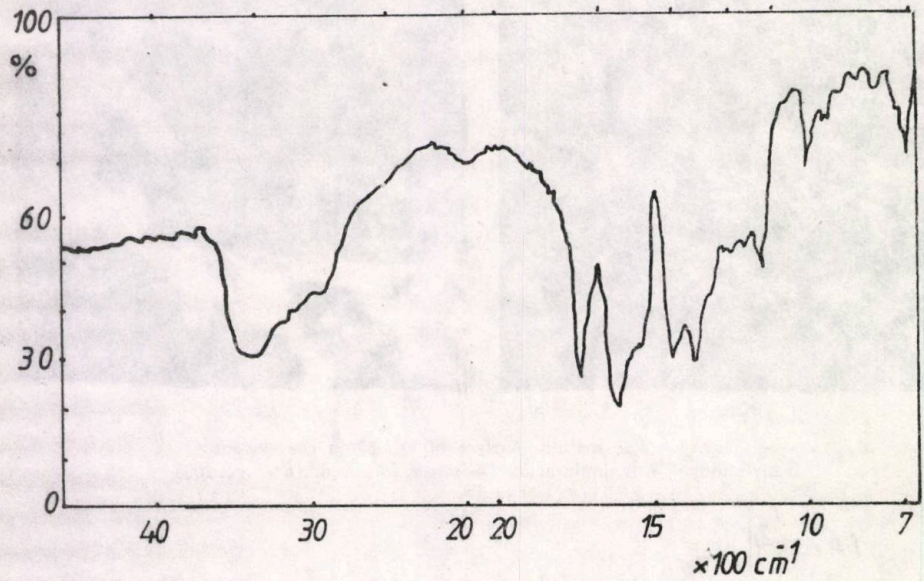

Fig. 3.– The IR spectrum of the corrosion compounds from OL 37 in the system methanol – 5% malonic acid – 5% water.

1,600...1,615 cm^{-1} corresponds to the COO$^-$-group from the malonic acid that is misplaced from the value presented in the free acid (1,675 cm^{-1}, [11]), fact that explains the oxygen bonding by two different bonds, a coordinative bond and the other a sample covalent one [12]. The presence of a peak with two maximum values at 1,000 cm^{-1} expresses the existence of methanol in the corrosion compound, and the peak at 1,725 cm^{-1} is characteristic to the CO groups from esters; the remaining maximums from the spectrum correspond to the vibration and rotation movements of C–C and C–H bonds [11], [12].

The same composition of the corrosive product is obtained by chemical-elements analysis, presented in Table 4.

This composition corresponds to a ratio of Fe/OOC–CH_2–COO of about 1/1 with a little excess in oxygen, hydrogen and carbon.

Analyzing the experimental results, the following corrosion mechanism is assigned:

$$Fe \rightarrow Fe^{2+} + 2e^-$$

Table 4
The Chemical Composition of the Corrosion Products

	OL 37	OL 50	OL 60
C, [%]	23.16	23.05	22.39
H, [%]	2.45	2.12	2.34
O, [%]	41.56	41.05	40.89
Fe, [%]	32.83	33.78	34.38

$$H_2O+\tfrac{1}{2}O_2+2e^- \rightarrow 2OH^-$$

$$Fe^{2+}+HO^-+\tfrac{1}{2}O_2+H_2O \rightarrow Fe(OH)_3$$

$$Fe(OH)_3+HOOC-CH_2-COOH \rightarrow Fe[(OOC-CH_2-COO)(OH)]_n+2H_2O$$

The assigned structure of the polymalonate compound of Fe(III) is presented in Fig. 4.

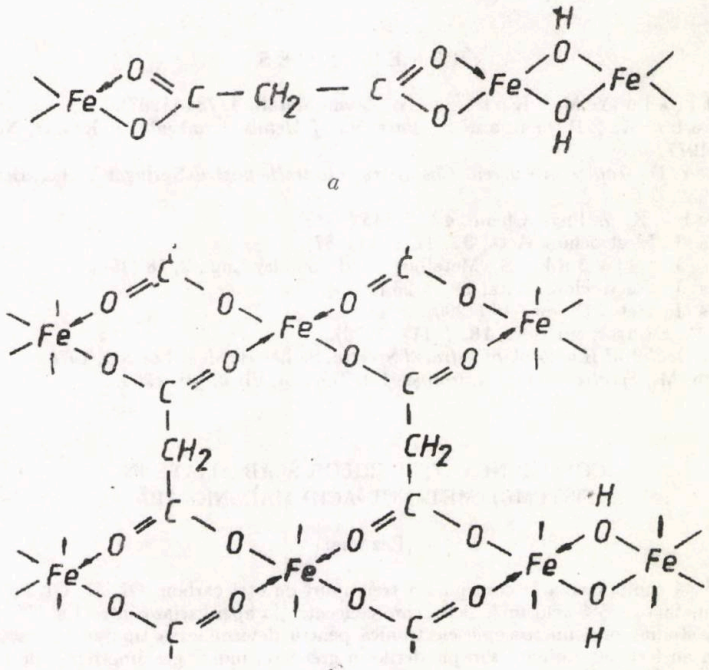

Fig. 4.– The structure from the polymalonate Fe(III); *a* – linear, *b* – cyclic.

In order to accomplish the six coordination of iron, it is possible to assign the participation of methanol, water or at the end of the polymeric chain, of an ester of malonic acid with methanol.

4. Conclusions

1. The corrosion rate increases with the increasing of water concentration of the corrosion solution until a value of 5% H_2O.

2. The corrosion rate decreases with the increasing of carbon concentration of steels, so that the most stable steel in the studied system is OL 60.

3. All types of steel present a pitting corrosion, very different from the corrosion in the organic mediums.

4. The assigned corrosion mechanism is a one with the complex compounds obtaining, the corrosion products being polymers.

Received, April 13, 1998

Technical University "Gh.Asachi", Jassy,
Department of Inorganic Chemistry,
** Research Center S.C.*
Chimenerg S.A., Craiova
and
*** Research Center S.C.*
Zecasin S.A., Ploieşti

REFERENCES

1. Kolotirkin Ye.M., Kossgy G., Zasch. Metall, **4**, 784 (1967).
2. Schwabe K., Herman S., *Passivity of Metals.* Frankental & Kruger, New Jersey, 1977, 68.
3. Degner D., *Topics in Current Chemistry, Electrochemistry.* Springer Verlag, Berlin, 1982, 232.
4. Schwabe K., Z. Phys. Chem., **48**, *9*, 145 (1980).
5. Banas J., Electrochim. Acta, **32**, *17*, 110 (1987).
6. Banas J., Stypula B., Metallurgy and Foundry Eng., **2**, 18 (1992).
7. Banas J., Electrochim. Acta, **18**, *3*, 26 (1985).
8. Banas J., Met. I Odlew., 16 (1990).
9. Hoar P., Electrochem. Soc., **18**, *4*, 117 (1970).
10. * * * *The Sadler of Handbook of Infrared Spectra.* Sadler Heyden, London, 1978.
11. Avram M., *Spectroscopia în infraroşu.* Ed. Tehnică, Bucureşti, 1960.

COROZIUNEA OŢELURILOR SLAB ALIATE ÎN SISTEMUL METANOL-ACID MALONIC-APĂ

(Rezumat)

Se studiază comportarea la coroziune a trei tipuri de oţel carbon: OL 37, OL 50 şi OL 60, în sistemul metanol – 5% acid malonic în care concentraţia apei variază între 1 şi 5%. Suprafaţa metalică s-a studiat prin microscopie electronică pentru determinarea tipului de atac corosiv şi de asemenea au fost determinaţi, din pierderile în greutate, indicii gravimetrici şi de penetraţie. Pentru concentraţia de 5% apă au fost trasate curbele de polarizare şi s-au determinat parametrii cinetici de coroziune. Din analiza produselor de coroziune prin difracţie de raze X, spectroscopie IR şi analiză elementară s-a propus un mecanism de coroziune.

BULETINUL INSTITUTULUI POLITEHNIC DIN IAŞI
Tomul XLIV (XLVIII), Fasc. 1-2, 1998
Secţia II
CHIMIE şi INGINERIE CHIMICĂ

D.C. 615.517; 54-92

ON THE COMPATIBILITY OF POLYSTYRENE WITH POLY(ETHYLENE-s-VINYL ACETATE) COPOLYMER

BY
N. AELENEI, MARCEL-IONEL POPA and *GABRIEL PĂDURARU

By osmometric and viscometric measurements was studied the compatibility of the polystyrene with the statistical copolymer poly(ethylene-s-vinyl acetate) in tetrahydrofuran solution. The study shows that the two polymers are incompatible in solution and incompatibility degree increases with increasing of copolymer content in mixture.

1. Introduction

From a practical point of view polymer mixture are very attractive materials, offering a possible compromise between physical-mechanical properties and production costs. In order to obtain a very stable polymer alloy a thermodynamical compatibility between its components is necessary. It is well known that less than 15% from the used polymer alloys are thermodynamical compatible, the others having a pseudo-compatibility in which the mixture maintains the properties in time as a result of a high viscosity, of the mechanical interpenetration of the chains, and, sometimes, due to the weak attractions, so that it is impossible to separate the components of the polymer alloy.

From thermodynamical point of view, the interaction between two polymers is estimated by the value and sign of the polymer–polymer interaction parameter, χ, the polymers for which $\chi \leq 0$ being considered compatible and the pairs having $\chi > 0$, incompatible. This parameter, having a Gibbs free energy character, contains energetical contributions – lies to the intermolecular forces – and entropical contributions – lies to length and flexibility of polymer chains. When the dispersion forces are dominating and the molecular weights of both polymers are big enough, the two contributions are positive and polymers are thermodynamically incompatible.

In order to be thermodynamically compatible, two polymers must have a negative mixing free energy. In this category can be included the polymer pairs which present strong attraction forces or specific interactions – like hydrogen bonds.

In practice is important to estimate the compatibility/incompatibility degree of a polymer pair and, especially, the optimal conditions to obtain a polymer alloy with great stability in solid phase. The compatibility studies in solid phase can be made

by DSC, thermogravimetry, microscopy, X-rays diffraction, mechanical and dynamical properties, etc. However these methods do not permit to estimate the polymer/polymer interaction parameter and can't offer quantitative information about thermodynamical interaction between the mixture components.

The estimation methods of the interaction parameter, χ, are based exclusively on the solution studies, using methods like osmometry, light scattering, viscometry, calorimetry, phase separation and so on.

The presence of the solvent can influence considerable the value of the polymer (2)/polymer (3) interaction parameter, χ_{23}, by changing chain flexibility and polymer/polymer contact points number. This is the reason why a clear difference between block and solution compatibilities must be made.

Introduction of a third component (1), which may be a common solvent or a low molecular weight plasticizer, produces a decrease of the polymer/polymer contact number and an increase of the chain flexibility, so that, at a specified concentration, the system becomes thermodynamically stable [1]. In a solvent (1)/polymer (2)/polymer (3) ternary system a phase separation may occur at a certain concentration, named critical concentration of miscibility. The critical concentration of miscibility can be obtained using the F l o r y - H u g g i n s theory supposing that the solvent have the same affinity for both polymers ($\chi_{13} = \chi_{12}$). It is already known that either critical concentration of miscibility and interaction parameter polymer/polymer, χ_{23}, depend on the affinity difference of the common solvent for the two polymers [1],...,[6], which may be expressed as $\Delta\chi = \chi_{12} - \chi_{13}$.

This quantity may be considered as a measure of incompatibility of two polymer in solution. It is considered that the maximum stability of a system solvent (1)/polymer (2)/polymer (3) is obtained when $\Delta\chi = 0$ [6], meaning that the affinity of the solvent for both polymers is the same. If the used solvent is a good one for both polymers then the separation of phases, which may occur at a certain concentration, is caused only by the incompatibility of polymers, being dependent on the interactions between polymers.

It was early recognized that the compatibility in solution depends on the nature of the functional groups of polymer [7], molecular weights of the polymers [8], and the nature of solvent [9]. Excepting the nature of functional groups of polymer which contributes directly on interactions between polymers, an important role has the nature of the common solvent used, so two polymers might be compatible in a solvent but incompatible in another one. This fact is important when it is desired to obtain polymer alloys by precipitation in solution and, especially, by solvent evaporation. A better compatibility can be obtained when the molecular weights of the two polymers are very different as values. Usually, when the molar weights of the two polymers are high they are incompatible.

Because of the fact that the polymer (2)/solvent (1), polymer (3)/solvent (1) and polymer (2)/polymer (3) interactions have a great importance for the size of the macromolecular coils in solution, and these dimensions influence appreciably the rheological properties of the solutions, the viscometric measurements can be also used for the analysis of the polymers compatibility. In this case, to estimate

the compatibility of the polymers in solutions is better to use the deviation of the limiting viscosity number from theoretic value calculated by additivity:

$$\Delta[\eta] = [\eta]_T - w_2[\eta]_{12} - w_3[\eta]_{13},$$

considering compatible the pairs of polymers for which $\Delta[\eta] > 0$ and incompatible those with $\Delta[\eta] < 0$.

In this paper we report some studies about the compatibility of polystyrene (PS) – rigid polymer with great tensible breaking and with little elongation at break (13%) – with poly(ethylene-s-vinyl acetate) (PEVA) copolymer – a low density polymer having a very great elongation of break (650...900%), both polymers having a great transparency.

2. Theory

Polymer/polymer interaction parameter, χ_{23}, and thermodynamic compatibility in dilute solutions can be evaluated by osmotic pressure measurements. Interaction parameter χ_{23} can be calculate from the second virial coefficient, A_{2T}, obtained for the solvent (1)/polymer (2)/polymer (3) ternary solutions from the linear dependence of reduced osmotic pressure (π/c) versus total polymer concentration in solution (c):

$$\frac{\pi}{c} = \frac{RT}{M_n} + RTA_{2T}c, \tag{1}$$

where:

$$A_{2T} = \frac{0.5 - \chi_T}{\rho^2 V_{m01}}, \tag{2}$$

with: χ_T – ternary interaction parameter, V_{m01} – molar volume of the solvent, and

$$\rho = \frac{\rho_2\rho_3}{\rho_2 w_3 + \rho_3 w_2} \tag{3}$$

– mean density of the polymer mixture. Here ρ_2 and ρ_3 are the densities of pure polymers; w_2 and w_3 – the weight fractions of polymers, in solid binary mixture.

According to F l o r y - H u g g i n s theory for ternary systems [10], the ternary interaction parameter can be obtained in the form:

$$\chi_T = \frac{\rho}{\rho_2}\chi_{12}w_2 + \frac{\rho}{\rho_3}\chi_{13}w_3 - \frac{\rho^2}{\rho_2\rho_3}\chi_{23}w_2w_3, \tag{4}$$

where χ_{12} and χ_{13} are the binary interaction parameters polymer (2)/solvent (1) and respectively, polymer (3)/solvent (1).

The polymer/polymer interaction parameter can be then evaluate with the relation:

$$\chi_{23} = \frac{\dfrac{\rho}{\rho_2}\chi_{12}w_2 + \dfrac{\rho}{\rho_3}\chi_{13}w_3 - \chi_T}{\dfrac{\rho^2}{\rho_3\rho_2}w_2w_3}. \tag{5}$$

The existence of a correlation between the limiting viscosity number and the second virial coefficient allows that the viscometric measurements can be also used to appreciate the thermodynamic compatibility of polymers in solution. Thus, based on S t o c k m a y e r - F i x m a n theory, one obtains:

$$A_2 = 205.5\frac{[\eta]}{M}\left(1 - \frac{1}{\alpha_\eta^3}\right), \tag{6}$$

where: A_2 is the second virial osmotic coefficient, $[\eta]$ – the limiting viscosity number and α_η – the expansion factor of the polymer in solution.

Using Eq. (6), the deviation of the limiting viscosity number from the mean ideal value, can be expressed as [10]:

$$\Delta[\eta] = \frac{M}{205.5\left(1 - \alpha_{\eta,T}^{-3}\right)} \times$$

$$\times \left[A_{2,T} - w_2 A_{2,(12)} \frac{M_2\left(1 - \alpha_{\eta,T}^{-3}\right)}{M\left(1 - \alpha_{\eta,2}^{-3}\right)} - w_3 A_{2,(13)} \frac{M_3\left(1 - \alpha_{\eta,T}^{-3}\right)}{M\left(1 - \alpha_{\eta,3}^{-3}\right)}\right], \tag{7}$$

where: $A_{2,T}$, $A_{2,(12)}$ and $A_{2,(13)}$ represent the second virial coefficients for polymer mixture, polymer (2), and polymer (3), in common solvent used; M, M_2, M_3 – molecular weights of the mixture and of the two polymers; $\alpha_{\eta,T}$, $\alpha_{\eta,2}$ and $\alpha_{\eta,3}$ – the expansion factors for mixture and for the two polymers.

The value of $\Delta[\eta]$, calculated with Eq. (7), should be equal with the experimental one only in case when the molecular weights and the expansion factors are identical for both polymers and mixture. In such a case the sign of $\Delta[\eta]$ is the same with the ΔA_2 sign.

The expansion factor for the mixture might be equal with that calculated one by addition only when between the two polymers doesn't exist repulse or attraction forces. When between polymers there are attraction forces, the polymers are compatible and $\Delta A_2 = A_{2,T} - w_2 A_{2,(12)} - w_3 A_{1,(13)} < 0$; a compression of the macromolecular coils take place in the solution, apparently the solvent quality is lowered, so that the expansion factor $\alpha_{\eta,T}$ is smaller than that calculated by additivity. In such a case, according to Eq. (7), $\Delta[\eta]$ should be higher than that calculated by additivity. The absolute values of $\Delta[\eta]$ depend as well on strength of the polymer/polymer interactions, that is why the solvent quality might be more important even than interactions between polymers. Usually the sign of $\Delta[\eta]$ is opposite to the ΔA_2 sign.

3. Experimental

Osmometric measurements were made at 27°C, with an automatic Hewlett-Packard 502 osmometer, using cellulose membranes of PECELL-600 type. Tetrahydrofuran (THF) stabilised with 0.05% hydroquinone was used as solvent. For each sample,

pure polymer or mixture, the osmotic pressure was measured for at least five concentrations, between 0.2 and 1.0 g.dl^{-1}, the solutions being obtained by diluting a concentrate solution of 1.0 g.dl^{-1}. M_n and the second virial coefficient were evaluated from π/c versus c diagram which was linear in all the cases.

The viscometric measurements, also in tetrahydrofuran, were carried out with an Ubbelohde-type viscometer with internal dilution, equipped with sintered glass filter. The dilutions were effected directly in viscometer starting from a concentration of 1 g.dl^{-1}. For each sample 6...7 measurements were made, at 27°±0.02°C. The limiting viscosity number was evaluated, graphically, by double extrapolation according to the H u g g i n s and F u o s s - M e a d equations.

Unfractionated polymers were used; polystyrene with specific gravity 1.06 g/cm^3 and poly(ethylene-s-vinyl acetate) of low density ($\rho = 0.92$ g/cm^3).

The ternary solutions solvent (1)/polymer (2)/polymer (3) were prepared at least with 30 h before the measurements.

4. Results and Discussions

The number average molecular weights, M_n, the second virial coefficient, $A_{2,T}$, and the limiting viscosity number in THF, $[\eta]$, for pure polymers and mixtures are presented in Table 1, versus concentration of poly(ethylene-s-vinyl acetate) from polymer mixture, expressed either as weight percentage (% PEVA) or molar fractions (x_2).

Table 1

Results of Osmometric and Viscometric Measurements, at 27° C, in Tetrahydrofuran

PEVA, [%]	0	20	40	60	80	100
x_2	0	0.4326	0.6703	0.8206	0.9242	1
M_n, [g.mol^{-1}]	109,800	76,800	62,100	46,300	39,400	36,000
$10^4 A_{2,T}$, [m^3.mol.kg^{-2}]	4.23	7.34	10.40	13.50	15.20	16.75
$[\eta]$, [dl.g^{-1}]	1.015	1.040	1.085	1.120	1.160	1.287

An appreciation of the precision for osmometric measurements, it can be made comparing the experimental values of the solid mixtures molecular weights with that calculated by additivity ($M_n = \sum_i x_i M_{ni}$), the averaging being based on molar fractions which are equal with numerical fractions. Fig. 1 shows a good linearity, within a limit of 2...3% errors, acceptable for osmometric measurements.

Sometimes, to appreciate the compatibility of two polymers the second virial coefficient for ternary mixture, $A_{2,T}$, determined by osmometry or light scattering, is used [12],...,[14].

When light scattering method is used it is necessary that one of the two polymers to be isorefractive with the used solvent, studying the manner in which his presence in solution influences the value of the second virial coefficient of the unisorefractive polymer, the polymers being considered compatible when A_2 increases with concentration of isorefractive polymer.

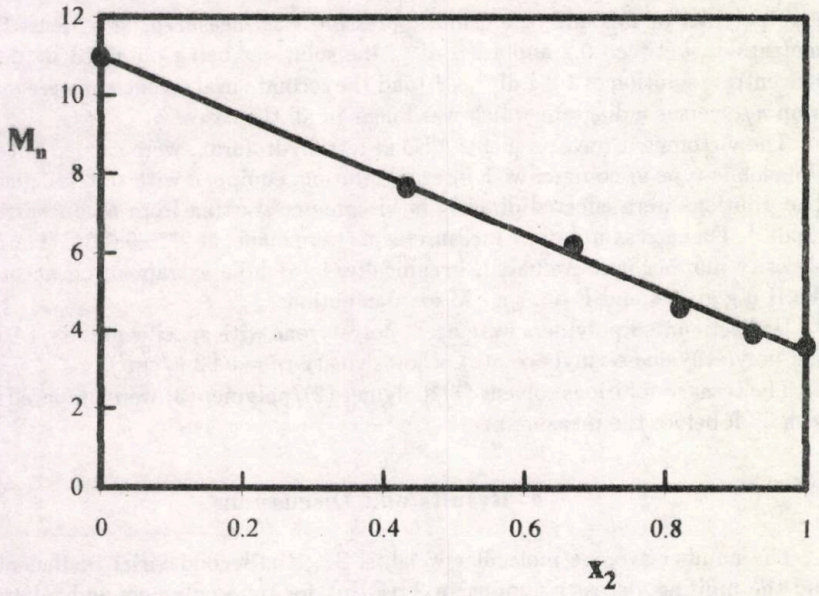

Fig. 1.– Number average molecular weight versus molar fraction of PEVA in solid mixture.

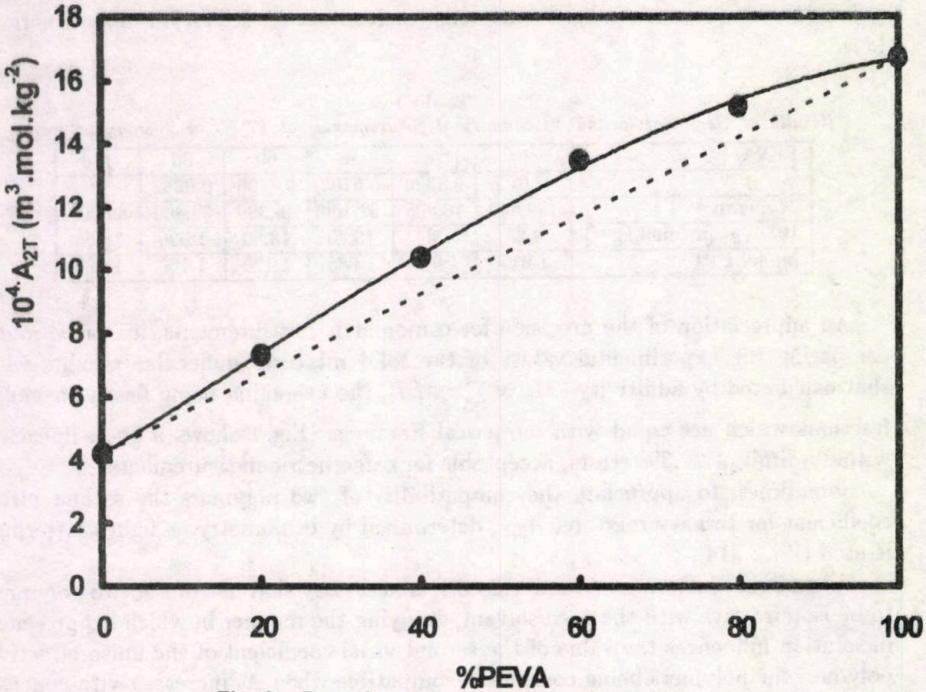

Fig. 2.– Dependence of the ternary second virial coefficient on gravimetric composition of the mixture.

In osmometric measurements the compatibility is estimated analysing the deviations from additivity of the second virial coefficient of the ternary system, the polymers being compatible when $\Delta A_{2,T} < 0$. In these cases it must be taken into account the averaging procedure in obtaining of the mean values, gravimetrical or numerical, because when the molecular weights of the polymers are very different and deviations from additivity are small, the averaging type can influences considerable the conclusions about compatibility, like in our case. The second ternary virial coefficient, $A_{2,T}$, is represented versus weight percentage of poly(ethylene-vinyl acetate) in Fig. 2, and versus molar fraction of PEVA in Fig. 3. As it can be seen from Fig. 2, $\Delta A_{2,T} > 0$ and the conclusion should be that the system PS/PEVA is incompatible in solution, otherwise according to the Fig. 3, $\Delta A_{2,T} < 0$ and consequently the system appears as a compatible one. Taking into account the fact that in osmometric experiments the solution composition are expressed in $g.cm^{-3}$ or in $g.dl^{-1}$, for calculating of the reference average value the weight polymer fractions must be used. On the same basis Eq. (4) was found for ternary interaction parameter. So, the osmometric data show the incompatibility of these two polymers.

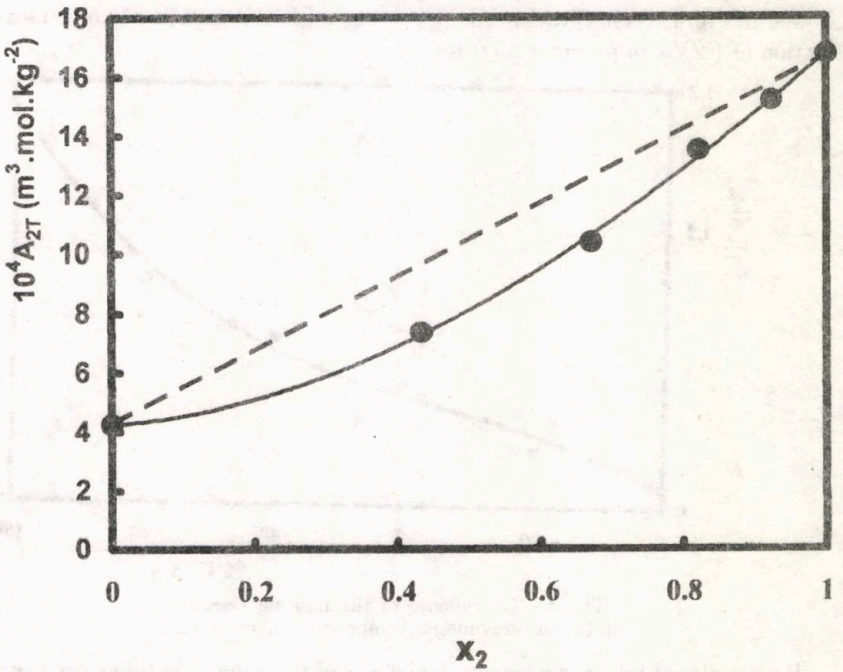

Fig. 3.– Dependence of the ternary second virial coefficient on molar composition of the mixture.

Based on the data from Table 1 and Eqs. (2),...,(5), the densities (ρ), ternary interaction parameter (χ_T) and polymer/polymer interaction parameter (χ_{23}) were calculated; the obtained values are shown in Table 2. The solvent and polymers

experimentally determined densities were used, namely: $\rho_1(\text{THF}) = 0.888$ g.cm^{-3}; $\rho_2(\text{PEVA}) = 0.920$ g.cm^{-3} and $\rho_3(\text{PS}) = 1.060$ g.cm^{-3}.

Table 2

Densities of Polymer Mixtures, χ_T, and χ_{23} for PS/PEVA/THF System at 27° C

PEVA, [%]	0	20	40	60	80	100
ρ, [g.cm^{-3}]	1.060	1.0287	0.9991	0.9713	0.9449	0.920
χ_T	χ_{13}=0.4635	0.4369	0.4157	0.3966	0.3898	χ_{12}=0.3848
χ_{23}	0	0.0518	0.05526	0.07335	0.06148	0

The positive values of the polymer/polymer interaction parameter indicate the incompatibility of polystyrene with poly(ethylene-s-vinyl acetate), in THF solutions, but low values of χ_{23} show that the incompatibility degree is rather low, so that by a mechanical mixing a pseudo-compatible mixture is easy to obtain. For this system the value $|\Delta\chi| = |\chi_{23} - \chi_{13}| = 0.0787$ is relatively low and indicate a selective sorbtion of the solvent against the two polymers; in this case THF is preferential adsorbed by poly(ethylene-s-vinyl acetate).

The dependence of limiting viscosity number on polymer mixture composition is showed in Fig. 4, versus gravimetric percentage of PEVA and in Fig. 5, versus molar fraction of PEVA in polymer mixture.

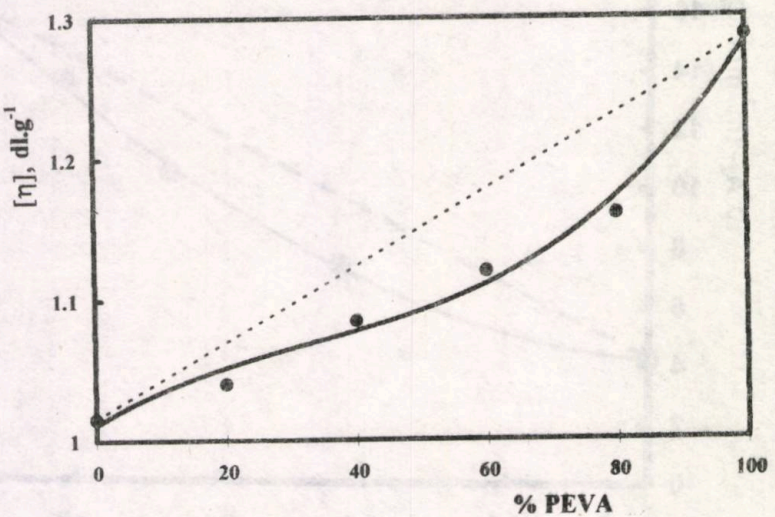

Fig. 4.– Dependence of the limiting viscosity number on gravimetric composition of the mixture.

Both plotts of $[\eta]$ show negative deviations of the experimental values from those calculated by additivity, which means that the two polymers are incompatible in THF, and the incompatibility degree increases with the content of copolymer in the polymer mixture. This can be explained by increasing of the contact number between polystyrene groups and vinyl acetate ones of the copolymer, being known that polystyrene and polyvinyl acetate are incompatible in THF [9], and polystyrene

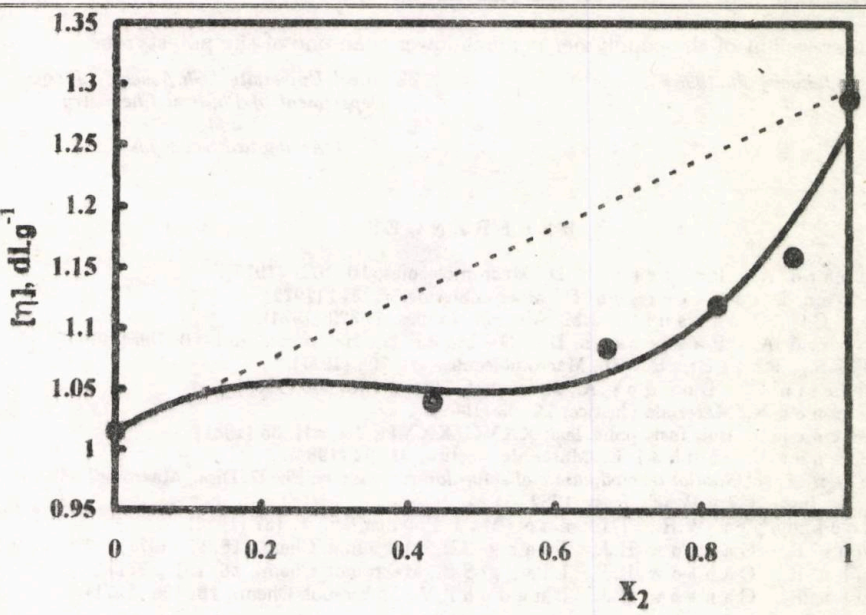

Fig. 5.- Dependence of the limiting viscosity number on molar composition of the mixture.

groups and the polyethylene groups are incompatible by their themselves structures. In solution macromolecular coils of the copolymer are much bigger than those of the polystyrene because THF is a better solvent for PEVA than for PS and, on the other hand, due to the repulsive forces existing between the functional groups of PEVA (s. the low density of this material). the increasing of the PS/PEVA contacts number in rich copolymer mixtures is facilitated also by the fact that molecular weight of the copolymer is much lower than that one of the polystyrene. The results of the viscometric analysis are in a good agrement with the osmometric results.

5. Conclusions

1° Osmometric and viscometric studies on compatibility of polystyrene and poly(ethylene-s-vinyl acetate) copolymer show that they are incompatible in tetrahydrofuran solution.

2° Polymer/polymer interaction parameter, χ_{23}, being normalised at the volume of a solvent molecule, should not depend on the ratio of the two polymers in mixture. From presented data it can be seen a well-marked dependence of this parameter on composition, this, perhaps, due to a preferential interaction between solvent and copolymer.

3° The incompatibility degree increases with increasing of the copolymer content in mixture and this can be explained by PS/PEVA contact number rise because the fact that tetrahydrofuran is a better solvent for colopymer than for polystyrene and

molecular weight of the copolymer is much lower than one of the polystyrene.

Received, January 30, 1998

Technical University "Gh.Asachi", Jassy,
Department of Physical Chemistry
and
** Antibiotice S.A., Jassy*

REFERENCES

1. Robard A., Patterson D., Macromolecules, **10**, 1021 (1977).
2. Zeman L., Patterson D., Macromolecules, **5**, 513 (1972).
3. Hsu C.C., Prausnitz J.M., Macromolecules, **7**, 320 (1974).
4. Robard A., Patterson D., Delmas G., Macromolecules, **10**, 706 (1977).
5. Su C.S., Patterson D., Macromolecules, **10**, 708 (1977).
6. Hugelin C., Dondos A., Makromol. Chem., **126**, 206 (1969).
7. Aelenei N., Materiale plastice, **19**, 93 (1982).
8. Aelenei N., Bul. Inst. polit. Iaşi, **XXVII(XXXI)**, *1-4*, s.II, 35 (1981).
9. Aelenei N., Mihai E., Materiale plastice, **21**, 92 (1984).
10. Aelenei N., *Studiul termodinamic al soluţiilor de polimeri.* Ph. D. Diss., Macromol. Chem. Inst. "Petru Poni", Jassy, 1982.
11. Stockmayer W.H., Fixman M., J. Polymer Sci., **1**, 137 (1963).
12. Kuhn R., Cantow H.J., Liang S.B., Makromol. Chem., **18**, 93 (1971).
13. Kuhn R., Cantow H.J., Liang S.B., Makromol. Chem., **18**, 101 (1971).
14. Kuhn R., Cantow H.J., Bugdohl V., Makromol. Chem., **18**, 109 (1971).

COMPATIBILITATEA POLISTIRENULUI CU COPOLIMERUL POLI(ETILEN-s-VINIL ACETAT)

(Rezumat)

Prin măsurători osmometrice si viscozimetrice s-a studiat compatibilitatea polistirenului cu copolimerul statistic poli(etilen-s-vinil acetat) în soluţie de tetrahidrofuran. Studiile relevă faptul că cei doi polimeri sunt incompatibili în soluţie, iar gradul de incompatibilitate creşte odată cu creşterea conţinutului de copolimer în amestec.

BULETINUL INSTITUTULUI POLITEHNIC DIN IAŞI
Tomul XLIV (XLVIII), Fasc. 1–2, 1998
Secţia II
CHIMIE şi INGINERIE CHIMICĂ

D.C. 620.193

CONSIDERATIONS ON CORROSION OF PIPE PRECIPITATORS

BY

ŞT. IVĂŞCAN, MARIA APOSTOLESCU, N. APOSTOLESCU, EDUARD-EMIL IOJOIU and FLORIN BANDRABUR

The pipe precipitators used for burning gases dedusting from black lyes burning, which are residual solutions from cellulose manufacturing, are submitted to a corrosion process both mechanically and electrochemically. We established a corrosion mechanism on the basis of thermodynamic calculations and experimental data obtained by the analysis of the corrosion products.

1. Introduction

The residual solutions resulting from the decrustation of the wooden mass in case of the cellulose manufacturing by the hydroxide-sodium sulphide alkali procedure, commonly referred to as black liquors, are complex systems of both organic and inorganic compounds. Their concentration lies between 13% and 20%, depending on the technological parameters of the decrustation process [1].

For recovering as much as possible the organic and inorganic components the black liquors are submitted to an working process where some difficulties arise due to the corrosion of the metallic equipment. The processing of the black liquors consists essentially in their concentration by evaporation followed by the burning in boilers of an especial building.

During the burning process the organic components are converted into gases (CO_2, CO, water vapour, SO_2, mercaptan derivatives) while the inorganic part turns into melt. Several chemical reaction proceed involving some of the inorganic compounds among which the reduction of sodium sulphate by the carbon is the most important:

$$Na_2SO_4 + C = Na_2S + CO_2$$

The reduction degree of the sulphate is lowered by an air excess which promotes at the same time a side reaction resulting in the sulphur dioxide formation:

$$Na_2S + CO_2 + \tfrac{3}{2}O_2 = Na_2CO_3 + SO_2$$

The gases resulting from the burning of the black liquors carry off great amounts of inorganic salts (Na_2SO_4, Na_2S, Na_2CO_3) so that they must be purified before evacuation into atmosphere for economical and ecological reasons.

The fine particles of size less than 0.30 μm are retained by the pipe precipitator. Under the operating conditions of the burning aggregates as well as those of the gas evacuation (low temperature, air excess, etc.) undesirable corrosion process of the metallic parts arise and develop especially in case of the pipe precipitator [2]. Their corrosion results in a decrease in the gas purification degree along with an increase in the atmosphere pollution.

In the present paper the conditions of destruction by corrosion of both electrodes and supporting belts in pipe precipitator are discussed on the basis of thermodynamic calculations and experimental data obtained by the analysis of the corrosion products.

2. Results and Discussion

Under the real operating (working) conditions the pipe precipitator under study shows the following characteristics: gas flow rate of about 111,000 m^3/h, average temperature of 130°C and yield of particle retention of 50% only, in comparison with the design value of 99%.

The burning gas enter in the pipe precipitator as different contents of carbon oxide and dioxide, water vapour, nitrogen and oxygen, sulphur oxides as well as alkaline dust.

Since the black liquors are also considered to be fuels for obtaining thermal energy during the cold periods, different amounts of black oil containing 2...4% sulphur (sulphur-containing organic compounds) are added.

Due to the catalytic action of the vanadium compounds (in the black oil) the sulphur dioxide is oxidized to sulphur trioxide which results in the formation of sulphuric acid.

Numerous chemical reactions can proceed, corrosion reactions of the metallic parts among them, by the interaction of the solid (electrodes and supporting belts) and gaseous phases with the participation of the liquid phase arising when the condensation point is attained.

The thermodynamic calculations [3] ($\Delta_R G$) of some possible reactions along with the physical-chemical data of the resulting corrosion products are indicative of the following reactions proceeding under the conditions of the pipe precipitator operation ($T = 400$ K) and determining the corrosion of the metallic mass:

(1) $$2Fe + \tfrac{3}{2}O_2 = Fe_2O_3, \quad \Delta_R G_T^0 = -712 \text{ kJ};$$

(2) $$SO_3 + H_2O = H_2SO_4, \quad \Delta_R G_T^0 = -61 \text{ kJ};$$

(3) $$Fe + H_2SO_4 + \tfrac{1}{2}O_2 = FeSO_4 + H_2O, \quad \Delta_R G_T^0 = -356 \text{ kJ};$$

(4) $$Fe_2O_3 + 3H_2SO_4 = Fe_2(SO_4)_3 + 3H_2O, \quad \Delta_R G_T^0 = -1,120 \text{ kJ};$$

(5) $$Fe + SO_2 + O_2 = FeSO_4, \quad \Delta_R G_T^0 = -476 \text{ kJ}.$$

Consequently the metallic mass is damaged by corrosion acting by means of these

Table 1
Characterization of Sodium Sulphate

Colour	White-gray
State	Dust
Composition:	
SO_4^{2-} (total content), [%]	53.03
CO_2 (total content), [%]	5.88
Fe (total content), [%]	0.78
water-insoluble, [%]	8.62
diluted HCl insoluble, [%]	6.47
or:	
Na_2SO_4, [%]	78.44
Na_2CO_3, [%]	14.16
Fe_2O_3, [%]	1.12

simultaneous reactions of different rates. Due to the operating conditions the rate-limiting reaction of the corrosion process is rather difficult to appreciate.

The analysis of sodium sulphate gathered at the pipe precipitator bottom (Table 1) as well as the corrosion products collected by scraping the metallic surfaces are indicative of a corrosion process developing by means of the reactions (1),...,(5).

The rather high amount of Fe ions (61%) is indicative for the degradation by corrosion of the metallic parts of the pipe precipitator. This amount is included in iron oxides and sulphate. The content of iron sulphate in comparison with the oxide one in the corrosion products depends on the burning conditions: air excess, amount of added black-oil and its sulphur content, etc.

The condition of burning proceeding really by means of an air excess along with the secondary air infiltrated through the leakinesses of the pipes can explain the high content of oxides in the corrosion products (Table 2).

The corrosion process could be seen to affect the whole surface under study. The corrosion products appeared as a brown-reddish adherent layer containing whitish-glass randomly distributed crystals which represent sodium sulphate.

Small regions of irregular shape where the metallic surface had been perforated by corrosion have also been noticed. Such corrosive attacks were noticed to be concentrated on the surfaces of the both supporting belts and electrodes. The appearance of these strongly corroded regions could be explained by the existence of the some internal strains resulting during the initial preparation of the metallic material as well as during the mounting stage. These strains increase the instability of the metallic material and, consequently, the local corrosion intensities. Apart from this, the hydrodynamic conditions of the pipe precipitator operation (high gas flow rate, high rate) determine the appearence of some process of mechanical erosion. The shocks

Table 2
Characterization of Corrosion Products

Source / Characteristics	Collected from electrodes		Collected from supporting belts
	Large pieces	Small pieces	
Colour	rusty	rusty	rusty
Adherency	good	good	good
Moisture content at 100°C, [%]	4.88	4.96	4.72
Layer thickness, [mm]	0.1...0.3	0.2...0.3	0.2...0.3
Composition:			
Fe (total content)	61.63	61.65	61.92
SO_4^{2-} (total content)	4.84	5.36	5.047
Na (total content)	0.978	1.252	1.225
insoluble in HCl conc. cold	1.62	1.82	1.59
or as compounds:			
Fe_2O_3	86.40	85.79	87.08
Na_2SO_4	3.018	3.865	3.835
$Fe_2(SO_4)_3$	3.890	3.815	3.468

caused by the gases "snatch" portions from the attacked metallic parts which are carried off together other particles along the evacuation routes. These shocks cause additional mechanical strains.

Based on the advanced and verified corrosion mechanism and taking the different factors involved into account the following possibilities of anticorrosive protection of the electrodes and supporting belts of the pipe precipitator could be considered: the improvement of the conditions of the burning gas evacuation by remaining the leakinesses along the whole route till the pipe precipitator inlet; protective coatings with metallic films chemically/electrochemically obtained or with electroconductive polymers especially in the more active regions [5]. The first possibility depends on the operation conditions and on the physical state of the equipment while the second requires experimental investigations performed under the real operating conditions of the pipe precipitator.

3. Conclusions

1° The corrosion process proceeds by a predominantly electrochemical mechanism, with formation of rusty and iron sulphate.

2° The air excess confers an oxidizing character to the gases which would explain the formation of an adherent film of corrosion products.

3° The formation of sulphuric acid is due to the presence of sulphur dioxide and trioxide, water vapour as well as to the attainment of the acid condensation point at lower temperature.

Received, November 9, 1997

Technical University "Gh. Asachi", Jassy,
Department of Inorganic
Substances Technology

REFERENCES

1. Diaconescu V., Obrocea P., *Tehnologia celulozei şi hârtiei.* Vol.I, Ed. Tehnică, Bucureşti, 1974.
2. Bratu E., *Operaţii şi utilaje în industria chimică.* Ed. Tehnică, Bucureşti, 1963.
3. Comes A., Ivăşcan Şt., Apostolecu M., Revista de Chimie, Bucureşti, **46**, *8*, 773-777 (1995).
4. * * *, *Manualul inginerului chimist.* Vol. **II**, Ed. Tehnică, Bucureşti, 1951.
5. Simionescu Cr. *et al.*, Materiale plastice, Bucureşti, *3-4*, 87 (1991).

CONSIDERAŢII ASUPRA COROZIUNII ELECTROFILTRELOR

(Rezumat)

Electrofiltrele utilizate pentru purificarea gazelor rezultate de la arderea leşiei bisulfitice de la fabricarea celulozei suferă un proces rapid de degradare, atât de natură mecanică cât şi electrochimică. Se stabileşte un mecanism de coroziune, verificat cu ajutorul datelor furnizate de analizele chimice ale produşilor de coroziune şi ale gazelor de ardere, precum şi de condiţiile de curgere ale acestora.

BULETINUL INSTITUTULUI POLITEHNIC DIN IAŞI
Tomul XLIV (XLVIII), Fasc. 1-2, 1998
Secţia II
CHIMIE şi INGINERIE CHIMICĂ

D.C. 669.38

STUDIES ON COPPER DEPOSITION FROM ACID SOLUTIONS ON STEEL CYLINDERS

BY

FLORIN BANDRABUR, ŞT. IVĂŞCAN and N. APOSTOLESCU

It was investigated at laboratory, pilot and industrial scale, the possibilities of replacing the cyanure electrolytes by acid ones in the process of the copper deposition on steel. To prevent the copper cementing, a thin layer of nickel was firstly deposed using galvanic methods. The layers obtained from the acide electrolyte show a particulary good adherence, metallic marked gloss and low porosity.

1. Introduction

The copper shows a more electropositive potential than the hydrogen and much more electropositive than the iron. As a consequence the copper deposition on ferrous supports shows the following features: a) the copper cementation previous to the deposition; the layer of the cemented copper is slightly adherent and porous; b) in case of the copper damaging local galvanic piles are created by means of which the corrosion processes intensity (the copper acts as a cathode and the iron as an anode). The copper deposition is made as a substratum for final depositions of nickel, chrome, silver.

The principal categories of electrolytes used for the copper deposition are the following:

a) the cyanide electrolytes, characterized by a remarkable penetrating capacity and a minimum energy consumption; the obtained copper deposits show a fine structure, uniform thickness, good adherence;

b) the sulphatic electrolytes which show a high chemical stability, current yield closed to 100% being only slightly sensitive toward impurities; their disadvantages consist in a rather low penetrating capacity and a deposit of a raw structure;

c) the fluoboric electrolytes recommended for quick depositions performed at high current densities (1,000...2,000 A/m^2) and temperatures of 60°...70°C;

d) the fluosilicate electrolytes ($CuSiF_6$, 300...450 g/l) have a rather low costs in comparison to the fluoboric ones; they allow high current densities (600...1,000 A/m^2) at the room temperature;

e) the alkaline electrolytes based on solution pyrophosphate, disodic phosphate

and copper sulphate which assure the direct copperplating of the steel.

The aim of the present paper is the finding of the possibilities of replacing the cyanure electrolytes by acid electrolytes in the process of the copper deposition directly on steel large-sized cylinders.

The replacing of the cyanure electrolytes, which show a high dispersing capacity, is required by the difficulties arising in the technological process and the working of the waste water as well as by the high toxicity.

The acid electrolytes are advantageous due to their simple composition, the stability of applying rather high current densities. The toxicity is low and the waste water can be easier worked at the industries scale.

2. Theoretical Bases of Copper Deposition from Acid Electrolytes

Several acid electrolytes are mentioned in literature for copper deposition [1], [2].

The researches at the laboratory and industrial pilot scales were made by deposing the copper directly from acide solutions of copper sulphate on large steel cylinders.

The fact is know that from the copper sulphate electrolytes the copper separates on the ferrous materials by cementing due to the high Cu^{2+} concentration to the Cu^{+} one. The electrolytic copper deposition is possible only when a first copper layer has been deposited from an alkaline bath. The copper sulphate (200...300 g/l) and the sulphuric acid (introduced for both conductivity increasing and preventing the cuprous sulphate from hydrolysis) are the principal components of the electrolyte:

$$CuSO_4 + H_2O = Cu_2O + H_2SO_4$$

Some additions of dextrine, gelatine, naphtalin disulphonic and thioureea (0.03... 0.05 g/l) can improve the penetrating strength and determine the obtaining of glossy depositions.

The equation characteristic of the electrochemical deposition of copper from acid solutions with copper soluble anodes is the following:

$$[CuSO_4 + H_2SO_4 + H_2O + A_1'']_1 + [Cu]_s + [K] \rightarrow [K + Cu]_s + [Cu]_s + [CuSO_4 + H_2SO_4 + H_2O + A_1'']_1$$

The principal electrode processes on the anode surface are:

$$Cu \longrightarrow Cu^{2+} + 2e^-, \quad \varepsilon^0 = 0.337 \text{ V};$$
$$Cu \longrightarrow Cu^{+} + 1e^-, \quad \varepsilon^0 = 0.521 \text{ V};$$
$$Cu^{+} \longrightarrow Cu^{2+} + 1e^-, \quad \varepsilon^0 = 0.153 \text{ V}.$$

At the standard temperature the equilibrium constant of the reaction:

$$Cu + Cu^{2+} \longrightarrow 2Cu^{+}$$

has a low value:

$$K = \frac{(C_{Cu^+})^2}{C_{Cu^{2+}}} = 0.5 \times 10^{-4}.$$

This indicates the Cu^{2+} ion formation to prevail by the dissolution of the copper soluble anode.

The cathodic process consists in the Cu^{2+} discharge on the steel support:

$$Cu^{2+} + 2e^- \longrightarrow Cu.$$

As regards the structure, the cathodic process of electrocrystallization is of the type of adsorption – reaction – formation and growth of germs in solid phase [3],...,[5]. The following macroscopic processes are the components of the electrode overall process:

a) the transfer of the Cu^{2+} ions from the electrolyte volume to the cathode surface;

b) the adsorption of the Cu^{2+} ions on the cathode surface;

c) the electrochemical reaction (charge transfer);

d) the crystallochemical reaction (formation and growth of the copper germs on the steel cathode).

By assuming the charge transfer as a limiting stage for the overall cathode process the current cathodic density (i_C) and the cathode cinetical potential (ε_C) can be correlated by the equation:

$$\ln i_C = \ln K_0 + \ln C_{Cu^{2+}} - \frac{\alpha F}{RT}\varepsilon_C.$$

3. Experimental

The copper deposition on a steel support was investigated at the laboratory scale by using an acid electrolyte containing $CuSO_4 \cdot 5H_2O$ (220 g/l), H_2SO_4, $d = 1.884$ g/l, (60 g/l) and additives (wetting agents, glass agents).

Since the copper layer deposited directly on the steel is not adherent, a thin layer of nickel is firstly deposed followed by the deposition of the copper layer (Fig. 1).

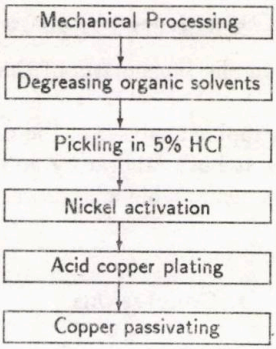

Fig. 1.– Simplified block diagram of the process.

The composition of the activation bath and the parameters of the deposition process of the nic'... layer on the steel support are given in Table 1.

Table 1

Composition and Parameters of the Activation Bath

Component	Concentration g/l	Temperature °C	Current density A/dm^2	Deposition time min.
Nickel chloride	180	55	0.5...1	1...3
Nickel sulphate	20			

Buffer substances and surface-active agents were also added in the activation bath.

The runs on the pilot and industrial scales were made on steel cathodes (cylinders of areas of 0.55 m^2) in electrolysis pans (electrolyte volume = 0.6 m^3) provided with systems of electrolyte stirring by air bubbling. The experimental data were processed statistically (Fig. 2) and an equation for calculating the thickness of the copper layer (d) as a function of the deposition time (τ) developed:

$$d = 0.7558\tau + 0.0532.$$

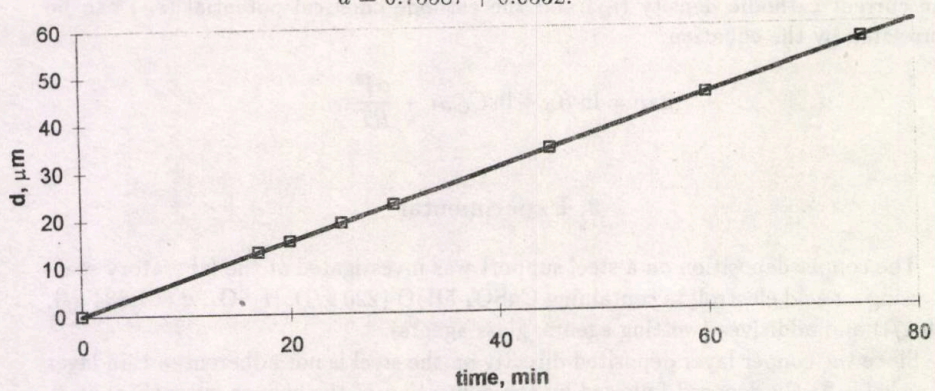

Fig. 2.– The thickness of the copper layer vs. time.

For the copper depositions on the inner parts of the cylindrical cathodes additional anodes were used.

The bulletins of the metallographic analyses of the depositions performed under the above mentioned conditions at both laboratory and industrial scales indicated that the copper layers showed a remarkable adherence, marked metallic gloss and low porosity.

4. Conclusions

The process of copper deposition from copper sulphate electrolytes on the surface of large-sized cylinders was investigated at the laboratory, pilot and industrial scales.

In order to prevent from the cementation process the copper depositions were made on an intermediary nickel layer.

The layers obtained from the acide electrolyte show a particularly good adherence, metallic marked gloss and low porosity.

Notations

K_0 – constant including the standard kinetic parameters;
α – symmetry factor;
F – Faraday constant;
R – universal gas constant;
T – temperature, [K].

Received, November 12, 1996

Technical University "Gh.Asachi", Jassy,
Department of Inorganic
Substances Technology

REFERENCES

1. Lainer V., Kudriavţev N., *Bazele galvanostegiei* (transl. from Russian). Vol.1, Ed. Tehnică, Bucureşti, 1956.
2. Oniciu L., Grünwald E., *Galvanotehnica.* Ed. Ştiinţ. şi Encicl., Bucureşti, 1980.
3. Calistru C., Leonte C., *Tehnologia substanţelor anorganice.* Ed. Did. şi Pedag., Bucureşti, 1972.
4. Bandrabur Fl., Szép Al., *Tehnologii electrochimice.* Univ. Tehn. „Gh.Asachi", Iaşi, 1992.
5. Ivăşcan Şt., Bandrabur Fl., Apostolescu M., Rev. Construcţia de maşini, **XL**, *3*, 153-156 (1988).

CERCETĂRI PRIVIND DEPUNEREA CUPRULUI DIN SOLUŢII ACIDE, PE CILINDRI DIN OŢEL

(Rezumat)

S-au cercetat, la scară de laborator, la nivel de pilot şi la scară industrială, posibilităţile de înlocuire a electroliţilor cianurici cu electroliţi acizi în procesul de depunere galvanică a cuprului pe cilindri de dimensiuni mari, confecţionaţi din oţel.

Pentru a preveni procesul de separare a cuprului prin cementare, depunerile electrolitice s-au realizat pe un strat superficial de nichel depus pe cale galvanică.

Depunerile galvanice de cupru obţinute din electrolitul acid prezintă o aderenţă deosebită, un luciu metalic pronunţat şi o porozitate redusă.

BULETINUL INSTITUTULUI POLITEHNIC DIN IAŞI
Tomul XLIV (XLVIII), Fasc. 1-2, 1998
Secţia II
CHIMIE şi INGINERIE CHIMICĂ

D.C. 667.212; 628.54; 661.183.28

REMOVAL THE TRIPHENYLMETHANIC DYES FROM WASTE WATERS USING ION EXCHANGERS (I)

BY

DANIELA ŞUTEU and AL. NACU

To establish the proper conditions to removal the triphenyl metanic Methyl Violet dye on cation exchange Purolite C-100, the following parameters: pH of solution, temperature, contact time and initial dye concentration were studied.

In accordance with Langmuir and Freundlich isotherms the sorption process was favourable.

1. Introduction

The presence of textile dyes in the waste water effluents of dyehouse operations is a growing environmental concern [1]. Dificulties arise in effectively and economically treating these effluents because they can contain a great variety of dyes and high concentrations of co-solutes, such as inorganic salts, sizing agents typity the adverse conditions posed.

For decontamination of waste waters impurified with dyes was proposed some traditionals methods such as: precipitation of the dyes with metallic salts [2], ion exchange [3],...,[6], sorption on different natural [4], [7],...,[10] or synthetic [11], [12] sorbents, coagulation, membrane filtration, aerobic biological treatment.

Because none of the traditional waste water-treatment methods are effective in decolorizing these effluents in a satisfactorily cost-effective, environmentally - sound manner it were studied the combined methods such as: ion-exchange - physical sorption or D o n n a n distribution on different supports [4], [12], [13].

The aim of this work is optim retention conditions establishment for triphenylmethanic dyes presents in waste waters by sorption on ionic resins from copolymers styrene divinylbenzene type.

2. Experimental

The sorption experiments of triphenylmethanic Methyl Violet dye

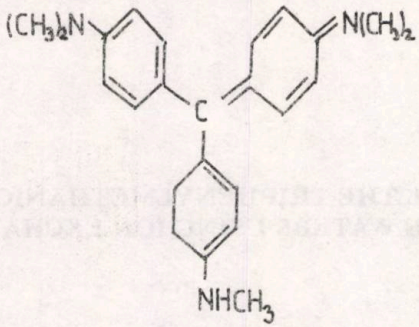

have been accomplished with using a stock aqueos solution 1.4×10^{-2} M from wich working solutions with $(1.4 \times 10^{-5} ... 5.6 \times 10^{-4})$ M concentrations were prepared.

Dye concentration was determined by spectrophotometric method using a Carl Zeis Jena model UV-Viz. spectrophotometer, at a wavelenght $\lambda_{max} = 580$ nm.

Strong acid cationite (Na^+ form): purolite C-100 have been resed as ion exchangers. This resin is styrene divinylbenzene copolymers, gel structure and ionic exchange capacity of 1.9 mechiv/ml.

The study of Methyl Violet dye retention has been carried out in static conditions, using samples of about 0.1 g cationite and 50 ml solution containing determined amounts of dye.

After a certain contact time this phases were separated by filtration and the unretained amount of dye was determined in solution by a spectrophotometric method.

3. Results and Discussion

Experimental data about sorption of triphenylmethanic dye from aqueous solutions on cation exchanger, the effect of pH of solution, temperature, contact time and initial concentration of dye have been studied.

The amount of Methyl Violet dye retained on cationit increases with contact time, reaching a maximum constant value after 48 hrs (Fig. 1). This time is necessary for diffusion of dye molecules into the functional groups from internal structure.

The results represented in Fig. 2 show greats values of retention of dye at acid pH (pH = 4...6.5 – Fig. 2), because the active form as Methyl Violet pH indicator was in acid solution, that is why a strong retention in this domain was possible.

The temperature of a solution affects the rate of diffusion of the adsorbate molecules through the solution to the adsorbent. The amount of dye retained increases with temperature (Fig. 3) and initial dye concentration.

The influences of temperature and initial dye concentration was represented using sorption isotherms at differents temperatures (Fig. 3).

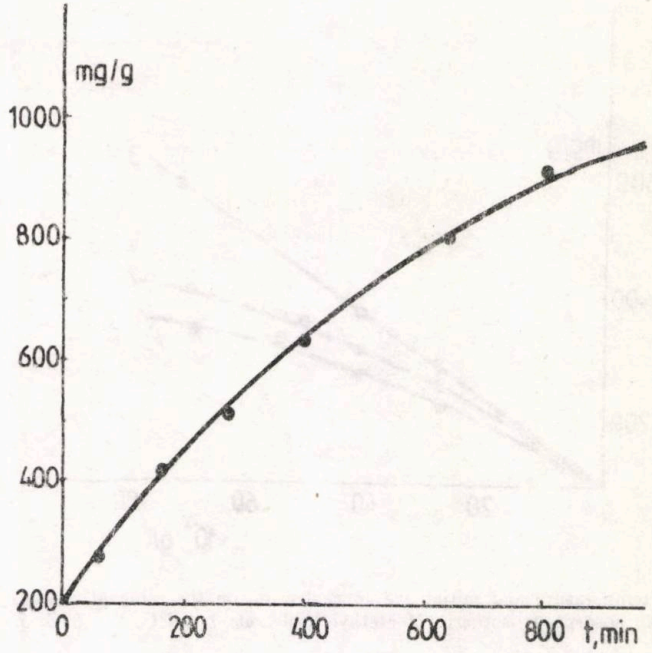

Fig. 1.– Effect of contact time on the removal of Methyl Violet on Purolite C-100; dye concentration: 0.025 g/L.

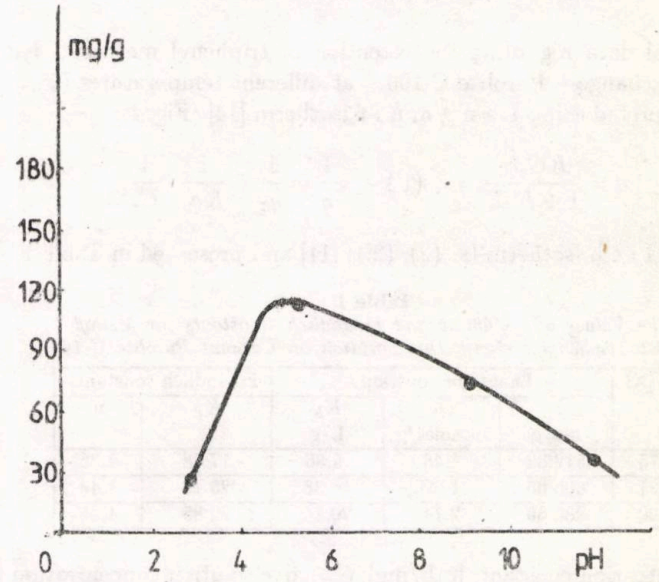

Fig. 2.– Effect of pH on the removal of Methyl Violet on Purolite C-100; dye concentration: 0.025 g/L.

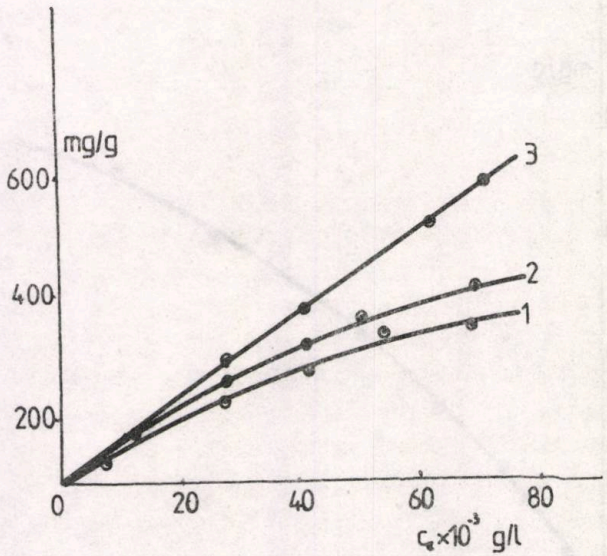

Fig. 3.– Effect of temperature and initial dye concentration on the removal of Methyl Violet on Purolite C-100; adsorption isotherm of Methyl Violet at: *1* – 2°C; *2* – 8°C; *3* – 17°C.

4. Sorption Isotherm

Experimental data regarding the retention of triphenyl methanic dye Methyl Violet on ion exchange – Purolite C-100 – at different temperatures (2°, 8°, 17°C) have been interpreted using L a n g m u i r isotherm [14] (Fig. 4):

$$(1) \qquad q = \frac{KC_e q_0}{1 + KC_e}, \quad \cdot \quad (1') \qquad \frac{1}{q} = \frac{1}{q_0} + \frac{1}{Kq_0} \cdot \frac{1}{C_e},$$

and F r e u n d l i c h isotherm (s. (2), (2′)) [11] and presented in Table 1.

Table 1

The Values of Langmuir and Freundlich Constants for Methyl Violet Triphenyl Metanic Dye Sorption on Cationit Purolite C-100

T, [K]	Langmuir constants			Freundlich constants	
	q_0 mg/g	Q_0 mmoles/g	K_L L/g	K_F	n
275	512.82	1.43	5.36	17.78	1.36
281	606.06	1.69	16.38	25.12	1.43
290	980.39	2.74	20.24	29.85	1.45

Here K is retention constant, [mL/mg]; C_e – dye solution concentration at equilibrium, [mg/mL]; q – retained dye amount, [mg/g]; q_0 – maximum sorption capacity, [mg/g]; (1′) represents the liniarized form of L a n g m u i r isotherm.

For ion exchange studied the plots $1/q$ versus $1/C_e$ (Fig. 4) at different temperatures allow calculation size of constant sorption K and maximum sorption capacity; the obtained results are given in Table 1.

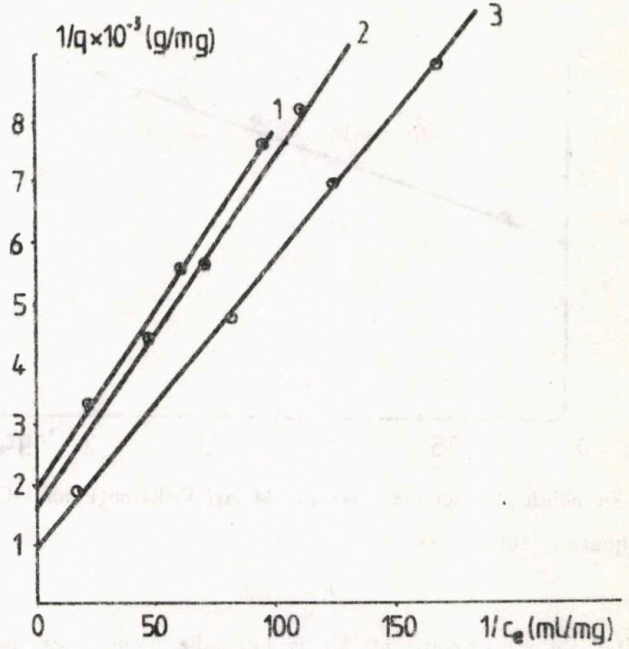

Fig. 4.– Langmuir plots in coordinates $1/q$ vs. $1/C_e$ for the removal of Methyl Violet on Puroline C-100 at: *1* – 2°C; *2* – 8°C; *3* – 17°C.

The F r e u n d l i c h equation has the general form [11]:

$$q_e = K_F C_e^{1/n}, \tag{2}$$

where: K_F and $1/n$ are characteristic constants; q_e – retention dye amount, [mg/g]; C_e – dye solution concentration at equilibrium, [mg/L].

In logarithmic form equation (2) becomes

$$\log q_e = \log K_F + \frac{1}{n} \log C_e, \tag{2'}$$

which is a straight line.

Fig. 5 shows typical F r e u n d l i c h plots for the dye studied and the Table 1 lists the F r e u n d l i c h constants K_F and n for this dye using various temperatures.

K_F was taken as a relative indicator of adsorption capacity, while $1/n$ is an indicative of the energy or intensity of the reaction. The magnitude of the exponent n gives an indication of the favourable character and capacity of the adsorbent/adsorbate system.

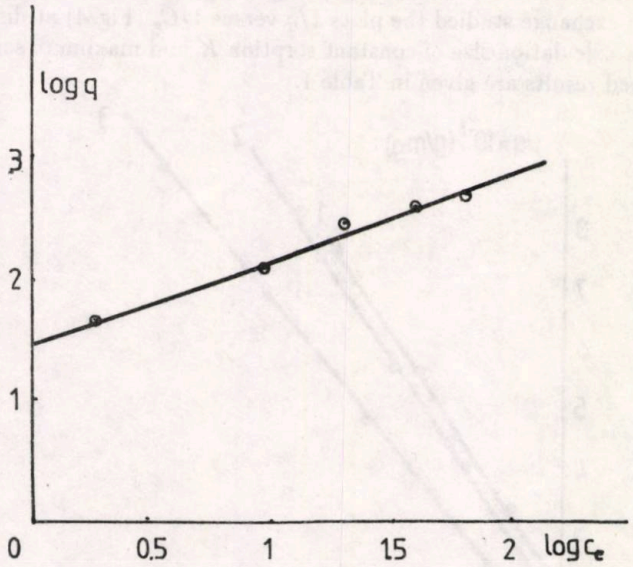

Fig. 5.– Freundlich plots for the removal of Methyl Violet on Purolite C-100 at 17°C.

With equation [14]:

$$K_L = q_0 b, \tag{3}$$

the size of L a n g m u i r constant, K_L, was calculated and it was used to determine thermodynamic parameters, were b is retention constant, [L/mg]; $b = 10^{-3}K$.

Table 1 shows that both the L a n g m u i r constants, F r e u n d l i c h constants and maximum sorbtion capacity (q_0) increase with temperature. The calculated values of q_0, [mg/g], are higher that theoretical capacity of ion exchange studied. This fact can be explained by the surfaces physical adsorption which occur simultaneously with the ion exchange process.

Values of $n > 1$ represent favourable sorption conditions according to the existent theories.

5. Conclusions

The factors affecting triphenyl metanic dye removal from aqueous solutions have been studied on Purolite C-100 using a static process.

For Methyl Violet dye, ion exchange Puroline C-100 is an excelent sorbent; the retention can be explained by an ion exchange process completed by a surface physical adsorption of the dye on the substate.

The L a n g m u i r and F r e u n d l i c h isotherms were shown to be favourable.

Received, June 8, 1997

Technical University "Gh.Asachi", Jassy,
Department of Analytical Chemistry

REFERENCES

1. P i e r c e J., J. Soc. Dyers Colour, **110**, 131 (1994).
2. M i a o l i n H o u, Dyes and Pigments, **18**, *35* (1992).
3. I g n a t o v Iu.I., Zhur. Fiz. Khim. **54**, *2*, 406 (1980).
4. L a s z l o J.A., S i m k o v i c h I., *Ion Exchange Developments and Applications*. Ed. by J.A. G r e i g, The Royal Society of Chemistry, Cambridge, 1996, 128.
5. C o o p e r P., J. Soc. Dyers Colour., **109**, *97* (1993).
6. R e i f e A., *Enciclopedia of Chemical Technology*. Fourth Edition, M. Howe-Grant, ed. John Wiley and Sons, New York, vol.**8**, 1993, 753.
7. S h u l e r M.L., *Utilization and Recycle of Agricultural Wasters and Residues*. CRC Press, Boca Raton, 1980, 23.
8. S h u k l a S.R., S a k h a r d a n t e V.D., Dyes and Pigments, **17**, 11 (1991).
9. N a m a s i v a y a m S., K a n c h a n a N., Chemosphere, **25**, 1691 (1992).
10. Mc K a y G., Chem. Eng. Res. Des., **61**, 29 (1983).
11. H w a n g M.C., C h e n K.M., J. Appl. Polym. Sci., **50**, 735 (1993).
12. Ş u t e u D., B î l b ă D., C r i s t i a n Gh., Cell. Chem. and Tech. (in press).
13. M u z z a r e l l i R.A.A., Adv. Chromatogr., **5**, 127 (1968).
14. Mc K a y G., B l a i r H.S., F e n d o n A., Indian J. Chem., **28A**, 356 (1989).

RECUPERAREA COLORANŢILOR TRIFENILMETANICI DIN APE REZIDUALE FOLOSIND SCHIMBĂTORI DE IONI

(Rezumat)

Au fost studiaţi parametrii de sorpţie (pH-ul soluţiei, temperatura, timpul de contact, concentraţia iniţială a colorantului în soluţie) pentru a stabili condiţiile optime de utilizare a schimbătorului de ioni Purolite C-100 la decontaminarea apelor reziduale impurificate cu coloranţi trifenilmetanici.

Procesul de sorpţie a fost apreciat favorabil cu ajutorul izotermelor Langmuir şi Freundlich precum şi al mărimilor caracteristice.

BULETINUL INSTITUTULUI POLITEHNIC DIN IAŞI
Tomul XLIV (XLVIII), Fasc. 1–2, 1998
Secţia II
CHIMIE şi INGINERIE CHIMICĂ

D.C. 541.141; 547.562.1; 621.384.2

PHOTODEGRADATION OF BISPHENOL-A IN WATER BY ULTRAVIOLET-ACTIVATED HYDROGEN PEROXIDE

BY

I. SIMINICEANU and *MARIANA NEAMŢU

Aqueous solutions of 0.52 mmol L^{-1} bisphenol-A (BPA) have been irradiated in a batch laboratory-scale photoreactor with UV-254 nm light and different doses of hydrogen peroxide added into the reaction mixture. The BPA concentration have been followed with time by a high performance liquid chromatograph (HPLC) equipped with a Diode Array Detector (DAD). After 20 min. of irradiation, the conversion of BPA was only 16.54% with no hydrogen peroxide but 98.13% with 0.4907 mmol L^{-1} H_2O_2 added. These results have shown the synergetic effects of H_2O_2 plus UV light on the degradation of BPA in water. Using a simple kinetic model, the apparent first-order constant has been derived from the experimental curves, at 298 K. The values of this constant ranged from 0.17×10^{-3} s^{-1} for UV with no H_2O_2 to 3.5×10^{-3} s^{-1} for UV with 0.4907 mmol L^{-1} hydrogen peroxide.

1. Introduction

Recent reports have suggested that background levels of industrial chemicals and other environmental pollutants may play a role in development of breast cancer at women and decreased male reproductive success. These suggestions have been supported by articles which have described the perils of exposure to endocrine-disrupting chemicals such as estrogenic organochlorine pesticides. Other industrial chemicals or intermediates that have been identified as estrogenic compounds include bisphenol-A [1].

Bisphenol-A (BPA) is a chemical produced in rather large quantities, used in the manufacture of polycarbonate-derived products, phenol red, and alkyl phenols and their derivatives which are extensively used for preparation of polyetoxylates in detergents. The main physical, chemical and toxicological properties of BPA are listed in Table 1.

The data in Table 1 show that BPA is contaminant for aquatic ecosystem having a solubility in water grater than its EC_{50}. On the other hand, the data on the biodegradability in natural waters of BPA are not concordant: D o r n *et al.* consider that BPA can be biodegradated in aquatic environment in days instead of years as suggested by EPA [2]. This ambiguity regarding the biodegradability of BPA on one hand, and their estrogenic and photoallergenic effects on the other hand, have

determined us to investigate the ways of destruction and/or removal of BPA from water. What method is the most suitable for BPA removal from water, taking into account that it can be present in a maximum concentration of 120 mg L^{-1}?

Recent developments in the field of chemical water treatment have led to an improvement in oxidative degradation procedures for organic compounds dissolved or dispersed in aquatic media in applying catalytic and photochemical methods. They are generally reffered to as *advanced oxidation processes* [3]. These processes rely on the generation of very reactive free radicals, such as hydroxyl radicals ($HO^{\cdot}$), to be considered as initiators of oxidative degradation. The H_2O_2/UV, O_3/UV, and $H_2O_2/O_3/UV$ procedures employ UV photolysis of H_2O_2 and/or O_3 in order to generate $HO^{\cdot}$ radicals. Among these procedures, the oxidation by hydrogen peroxide activated by UV radiation (H_2O_2/UV) brings a number of advantages in comparison to others: commercial availability of the oxidant, thermal stability and storage on-site, infinite solubility in water, no mass transfer problems associated with gases (O_3), high quantum yeald in $OH^{\cdot}$ radicals, minimal capital investment, and relatively simple operation procedure [3].

Table 1
Physical, Chemical and Toxicological Properties of BPA

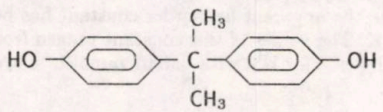

Chemical structure

Name: 2,2′-Bis(*p*-hydroxyphenyl)/propane/Bisphenol-A	
Molecular weight	228.27 g mol^{-1}
Solubility in water at 298 K	120.00 mg L^{-1}
Solubility in ethanol at 293 K	60.6%
Melting point	330.4 K
Freezing point	116.6 K
Heat of formation	−7,809.07 J mol^{-1}
Aquatic toxicity/EC/LC_{50}	
Algae (*Selanastrum capricornutum*)	2.7...3.1 mg L^{-1}
Invertebrates (*Daphnia magna*)	10.2...15.5 mg L^{-1}
Fish (*Pimephales promelas*)	4.6...4.7 mg L^{-1}
Log octanol-water partition (K_{OW})	2.2...3.84

The aim of this study was to investigate the photodegradation of BPA in water system by UV-activated oxidation with H_2O_2. The experimental curves concentration vs. time obtained are kinetically interpreted and the kinetic constants derived. These kinetic data can be used for the commercial-scale photoreactor design.

2. Experimental

a) *Materials.* The aqueous BPA solutions of 0.52 mmol L^{-1} have been prepared with double distilled deionised water (conductivity 0.056 μS) and BPA purchased

from Fluka AG and stirred at 298 K for 48 hrs. Then, hydrogen peroxide of 30% H_2O_2 from Merck has been added at three level: 25, 37.5 and 59 mL per litter of solution. These correspond to the molar concentration of 245.338; 368.0 and 490.673 μmol H_2O_2 L^{-1}, respectively.

b) *Photolysis Procedure.* The aqueous solutions prepared as above were irradiated with an UV low pressure mercury lamp Heraeus/Hanau whose spectrum is rich in 254 nm line, immersed in a batch photoreactor. The experimental equipment has been presented in a previous paper [5].

c) *Analytical Method.* The concentration of BPA during irradiation has been measured by a high performance liquid chromatograph (HPLC) equipped with a Diode Array Detector (DAD). The analytical method has been minutely described in a previous paper, devoted to the nitromusks degradation [6].

3. Results and Discussion

The concentration of BPA have been followed in time at 298 K and pH = 7.0 for four different initial concentrations of H_2O_2: 0.0; 0.2453; 0.3680 and 0.4907 mmol L^{-1}. The obtained kinetic curves C_{BPA} vs. time are presented in Fig. 1.

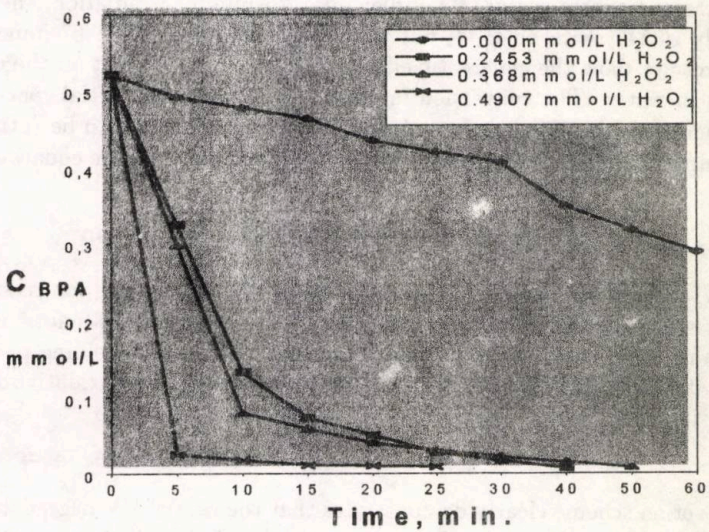

Fig. 1.– The experimental kinetic curves C_{BPA} vs. time at 298 K.

By defining the fraction conversion of BPA:

$$\eta = \frac{C^0_{BPA} - C_{BPA}}{C^0_{BPA}},$$

the kinetic curves conversion vs. time from Fig. 2 have been generated.

It is noteworthy that, when exposed to UV light with no H_2O_2 present, a small conversion was observed. In the presence of both H_2O_2 and UV light the conversion

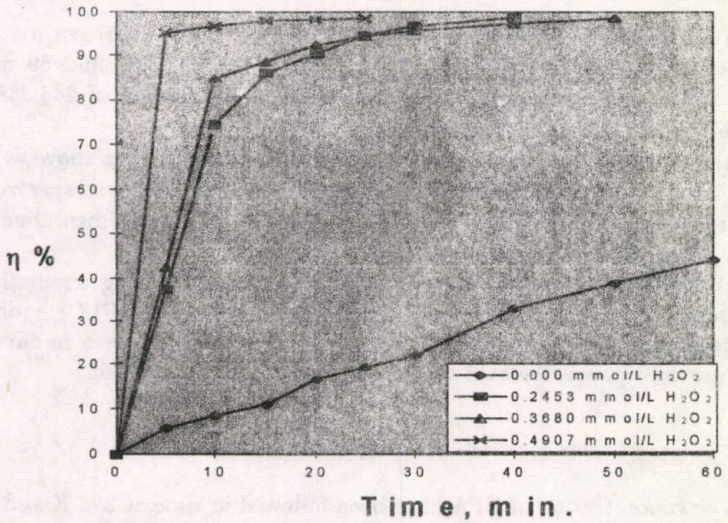

Fig. 2.– The experimental curves conversion vs. time at 298 K.

was increased substantially. Example: after 20 min. of irradiation, the conversion was only 16.54% with no H_2O_2 but as high as 98.13% with 0.4907 mmol L^{-1} H_2O_2. These results show the synergetic effects of H_2O_2 plus UV light on the degradation of BPA in water. The conversion increased with increasing initial concentration of hydrogen peroxide. Nevertheless, these laboratory-scale data can be extrapolated to the commercial-scale photoreactor only on the basis of a kinetic equation.

4. The Kinetic Constant Determination

a) *The UV Process.* In the absence of H_2O_2, the photooxidation reactions of the organic substrate (RX) imply in most cases a homolysis (Eq.(1)) to form radicals ($R^{\cdot}$) which then react with molecular oxygen dissolved in water yielding peroxyradicals ($RO_2^{\cdot}$). These intermediates initiate thermal-chain reactions of oxidative degradation, leading finally to carbon dioxide, water, and inorganic salts [3]:

(1) $\mathrm{RX} + h\nu = \mathrm{R}^{\cdot} + \mathrm{X}^{\cdot}$ (2) $\mathrm{R}^{\cdot} + \mathrm{O}_2 = \mathrm{RO}_2^{\cdot} \rightarrow \rightarrow$

This reaction scheme clearly demonstrates that the rate of UV degradation process, primary based on the production and reactivity of radical intermediates, depends on the energy needed in order to homolyse a given chemical bond as well on the concentration of dissolved molecular oxygen. Formally, the global degradation rate of the substrate (RX or A, for convenience) can be considered of pseudo-first order:

(3) $$\frac{\mathrm{d}C_\mathrm{A}}{\mathrm{d}\tau} = k_{ap} C_\mathrm{A}.$$

b) *The UV/H_2O_2 Process.* The chemistry of hydrogen peroxide UV reactions involves generation of peroxyl radicals ($HO^{\cdot}$) by the photochemical action UV light

on H_2O_2. The most commonly accepted mechanism for the photolysis of H_2O_2 is the cleavage of the molecule into hydroxyl radicals with a quantum yield of two $HO^{\cdot}$ formed per quantum of radiation absorbed:

$$H_2O_2 + 2h\nu = 2HO^{\cdot} \quad (4)$$

The hydroxyl radicals attack the organic species (RX or A) by abstracting a hydrogen atom or by electrophilic addition to the double bonds of unsaturated molecules:

$$A + HO. = \text{products} \quad (5)$$

In the same time, the hydroxyl radicals can decompose hydrogen peroxide in excess, producing hydroperoxyl radicals ($HO_2^{\cdot}$):

$$HO^{\cdot} + H_2O_2 = H_2O + HO_2^{\cdot} \quad (6)$$

The radicals $HO_2^{\cdot}$ are much less reactive that $HO^{\cdot}$ and do not contribute to the oxidative degradation of organic substances. On the other hand, hydrogen peroxide is known to decompose by a dismutation reaction (Eq.(7)) with a maximum rate at the pH of its pK value [3]:

$$HO_2^{\cdot} + H_2O_2 = H_2O + O_2 + HO^{\cdot} \quad (7)$$

By adding the equations (6) and (7) it results:

$$2H_2O_2 = 2H_2O + O_2 \quad (8)$$

In this way it has been demonstrated that reaction (6) is undesirable, wasting energy (UV) as well as oxidant (H_2O_2). Therefore, the pH of the system must be controlled and the local excess of H_2O_2 avoided. In natural and waste waters practically all solutes compete for the $HO^{\cdot}$ radicals, including bicarbonate ion which can be present at concentrations of several $mmol^{-1}\ L^{-1}$:

$$HO^{\cdot} + HCO_3^- = H_2O + CO_3^{\cdot -} \quad (9)$$

The HCO_3^- ions are powerful scavengers for $HO^{\cdot}$ radicals, the second-order rate constant of the reaction (9) being of about 1.1×10^7 L mol^{-1} s^{-1} [4],[5].

Assuming that the degradation of A is only due to the direct reaction between A and $HO^{\cdot}$ radicals, the rate of the UV/H_2O_2 degradation process may be expressed by the equation:

$$-\frac{dC_A}{d\tau} = k_A C_A C_{HO^{\cdot}}, \quad (10)$$

where k_A is the absolute second-order rate constant.

The concentration of hydroxyl radicals can be derived from a material balance of $HO^{\cdot}$: the rate of $HO^{\cdot}$ generation in the reaction (4) equals the rate of $HO^{\cdot}$ consumption in the reactions (5), (6) and (9). For a steady-state operation, the $HO^{\cdot}$

concentration may be considered constant and the equation (10) becomes of the form (3).

The obtained data for both UV and UV/H_2O_2 processes (Fig. 2) may be correlated in such a way through the same simple equation (3). Using the integral method, this becomes:

$$-\int_{C_A^0}^{C_A} \frac{dC_A}{C_A} = k_{ap} \int_0^{\tau} d\tau. \tag{11}$$

On the basis of the equation (11), the four straight lines in Fig. 3 have been drawn by linear regression using the experimental data.

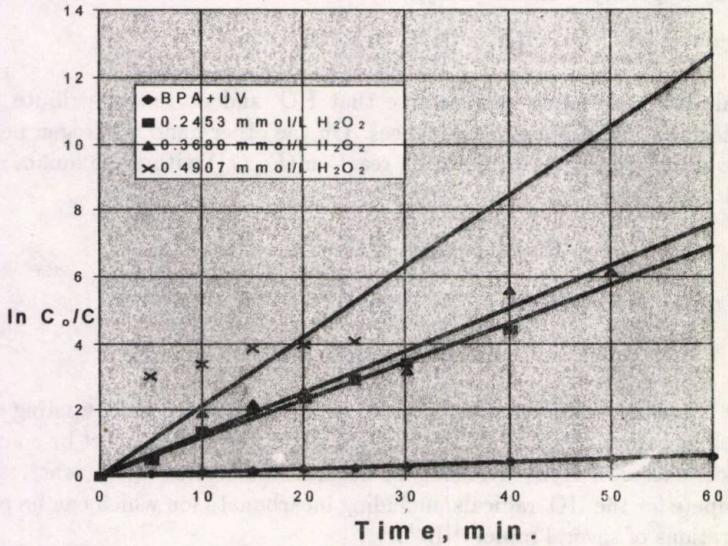

Fig. 3.– The apparent first-order rate constant determined by the integral method.

The pseudo-first order rate constants obtained from the slopes of the linear regions of these plots are listed in Table 2.

Table 2

Apparent First-order Rate Constants for the BPA Photodegradation at 298 K

$C^0_{H_2O_2}/C^0_{BPA}$	0.000	0.4718	0.7077	0.9436
$k_{ap} \times 10^3$, [s^{-1}]	0.170	1.920	2.100	3.510
k_{ap}/k_{UV}	1.000	11.294	12.352	20.647

The first-order rate constant in the presence of hydrogen peroxide at an initial molar ratio H_2O_2/BPA of 0.9436 is over twenty times grater than that with no H_2O_2. From a chemical reaction engineering point of view this means that the volume of the photoreactor for the same flow rate of water treated will be over twenty times smaller. This result has a great practical significance.

5. Conclusions

The bisfenol-A has been recently identified as environmental pollutant with estrogenic and photoallergenic effects. In order to apply oxidative treatment to improve the quality of drinking water, investigations have been made concerning the degradation rates of BPA with UV radiation as well as with UV-activated hydrogen peroxide oxidation. The results presented in this paper show the advantage of the UV/H_2O_2 process. The first order rate constant in the presence of hydrogen peroxide at an initial molar ratio $H_2O_2/BPA = 0.9436$ was over twenty times greater than that with no H_2O_2. The laboratory-scale kinetic data obtained can be extrapolated to commercial-scale photoreactor for water treatment.

Notations

A – organic substrate of the general formula RX;
BPA – bisphenol-A;
C_A – molar concentration of A, [mmol L^{-1}];
k_{ap} – apparent first-order rate constant, [s^{-1}];
k_A – absolute second-order rate constant, [L mol s^{-1}];
η_A – fractional conversion of A;
τ – irradiation/retention time, [s].

A c k n o w l e d g e m e n t s. This research, performed in the IOC laboratories directed by Professor A. K e t t r u p, has been financially supported by a grant from the German Academic Exchange Service – DAAD.

Received, February 3, 1997

Technical University "Gh.Asachi", Jassy,
Department of Inorganic
Substances Technology
and
**State University of Moldova,*
Kishinew

REFERENCES

1. S a f e H.S., Environmental Health Perspective, **103**, *4*, 347 (1995).
2. D o r n B.P., C h o u C.S., G e n t e m p o J.J., Chemosphere, **16**, *7*, 1501 (1987).
3. L e g r i n i O., O l i v e r o s E., B r a u n A.M., Chem. Rev., **93**, 671 (1993).
4. S c h e c k K.C., F r i m m e l H.F., Wat. Res., **29**, *10*, 2346 (1995).
5. N e a m ţ u M., S i m i n i c e a n u I., An. Şt. Univ. „Al.I. Cuza", Iaşi, **4**, s. Chim., 177 (1996).
6. N e a m ţ u M., S i m i n i c e a n u I., Chem. Rev., Bucharest, **48** (1997) (in print).

FOTODEGRADAREA BISFENOLULUI-A DIN APĂ CU PEROXID DE HIDROGEN ACTIVAT CU RADIAŢII ULTRAVIOLETE

(Rezumat)

Soluţii apoase cu 0.52 mmol/L bisfenol-A au fost iradiate într-un fotoreactor discontinuu cu agitare folosind UV-254 nm şi diferite doze de apă oxigenată. S-a determinat variaţia concentraţiei bisfenolului în timp prin metoda cromatografică HPLC-DAD. Rezultatele obţinute pun în evidenţă efectul sinergetic al peroxidului de hidrogen şi al radiaţiilor UV asupra degradării bisfenolului din apă. Constanta vitezei de degradare este de peste 20 ori mai mare cu UV şi 0,4907 mmol/L peroxid de hidrogen decât numai cu UV.

BULETINUL INSTITUTULUI POLITEHNIC DIN IAŞI
Tomul XLIV (XLVIII), Fasc. 1–2, 1998
Secţia II
CHIMIE şi INGINERIE CHIMICĂ

D.C. 66.069; 576.153

LIQUID–LIQUID EXTRACTION OF BIOSYNTHESIS PRODUCTS DIRECTLY FROM FERMENTATION BROTHS
I. MASS TRANSFER TO DROPS

BY

DAN CAŞCAVAL, CORNELIU ONISCU, LILIANA MARIN and VLAD ROŞCA

The extraction of butanol from simulated fermentation broths is studied. For this purpose the influence of drop diameter on its terminal velocity and on the mass transfer coefficients for different aqueous solution viscosities was settled.

1. Introduction

Many biosynthesis processes are inhibited by product formation, especially the batch system in which the final extracellular product concentration is high. The productivity of these fermentation processes can be significantly increased by recovery *in situ* the biosynthesis product from the cultivation medium during its formation.

Generally, two techniques can be used for the direct separation from the fermentation broths: a) the first utilises an extern separator and the fermentation broths are recirculated to the bioreactor; b) direct product extraction from the broth inside the bioreactor (*in situ* extraction).

The methods applied on direct separation are: adsorption, distillation, precipitation, reverse osmosis, electrophoresis, liquid–liquid extraction. The extraction of extracellular products directly from fermentation medium has been used at pilot plant for alcohols, carboxylic acids and some antibiotics separation, taking into account the compatibility between the microorganisms and the solvent, respectively [1]: a) the solvent toxicity; b) high values of the distribution coefficient of the solute between solvent and fermentation liquid; c) the formation of reduced stability emulsions; d) the easy recovery of the solvent after the extraction.

Moreover, an important factor is the fermentation broth characteristics, especially

the rheological behaviour which significantly influences the mass transfer process rate.

In situ extraction presents certain advantages in comparison with extraction in a distinct equipment [2], namely: a) in the second case, the product losses can be considerable; b) if the cellular mass is filtered before the extraction, the product concentration in liquid are reduced by washing the precipitate on the filter; c) *in situ* extraction avoids the product inhibition; d) the extraction inside the bioreactor simplifies the biotechnological flux.

However, a major problem in direct extraction is the choice and design of the adequate extraction equipment, because it is necessary to obtain high mass transfer area by dispersing the solvent inside the fermentation broth which has a pseudoplastic behaviour and high viscosities, taking into account the shear fields influence on the microorganisms.

The production of acetone and butanol by *Clostridium acetobutylicum* is impaired by butanol inhibition (acetone inhibition can be neglected comparative to that of butanol). In previous works for "in extraction" of butanol have been used dibutyl phalate [3], oleyl alcohol [4] and n-dodecanol [5] as solvent. In this paper the butanol extraction by 1,2-dichloroethane from simulated fermentation medium is carried out. The solvent has been dispersed by a nozzle. In the first part, the influence of the drops size on the solvent drops terminal velocities has been settled, and in the second part the dependence between the butanol mass transfer coefficient values and the drops size and the liquid viscosity has been established.

2. Materials and Method

The experimental equipment consists of a glass column (*1*) of 40 mm inner diameter and 760 mm height, provided with a nozzle (*2*) which disperses the solvent on drops and a microburette (*3*) at the top (Fig. 1). The solvent is evacuated through the valve (*4*) at the bottom. For simulation of the fermentation broths the carboxymethylcellulose sodium salt solutions at different concentrations have been used. These solutions exhibit a pseudoplastic behaviour similarly to that of *Clostridium acetobutylicum* fermentation medium. The viscosity of these solutions was 2.9, 5.7, 12.1, 44.6 cP, respectively 1 cP for water, being measured by means of an Ostwald viscometer. The butanol concentration in aqueous phase was 5% corresponding to the final fermentation concentration.

1,2-dichloroethane dispersed as drops was the solvent used. The drops diameter was varied between 1.65×10^{-3} and 6.02×10^{-3} m.

For determination of the solvent drops terminal velocities it has been measured the time of the drops fall for 400 mm, after a drops freely fall for 340 mm from the column top.

The butanol mass transfer process development was followed by dosing the butanol concentration in organic phase by means of an Abbe refractometer. The mass transfer coefficients of butanol was calculated using the relationship:

$$M = kA\Delta Ct,$$

where: M is the amount of the butanol extracted; k – the butanol mass transfer coefficient; A – the overall interfacial area; ΔC – the mass transfer potential; t – the extraction time.

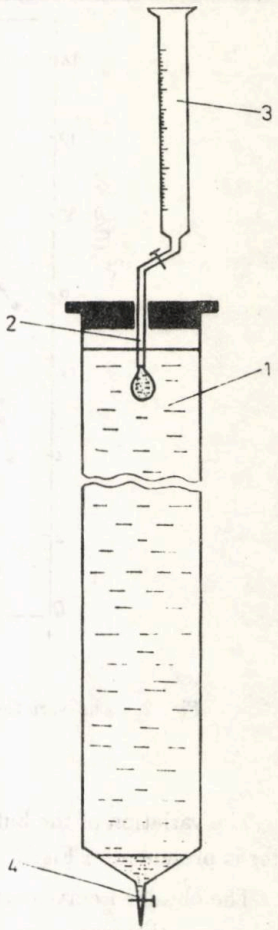

Fig. 1.– The experimental equipment.

3. Results and Discussions

3.1. Drop Velocity

The dependence between the solvent drops fall velocities and the drops size is depicted in Fig. 2. As can seen, for all solution viscosities the curve configuration presents a maximum corresponding to the drop pulsation appearance, this phenomenon reducing the drop velocity. By increasing the solution viscosity the drop pulsations are reduced and the falling drops trajectory becomes linear, comparative to the undulated drop fall in low viscosity solutions. Moreover, for the same diameter of the drops the corresponding velocities are decreased by the viscosity increase, reducing the Reynolds number, thus affecting the mass transfer rate.

Furthermore, the coalescence rate of the solvent drops at the column bottom is hindered by the high viscosity. If the continuous phase viscosity is high the solution between the drops cannot flow fast enough remaining as a dispersed phase included in the solvent one. In real fermentation processes the increasing of the coalescence time, and the hindering of the phases separation respectively, is the result both of the viscosity increase and of the adsorption of certain fermentation broth components (soluble proteins or cells) on the drops surface.

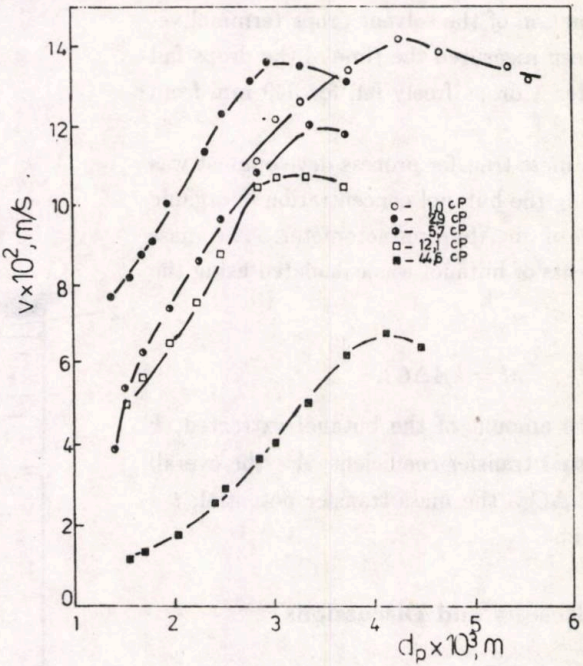

Fig. 2.– The variation of drops terminal velocity in function of drops size.

3.2. Mass Transfer to Drops

The variation of the butanol mass transfer coefficients in function of drops diameter is presented in Fig. 3.

The obtained curves are analogous to the variation of the terminal velocity with drops size, the maximum value corresponding to the maximum of the falling drops velocity, or to the maximum of the Reynolds number respectively. By increasing the aqueous solution viscosity the decreasing of the mass transfer coefficient maximum values has been observed. For example, the maximum value of butanol mass transfer coefficient for water is about 62 times greater than the maximum value for solution with 44.6 cP viscosity. It can see also the increase of the drop diameter corresponding to the maximum value of the mass transfer rate with the increase in solution viscosity.

As it was to be expected, at the same solvent drops size the mass transfer coefficients are reduced with the continuous phase viscosity increase, this mass transfer rate decrease being significant for largest drops (Fig. 4). The observed phenomenon is explained by the pulsations of the drops which are important especially for largest drops in low viscosity solutions, because of the increase of the Reynolds number by the drop pulsations appearance.

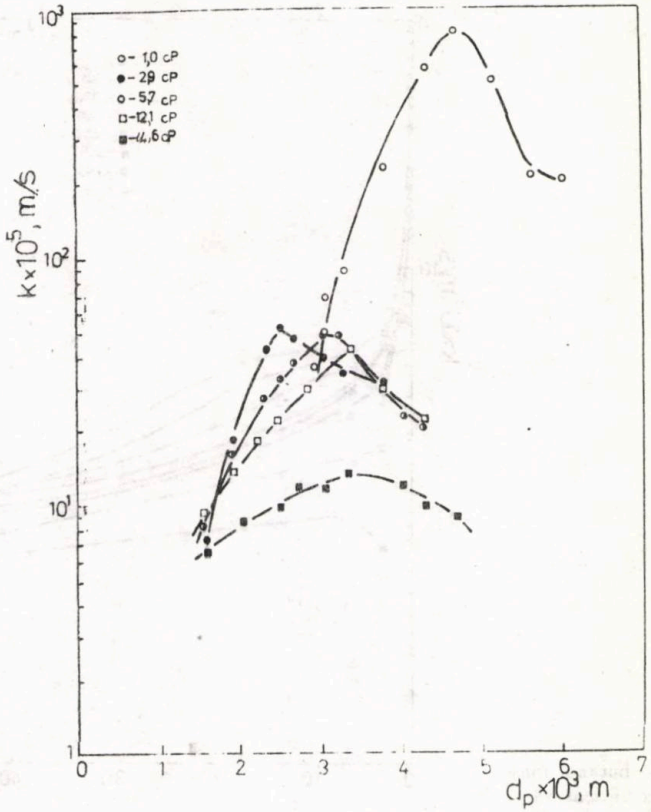

Fig. 3.– The butanol mass transfer coefficient vs. drops size.

The values of the mass transfer coefficients for a real fermentation can be lower than the values determined in this study owing to the additional resistance to mass transfer due to the soluble proteins or cells adsorption on the drops surface.

4. Conclusions

The experimental data indicated the decisively influence of the rheological characteristics, namely the aqueous phase viscosity, on the mass transfer rate. The dispersion of the solvent by certain nozzles is a compatible method of *in situ* extraction with the industrial fermentations, in this case a low shear effect on microorganisms being created. Furthermore, by increasing the fermentation broth viscosity large size drops must be used.

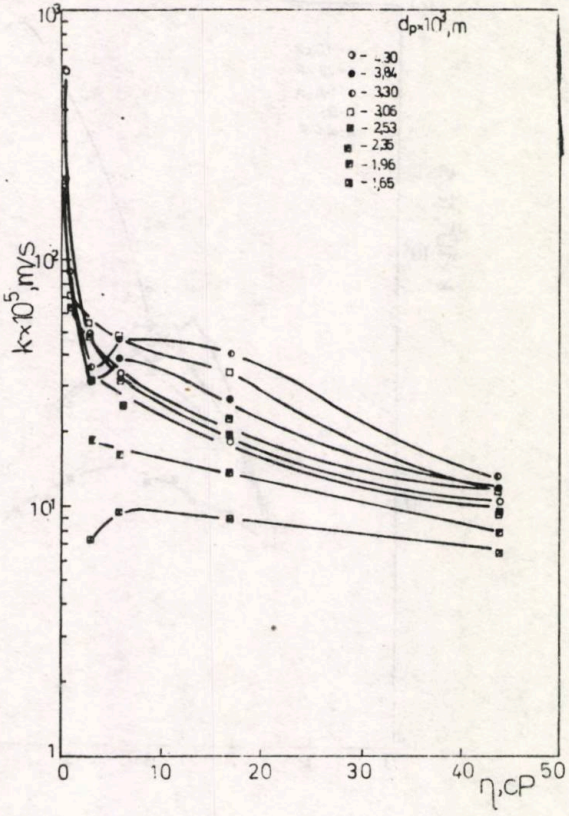

Fig. 4.– The butanol mass transfer coefficient vs. aqueous phase viscosity.

In further works a mathematical correlation between mass transfer coefficient and rheological characteristics or experimental conditions will be developed.

Received, May 13, 1996

Technical University "Gh. Asachi", Jassy,
Department of Organic Industries

REFERENCES

1. Rehm H.J., Reed G., Puhler A., Stadler P. (Eds.), *Biotechnology.* Vol. **3**, Weinheim, Germany, 1993.
2. Job C., Blass E., The Chem. Engn. J., **56**, *B1* (1994).
3. Waymon M., Parekh R., J. Ferm. Technol., **65**, 295 (1987).
4. Roffler S., Blanch H.W., Wilke C.R., Biotechnol. Bioengn., **31**, 135 (1988).
5. Eckert G., Schugerl K., Appl. Microbiol. Biotechnol., **27**, 211 (1987).

EXTRACŢIA LICHID–LICHID A PRODUSELOR DE BIOSINTEZĂ DIRECT DIN LICHIDELE DE FERMENTAŢIE

I. Transferul de masă către picături

(Rezumat)

Se prezintă rezultatele experimentale obţinute cu privire la extracţia butanolului din soluţii apoase care simulează comportarea lichidelor de fermentaţie, stabilindu-se influenţa diametrului picăturilor de solvent asupra vitezei terminale de deplasare a acestora şi asupra coeficienţilor de transfer de masă corespunzători unor faze apoase de viscozităţi diferite.

BULETINUL INSTITUTULUI POLITEHNIC DIN IAŞI
Tomul XLIV (XLVIII), Fasc. 1–2, 1998
Secţia II
CHIMIE şi INGINERIE CHIMICĂ

D.C. 547.281.2; 661.183.42

ALDOL CONDENSATION OF FORMALDEHYDE AND ACETALDEHYDE OVER THE ALKALI TREATED VOLCANIC TUFFS

BY

EMIL DUMITRIU and V. HULEA

The aldol condensation of acetaldehyde with formaldehyde to produce acrolein has been studied. The native and modified samples of volcanic tuff have been used as catalysts in the gas phase condensation of the aldehydes over a temperature range of 498...698 K. The catalytic properties were analyzed in relation to both the nature of crystalline phases of the catalysts and the catalyst porosity.

1. Introduction

One of the most important methods of synthesis of the α,β-unsaturated aldehydes is based on the aldol condensation reaction which can be described by the following equation:

$$R{-}CH_2{-}CHO + CH_2O \rightarrow HO{-}CH_2{-}CH(R){-}CHO \rightarrow CH_2{=}C(R){-}CHO + H_2O$$

where R = H, alkyl, aryl, aralkyl, cycloalkyl, etc. An important application of this reaction consists of the condensation of acetaldehyde with formaldehyde to produce acrolein.

Though the aldol condensation can be performed in homogeneous catalysis, however better yields have been obtained applying the heterogeneous catalysis. Performing this condensation in the gas-phase results in high yields and an appreciable selectivity. The heterogeneous catalytic systems are mostly based on the metal oxides having acidic or basic properties [1],...,[3]. The selectivity is considerably enhanced when the process is carried out on the zeolite catalysts which can inhibit the formation of bulkier reaction products [4],...,[7] due to the spatial constraints imposed by the size of pores.

Therefore, starting from these aspects it was considered as timely to study the reaction of acrolein synthesis by aldol condensation in the presence of the native and modified volcanic tuffs; as is known, the volcanic tuffs contain mainly small pore natural zeolites such as: clinoptilolite, analcime, heulandite, philipsite, etc. This

study extends our previous investigations on the application of volcanic tuffs in the aldol condensation [7] by the use of hydrothermally modified tuffs having different crystalline phases, aiming to obtain a catalyst with more uniform properties than the parent material.

2. Experimental

2.1. Catalyst Preparation

The volcanic tuff (Marsid deposit, Romania) used as a raw material containing 60...62% clinoptilolite had the following composition: 68.54% SiO_2, 11.95% Al_2O_3, 0.40% Na_2O, 2.80% K_2O, 3.35% CaO, 0.70% MgO and 0.86 wt % Fe_2O_3. The other properties were: the loss on calcination reached 11.40% at 773 K, the ion exchange capacity of 0.4...1.70 mequiv/g hydrated tuff and the adsorption capacity for water of 8.0 wt %. The native volcanic tuff was grounded, sieved, washed with a large amount of deionized water and dried at 473 K.

The samples of modified volcanic tuff were obtained by the alkali treatment of the parent material. The main variables of the chemical treatment were: the ratio between the solid and liquid phase, the nature and the concentration of the alkaline reagent, temperature and pressure. Typically, 30 g of native tuff were immersed into 100 mL alkali solution in a stainless steel autoclave and this mixture was heated under (or without) autogene pressure at constant temperature for a certain reaction time. Then, the sample was removed by filtration and the solid material was washed with a large amount of deionized water. The composition of samples was determined by chemical analysis and the nature of the crystalline phase was established by the X-ray diffraction technique.

Then, all samples were ion exchanged with 0.1 M solution of NH_4Cl three times for 24 hrs at 363 K, washed with a large amount of deionized water and calcined at 773 K in order to obtain the H^+ form.

2.2. Reagents

Formaldehyde (Merck) was used as aqueous solution containing 36 wt % formaldehyde (FA) and stabilized with 12% methanol.

Acetaldehyde (AA) was pure Fluka reagent.

2.3. Catalyst Testing

The reactions were carried out in a pulse type microreactor (stainless steel, i.d. 3 mm and 80 mm length) under the following conditions: weight of catalyst, 0.02...0.04 g; particle size, 0.25...0.43 mm and 5 mm high bed; nitrogen flow rate, 30 $mL.min^{-1}$; pressure, 140 kPa; pulse size, 0.3 μL. The microreactor was coupled with a gas chromatograph equipped with two columns, one filled with Carbowax 20 M on Chromosorb W and the second filled with Porapak N.

The catalyst was activated before use in an air flow at 773 K, then it was cooled to the reaction temperature under a stream of nitrogen.

3. Results and Discussion

3.1. Volcanic Tuff Treatment

As was already shown, the samples of native volcanic tuff were processed by alkaline hydrothermal treatments. The results of these treatments were dependent on the alkali concentration, temperature and pressure.

Thus, when the volcanic tuff was treated with NaOH at 373 K, the amorphous silica, clay materials and clinoptilolite were solubilized and a progressive recrystallization took place. Finally, the Pc zeolite (T_{Pc} sample) was formed which contain quartz, mica and illite in small amounts.

If the alkaline treatment was performed at 473 K using a solution of sodium hydroxide or a mixture of sodium aluminate and sodium hydroxide, a sample was obtained which contained mainly analcime with various amounts of clinoptilolite ($T_{cli+ana}$ and T_{ana} samples).

Using only sodium aluminate caused a decrease of the mole ratios SiO_2/Al_2O_3, Na_2O/Al_2O_3 and H_2O/Na_2O and the recrystallization of native clinoptilolite into chabazite (T_{cha} sample).

The analysis of the X-ray diffractograms allowed establishing the nature of crystalline phases for each sample as shown in Table 1.

Table 1
The Treatment Conditions for the Samples of Volcanic Tuff

Sample	Chemical treatment				Composition of crystalline phase, [%]				
	Reagent	Conc.	Temp. K	Time h	cli	cha	ana	Pc	Illite
Tuff (T)	–	–	–	–	93...95				7...5
T_{Pc}	NaOH	3N	373	24				88...91	12...9
$T_{cli+ana}$	NaOH	4N	473	24	22...24		78...76		
T_{cha}	$NaAlO_2$	1N	373	24	13...15	87...85			

3.2. Aldol Condensation

The aim of our study was testing of the catalysts described above in aldol condensation of acetaldehyde and formaldehyde. The main objectives of these tests were: the catalytic activity and selectivity in relation to the nature of the crystalline phase and the resistance to cocking in dependence on the operating conditions.

a) *Catalytic Activity.* At the beginning, the catalytic activity as function of the reaction temperature was investigated. The condensation reactions were performed within the temperature range of 498...698 K and the catalytic activity was estimated on the basis of the acetaldehyde conversion to acrolein.

It can be seen from Fig. 1 that the nature of the crystalline phase exerts a certain influence on the catalytic activity of the tested samples. The obtained results are expressed as relative activities, i.e. the ratio between the activities of modified and native tuffs (the mean values of the first five pulses). Two domains can be distinguished: one ranging between 498 and 573 K, when the relative activities of

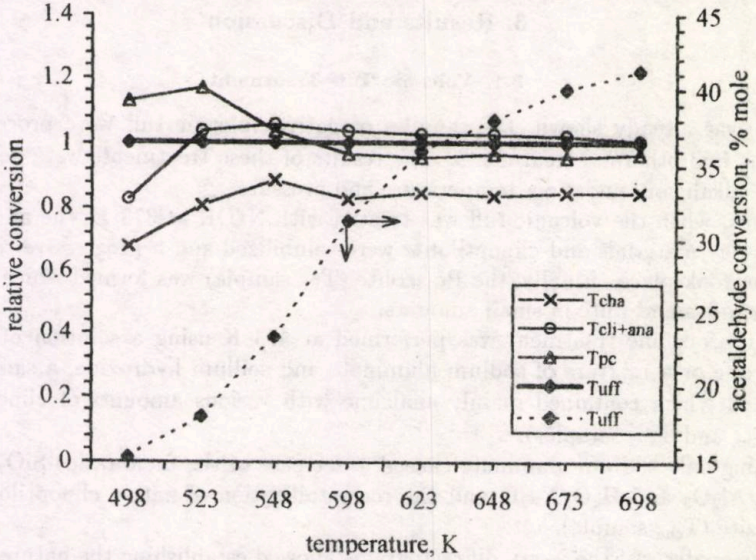

Fig. 1.– The influence of reaction temperature on the conversion of acetaldehyde, 1:1 mole ratio of reagents: — relative conversion; --- conversion of acetaldehyde.

the modified tuffs rapidly increase with the reaction temperature and reach the maximum value at about 548 K, and the second region between 573 and 698 K, when the relative activities are kept approximately constant.

One can also note that only the crystalline phase containing clinoptilolite and analcime has a higher activity than the native volcanic tuff, whereas the activities of other alkali treated samples are lower. Therefore, the following order of catalytic activities of the fresh activated samples was obtained:

$$T_{cli+ana} > T > T_{Pc} > T_{cha}$$

and this order could be correlated with the alumina to silica ratio:

Zeolite	Analcime	Pc	Chabazite	Clinoptilolite
Pore size, [Å]	2.6	3.5	3.7×4.2	4.0×5.5
Si/Al	1.7...2.8	1...1.25	1.7...3.8	4...5.1

b) *Catalytic Selectivity.* It is worthwhile to note that the ratio between the aldol cross-condensation and the aldol self-condensation of acetaldehyde increases with the reaction temperature. Above 613 K the cross-aldol condensation was the main reaction for all catalysts (Fig. 2).

The decrease of the acetaldehyde conversion to crotonaldehyde with increase of temperature contradicts the thermodynamic data when the yield at 598 K is about 49% [1]. This is possible according as the crotonaldehyde is decomposed by the following route:

$$CH_3{-}CH{=}CH{-}CHO \longrightarrow CH_3{-}CH{=}CH_2 + CO$$

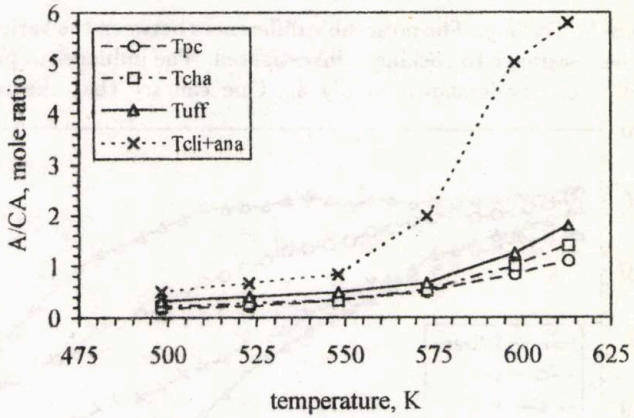

Fig. 2.– The influence of reaction temperature on the selectivity to acrolein: A – acrolein; CA – crotonaldehyde; 1:1 mole ratio of reagents.

and propene, as well as crotonaldehyde, involve a cocking process.

It should be noted that the carbon monoxide could also result from the following reactions:

$$CH_3{-}CHO \longrightarrow CH_4 + CO, \quad HCHO \longrightarrow H_2 + CO$$

The GC analysis revealed that a small amount of light products results at high temperatures.

As can be seen from Fig. 2, the catalytic selectivities of the tested catalysts are disposed by the following order:

$$T_{cli+ana} > T > T_{cha} > T_{Pc}.$$

As compared with other catalysts, the samples of alkali treated tuff show a good selectivity; e.g. for mordenite at 573 K an acrolein/crotonaldehyde mole ratio of 1:1 was obtained, while for Y faujasite [6] at 543 K this ratio was about 1:8. It can mean that the pore size of 6.6 Å for M and 7.3 Å for Y are responsible for the formation of crotonaldehyde, a bulkier condensation product. Therefore, shape selectivity could be taken into account in the case of the native and alkali treated tuffs, when both the small pore openings and the small cavities of these crystalline structures do not permit the formation of branched or longer reaction products.

However, as can be seen from the order of selectivities shown above this is better correlated with the Si/Al ratio than the mean size of pores of the tested catalysts. It is well-known that the acidity of zeolites is determined by the Si/Al ratio of the framework, therefore in order to explain the selectivities of these catalysts the acidic properties of active centers could be taken into account, too. It seems that in the case of the aldol condensation of lower aldehydes on zeolites having relatively near pore sizes the competition between cross- and self-condensation is mainly influenced by the acid–base properties of active sites. Moreover, the reaction temperature influences this competition, as can be seen from Fig. 2.

c) *Resistance to Cocking.* The noticeable differences between the various catalysts appear when the resistance to cocking is investigated. The influence of pulse number on the catalytic activity is shown in Fig. 3. One can see that the resistance to

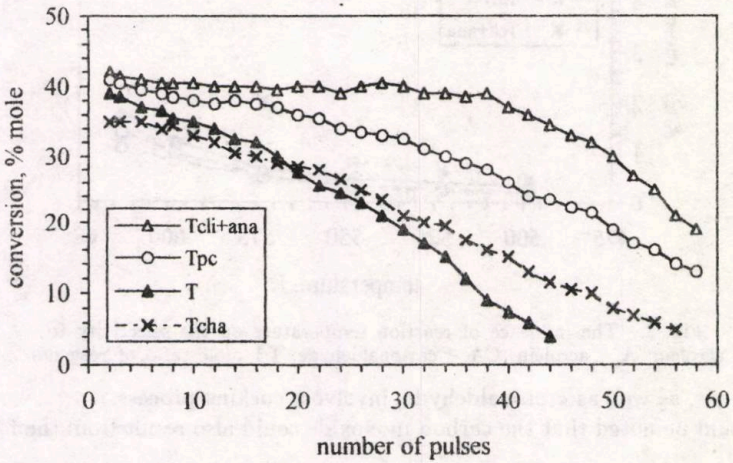

Fig. 3.– The conversion of acetaldehyde to acrolein vs. the number of pulses; reaction temperature 623 K; 1:1 mole ratio of reagents.

cocking does not correlate to the catalytic activity as shown in Fig. 1. Thus, the native volcanic tuff which showed a high catalytic activity in a fresh activated state, is now the least resistant catalyst, whereas the $T_{cli+ana}$ sample exhibits the highest resistance to cocking. One can state that the presence of the analcime phase has a benefic role and increases the resistance to cocking. This behaviour is surprising, because analcime has a unidimensional channel system, with the opening of 2.6 Å, when a fast deactivation of the zeolite could be supposed in the result of pore blocking by coke.

Generally, the modified volcanic tuffs are more stable to cocking than the native one, which has an inhomogeneous cation distribution. This is possible since acrolein formed initially is converted to unidentified polymers under the action of acidic sites present on the native volcanic tuff and thus a relatively fast deactivation takes place.

d) *Influence of the Mole Ratio of Reagents.* Another objective of our study consisted of the investigation of the reagents mole ratio influence on the conversion of limiting reagent. The experiments were performed using the most active and resistant catalyst ($T_{cli+ana}$) and the results are compared with those obtained on the native tuff.

As shown in Fig. 4, the excess of acetaldehyde has a stronger influence on the conversion of formaldehyde to acrolein than the excess of formaldehyde on the conversion of acetaldehyde to acrolein. The behaviour in the latter case can be explained by the reduction of the partial pressure of reagents when the content of water in the feed mixture is increased.

The equimolar ratio seems to be more suitable for the aldol condensation be-

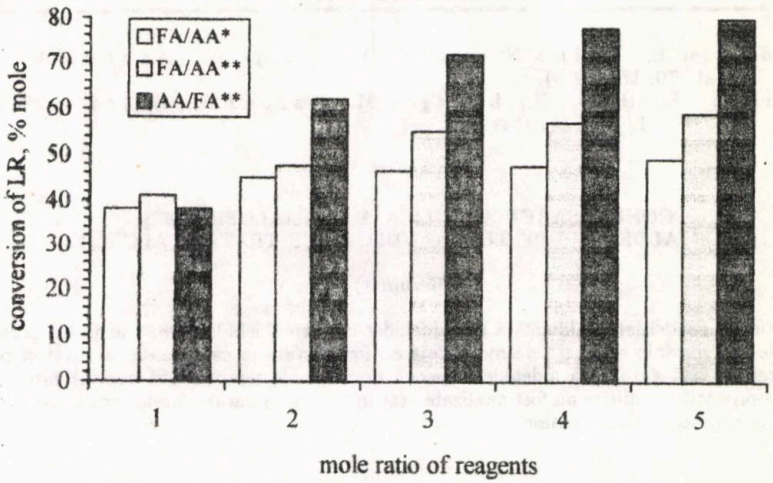

Fig. 4.– The influence of the mole ratio of reagents on the conversion of limiting reagent (LR) to acrolein: (*) native volcanic tuff; (**) $T_{cli+ana}$; reaction temperature 623 K.

cause, at a high excess of acetaldehyde, the side reactions (aldol self-condensation, crotonaldehyde decomposition, etc.) are intensified, while a high excess of formaldehyde decreases the productivity of catalyst (it should be mentioned that traces of HCOOH and $HCOOCH_3$ were identified at high ratios FA/AA).

4. Conclusions

The results of our study reveal that the catalysts based on alkali treated tuff are suitable for the aldol cross-condensation of acetaldehyde with formaldehyde. They exhibit a high catalytic activity and selectivity for acrolein synthesis and their resistance to cocking is higher than that of the native volcanic tuff. An important advantage of the alkali treated samples is an easier control of catalytic properties resulting from a more homogeneous composition of the samples.

A c k n o w l e d g e m e n t s. The authors thank Dr. N. B î l b ă for the delivered samples of volcanic tuff and their X-ray diffraction analysis.

Received, November 5, 1997

Technical University "Gh.Asachi", Jassy, Department of Organic Industries

REFERENCES

1. M a l i n o w s k i S., J e d r z e j e w s k a H., B a s i n s k i S., Chim. Ind. (Paris), **85**, *6*, 885 (1961).
2. A i M., Bull. Chem. Soc. Jpn., **64**, 1342 (1991).
3. A i M., Bull. Chem. Soc. Jpn., **64**, 1346 (1991).
4. C h e n N.Y., G a r w o o d W.E., D w y e r F.G., *Shape Selective Catalysis in Industrial Applications*. Marcel Dekker, New York, 1989, 131.
5. H ö l d e r i c h W.F., in: *Acid-Base Catalysis*, T a n a b e K., H a t t o r i H., Y a m a g u c h i T., T a n a k a T. (Eds.), Kodansha, Tokyo, 1989, 1.

6. Dumitriu E., Bilbă N., Hulea V., Cârje G., Azzouz A., J. Mol. Catal., **79**, 175 (1993).
7. Dumitriu E., Bilbă N., Lupaşcu M., Azzouz A., Hulea V., Nibou D., J. Catal., **147**, 133 (1994).

CONDENSAREA ALDOLICĂ A FORMALDEHIDEI ŞI ACETALDEHIDEI PE TUFURI VULCANICE TRATATE ALCALIN

(Rezumat)

S-a studiat condensarea aldolică a acetaldehidei cu formaldehida pentru a obţine acroleina. Probele de tuf vulcanic nativ şi cele modificate au fost testate în calitate de catalizatori pentru condensarea în fază gazoasă a aldehidelor pe un domeniu de temperatură cuprins între 498 şi 698 K. Proprietăţile catalitice au fost analizate atât în raport cu natura fazelor cristaline, cât şi în raport cu porozitatea catalizatorilor.

BULETINUL INSTITUTULUI POLITEHNIC DIN IAŞI
Tomul XLIV (XLVIII), Fasc. 1–2, 1998
Secţia II
CHIMIE şi INGINERIE CHIMICĂ

D.C. 66.095.2; 678.745

THE INFLUENCE OF SOME PARAMETERS ON FREE RADICAL POLYMERIZATION OF METHYL METHACRYLATE

BY

SILVIA CURTEANU and VICTOR BULACOVSCHI

The influence of different parameters on the discontinuous bulk radical polymerization of methyl methacrylate (MMA) by model simulation is studied. The applied model makes use of a kinetic diagram involving the decomposition of an initiator, propagation and termination by disproportionation as well as of relationships including the gel and glass effects. In previous papers [1],...,[3] numerous simulation results and their comparison with the experimental data have been discussed. In this study the influence of the initial conditions, temperature and volume contraction on the conversion, molecular weights and reaction rate are followed. The results thus obtained by simulation represent a stage in the model validation and a possibility of getting easily additional information on the polymerization process under study.

1. Introduction

In recent years, polymer reaction engineers have started focusing their attention on the mathematical modelling of various physical phenomena in industrial polymerization reactors. One such aspect – diffusion-controlled reactions – plays an important role in free radical chain growth polymerizations.

From the vast array of published experimental data, it is well-known that classical low-conversion free radical kinetics do not apply over the entire conversion range in concentrated polymerizing systems. In particular, many such polymerizations exhibit a large autoacceleration of the rate of polymerization with an associated increase in the molecular weight of the polymer on the order of 20...30% in polymer content, even under isothermal conditions. This autoacceleration, known as the Trommsdorff or *gel effect*, is the result of a drastic decrease in the rate of chain termination steps due to increasing viscosity of the reaction mass. The gel effect leads to higher monomer conversions than predicted by models using constant values of the rate constants, determined from low conversion data.

In the later stages of reaction, the glass transition temperature becomes higher than the polymerization one, and the reaction mixture becomes glassy in nature. Then the propagation rate constant also becomes diffusion controlled. As a consequence, the reaction stops shortly before the complete monomer conversion. This

effect is referred to as the *glass effect*. In addition to this, the initiator efficiency decreases with time at high monomer conversions. This is so-called *cage effect*.

In conclusion, in free radical polymerization, the termination, propagation and initiation reactions become diffusion-controlled as the conversion of the monomer increases and the viscosity of the reaction mass increases too. A good model is required to account for these effects mathematically, so that it can be used for design, optimization and control purposes. A sample polymerization system exhibiting these phenomena is that of polymethyl methacrylate (PMMA), an important commodity plastic.

2. Modelling of Free Radical Polymerization of MMA

A model based on the following kinetic diagram was proposed and verified for the batch bulk isothermal polymerization of MMA:

Initiation: $\mathrm{I} \xrightarrow{k_d} 2\mathrm{R}^*$

$\mathrm{R}^* + \mathrm{M} \xrightarrow{k_i} \mathrm{P}_1$

Propagation: $\mathrm{P}_n^* + \mathrm{M} \xrightarrow{k_p} \mathrm{P}_{n+1}^*$

Termination by disproportionation: $\mathrm{P}_n^* + \mathrm{P}_m^* \xrightarrow{k_t} \mathrm{D}_n + \mathrm{D}_m$

where I is the initiator, R^* – the initiating radical, M – the monomer, P_n^* – the polymer growing chain of length n, and D_n – the dead polymer of length n.

Assuming the steady-state and that no monomer is consumed in the initiation stage, one obtains the following kinetic equations based on the kinetic diagram:

(1) $$\frac{\mathrm{dI}}{\mathrm{d}t} = -k_d\mathrm{I} - \mathrm{I}\varepsilon\frac{1-x}{1+\varepsilon x}\lambda_0 k_p, \qquad (2) \quad \frac{\mathrm{d}x}{\mathrm{d}t} = k_p(1-x)\lambda_0,$$

(3) $$\frac{\mathrm{d}\lambda_0}{\mathrm{d}t} = 2fk_d\mathrm{I} - k_t\lambda_0^2 - \lambda_0^2\varepsilon\frac{1-x}{1+\varepsilon x}k_p,$$

(4) $$\frac{\mathrm{d}\lambda_1}{\mathrm{d}t} = k_p\mathrm{M}_0\frac{1-x}{1+\varepsilon x}\lambda_0 - k_t\lambda_0\lambda_1 - \lambda_0\lambda_1\varepsilon\frac{1-x}{1+\varepsilon x}k_p,$$

(5) $$\frac{\mathrm{d}\lambda_2}{\mathrm{d}t} = k_p\mathrm{M}_0\frac{1-x}{1+\varepsilon x}(2\lambda_1+\lambda_0) - k_t\lambda_0\lambda_2 - \lambda_0\lambda_2\varepsilon\frac{1-x}{1+\varepsilon x}k_p,$$

(6) $$\frac{\mathrm{d}\mu_0}{\mathrm{d}t} = k_t\lambda_0^2 - \mu_0\lambda_0\varepsilon\frac{1-x}{1+\varepsilon x}k_p,$$

(7) $$\frac{\mathrm{d}\mu_1}{\mathrm{d}t} = k_t\lambda_0\lambda_1 - \mu_1\lambda_0\varepsilon\frac{1-x}{1+\varepsilon x}k_p, \qquad (8) \quad \frac{\mathrm{d}\mu_2}{\mathrm{d}t} = k_t\lambda_0\lambda_2 - \mu_2\lambda_0\varepsilon\frac{1-x}{1+\varepsilon x}k_p.$$

The following relationships take into account the gel and glass effects completing the kinetic model (C h i u's model [4]):

$$\frac{1}{k_t} = \frac{1}{k_{t0}} + \theta_t(T, \mathrm{I}_0) \frac{\lambda_0}{\exp\left[\dfrac{2.303\Phi_m}{A(T) + B\Phi_m}\right]}, \tag{9}$$

$$\frac{1}{k_p} = \frac{1}{k_{p0}} + \theta_p(T) \frac{\lambda_0}{\exp\left[\dfrac{2.303\Phi_m}{A(T) + B\Phi_m}\right]}, \tag{10}$$

where: x represents conversion of the monomer, λ_k – the moments of the macroradicals and μ_k – the moments of the dead polymer.

The numerical values and the computing equations for some of the parameters are presented in Table 1.

Table 1

Parameters Used for MMA Polymerization

$k_d^0 = 1.053 \times 10^{15}\ \mathrm{s}^{-1}$ (for initiation with AIBN);
$k_{p0}^0 = 4.917 \times 10^2\ \mathrm{m}^3/(\mathrm{mol\ s})$; $k_{t0}^0 = 9.8 \times 10^4\ \mathrm{m}^3/(\mathrm{mol\ s})$;
$E_d = 1.2845 \times 10^5$ J/mol; $E_p = 1.822 \times 10^4$ J/mol; $E_t = 2.937 \times 10^3$ J/mol;
$f = 0.58$ (AIBN); $B = 0.03$; $C_1 = 0.15998$; $C_2 = 7.812 \times 10^{-6}\ \mathrm{K}^{-2}$; $T_{gp} = 387$ K;
$\theta_p^0 = 3.99822 \times 10^{-12}$ s; $E_{\theta p} = 1.02451 \times 10^5$ J/mol;
$\theta_t^0 = 2.8883 \times 10^{-18}$ (mol s)/m^3; $E_{\theta t} = 1.48924 \times 10^5$ J/mol;
$\varepsilon = -(0.1946 + 0.916 \times 10^{-3}T,\ [^\circ\mathrm{C}])$; $\Phi_m = \dfrac{1-x}{1+\varepsilon x}$;
$\theta_t = \dfrac{\vartheta_t^0}{\mathrm{I}_0} \exp[E_{\theta t}/(RT)]$; $\theta_p = \theta_p^0 \exp[E_{\theta p}/(RT)]$;
$A(T) = C_1 - C_2(T - T_{gp})^2$; $\lambda_k = \sum_{n=1}^{\infty} n^k \mathrm{P}_n$; $\mu_k = \sum_{n=1}^{\infty} n^k \mathrm{D}_n$;
$\mathrm{DP}_n = \dfrac{\lambda_1 + \mu_1}{\lambda_0 + \mu_0}$; $\mathrm{DP}_w = \dfrac{\lambda_2 + \mu_2}{\lambda_1 + \mu_1}$.

One should observe that the model predictions reasonable agree with the experimental data for high concentrations, when the kinetics of the process is controlled by diffusion [1].

3. Influence of the Initial Monomer and Initiator Concentrations

The influence of the initial conditions is studied by means of the model simulation using a programme for solving the differential equations of the Stiff type. The simulation was made over the time interval of 0...350 min., with a variable step calculated as part of the algorithm for the equation system solving.

The modification of the MMA initial concentration does not affect the shape of the conversion curve, causing instead the modification of the number average polymerization degree and the molecular weight of the polymer (Figs. 1 and 2).

The increase in the initial monomer concentration results in the molecular weight increase. Although this piece of information would seem rather common place if must be taken as a simulation result, hence as a step of the model validation.

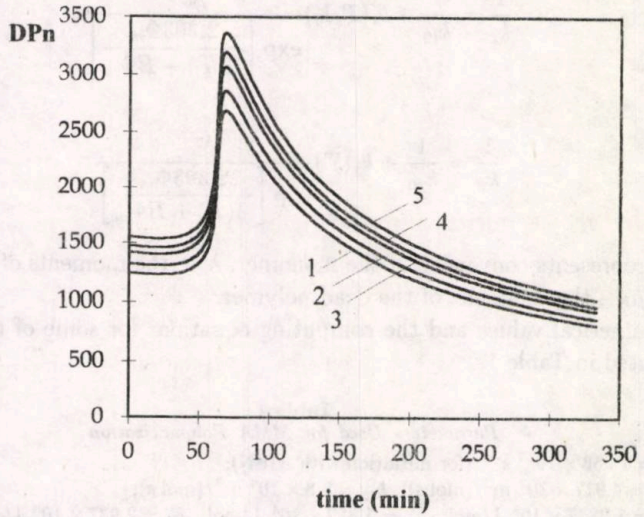

Fig. 1.– The influence of the initial concentration of monomer on the number average degree of polymerization in the following conditions: *1* – M_0 = 8,000 mol/m^3; *2* – 8,500 mol/m^3; *3* – 9,130 mol/m^3; *4* – 9,500 mol/m^3; *5* – 10,000 mol/m^3.

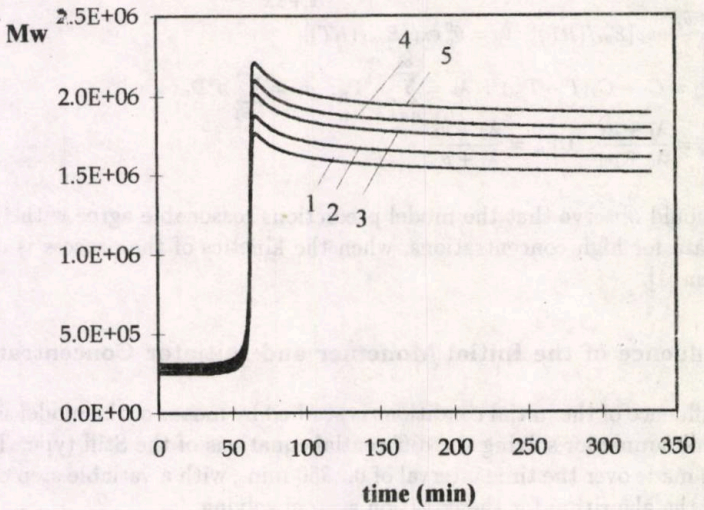

Fig. 2.– The influence of the initial concentration of monomer on the molecular weight in the following conditions: *1* – M_0 = 8,000 mol/m^3; *2* – 8,500 mol/m^3; *3* – 9,130 mol/m^3; *4* – 9,500 mol/m^3; *5* – 10,000 mol/m^3.

The acceleration of the MMA polymerization process with the increasing initiator concentration is illustrated in Fig. 3.

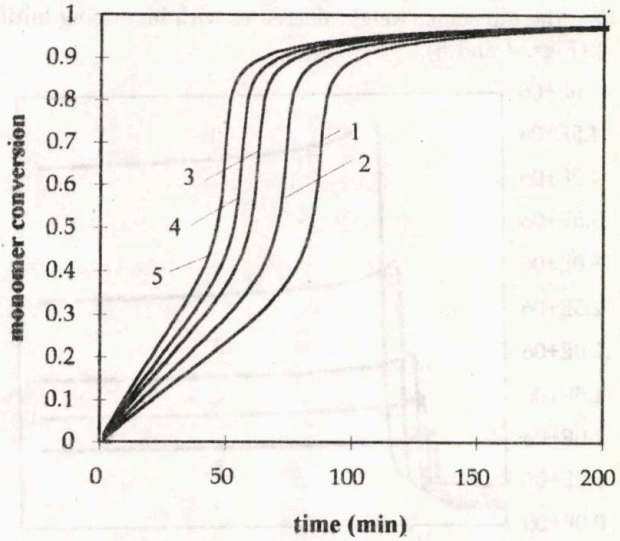

Fig. 3.– The influence of the initiator concentration on the monomer conversion in the following conditions: *1* – I_0 = 10 mol/m^3; *2* – 15.75 mol/m^3; *3* – 25.8 mol/m^3; *4* – 35 mol/m^3; *5* – 50 mol/m^3.

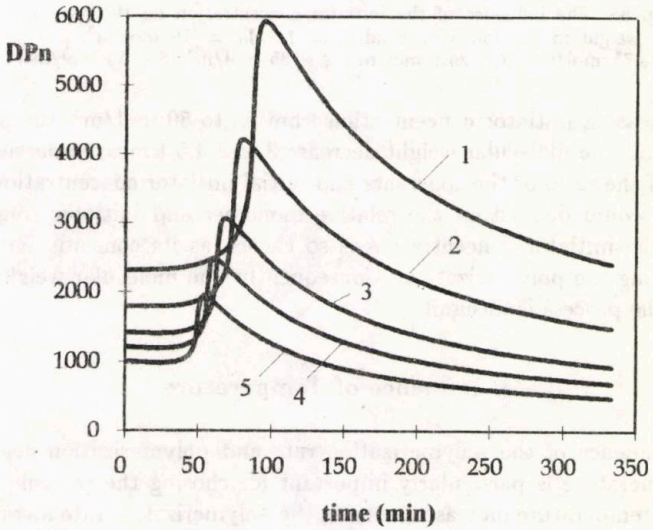

Fig. 4.– The influence of the initiator concentration on the number average polymerization degree in the following conditions: *1* – I_0 = 10 mol/m^3; *2* – 15.75 mol/m^3; *3* – 25.8 mol/m^3; *4* – 35 mol/m^3; *5* – 50 mol/m^3.

While the reaction time is of 50 min. for $I_0 = 50$ mol/m^3 (70°C) it attains to about 80 min. for $I_0 = 10$ mol/m^3.

The polymerization degree is inversely proportional to the initiator concentration square root, so that the molecular weight decreases with increasing initiator amount ($DP_n \sim \Delta M/\Delta I$) (Figs. 4 and 5).

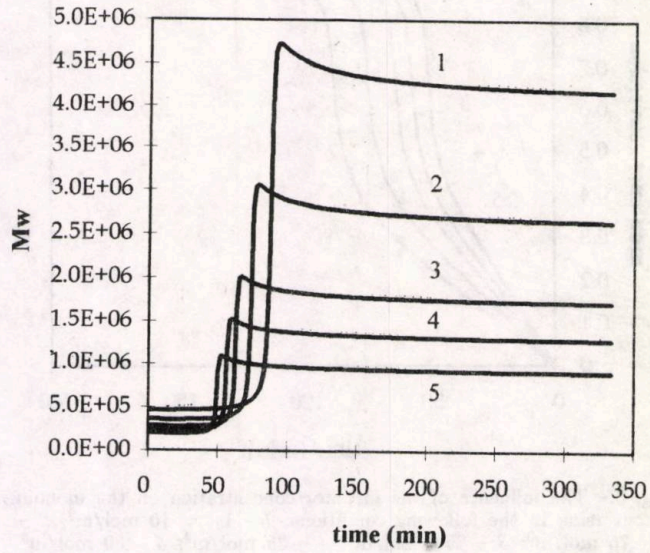

Fig. 5.– The influence of the initiator concentration on the molecular weight in the following conditions: *1* – $I_0 = 10$ mol/m^3; *2* – 15.75 mol/m^3; *3* – 25.8 mol/m^3; *4* – 35 mol/m^3; *5* – 50 mol/m^3.

With increasing initiator concentration from 10 to 50 mol/m^3, the polymerization degree and the molecular weight decrease 3 and 4.5 times, respectively. Thus, in function of the ratio of the constants and initial initiator concentration, the DP_n modification would depend on the relative monomer and initiator consumptions. Practically, the initiator concentration is so chosen as its consumption to be not complete during the polymerization. Consequently, the molecular weight modification during the process is unsignificant.

4. Influence of Temperature

The dependence of the polymerization rate and polymerization degree on the reaction temperature is particularly important for chosing the working procedure. The reaction temperature increase results in the polymerization rate increase (Fig. 6) and polymer molecular weight decrease (Fig. 7). The quantitative correlating of the above mentioned parameters is much more complex due to the dependence of the polymerization rate and polymerization degree on the rate constants k_d, k_p, k_t

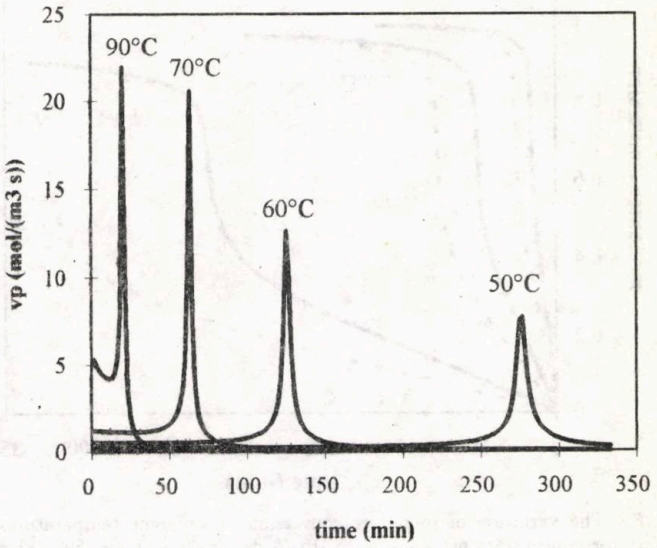

Fig. 6.– The variation of polymerization rate at different temperatures.

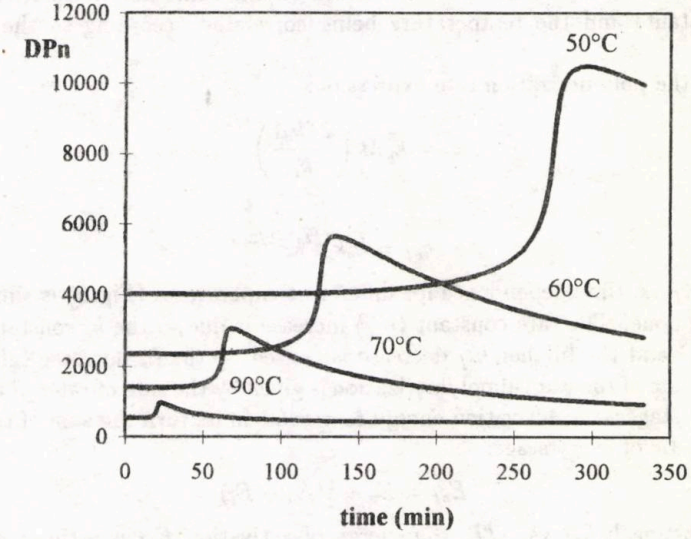

Fig. 7.– The variation of number average polymerization degree at different temperatures.

The conversion is also influenced by temperature in the following two directions: the maximum conversion increases with increasing temperature and, on the other hand, the jump characteristic to the gel effect appears at shorter times for higher temperature (Fig. 8).

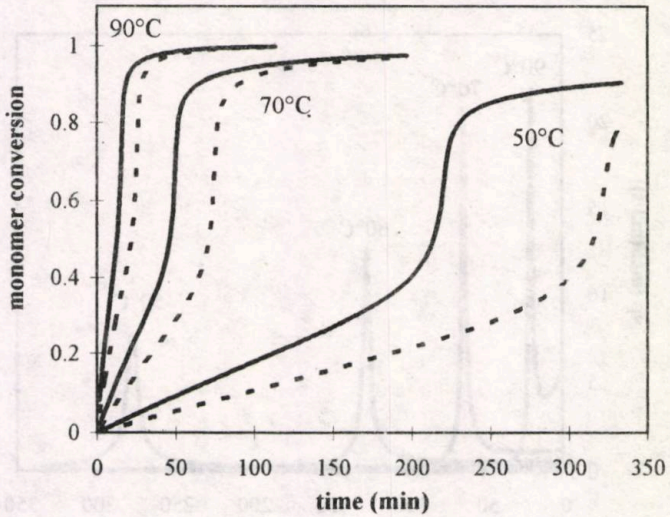

Fig. 8.– The variation of monomer conversion at different temperatures and initiator concentrations: - - - I_0 = 15.75 mol/m^3; — I_0 = 50 mol/m^3.

The temperature influence on the polymerization rate, average polymerization degree and conversion can be settled based on the same kinetic relationships, the rate constants and the temperature being correlated according to the Arrhenius equation.

From the polymerization rate expression:

$$v_p = k_p M \left(\frac{2 f k_d \mathrm{I}}{k_t} \right)^{1/2}, \tag{11}$$

it follows:

$$k_{ef} = k_p k_d^{1/2} k_t^{-1/2}. \tag{12}$$

The k_{ef} vs. time dependence for different temperatures (Fig. 9) is similar to the v_p vs. time one. The rate constant (k_{ef}) increase is due to the k_t constant decrease (gel effect) and the further k_{ef} decrease is caused by the k_p decrease (glass effect). Since the rate of the radical polymerization is given by the sum of rates of the process successive stages, the activation energy represents in its turn the sum of the energies characteristic of every stage:

$$E_{ef} = E_p + \tfrac{1}{2}(E_d - E_t). \tag{13}$$

By plotting $\ln k_{ef}$ vs. $1/T$, the energy of activation E_{ef} is estimated from the straight line slope and the preexponential factor in the Arrhenius equation from the straight line intercept.

According to the relation:

$$\ln k_{ef} = \ln A_{ef} - \frac{E_{ef}}{RT} \tag{14}$$

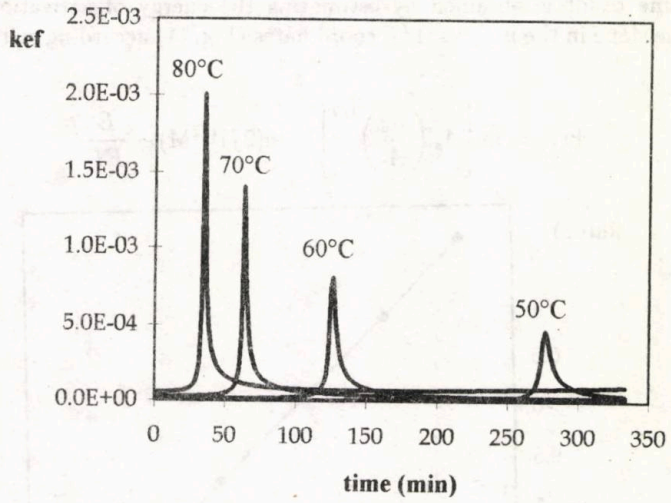

Fig. 9.– The variation of effective rate constant at different temperatures.

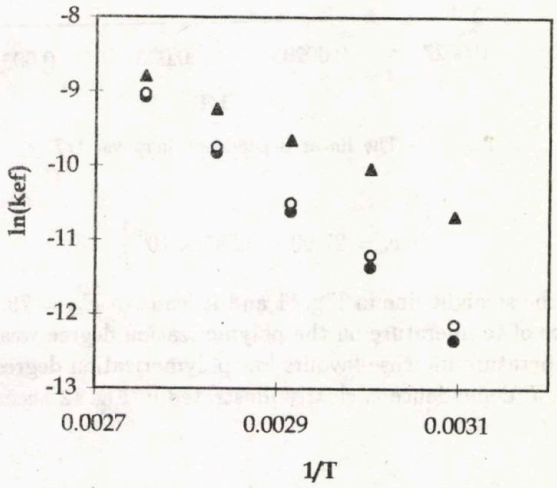

Fig. 10.– The temperature dependence of rate constant at different conversions: ▲ – $x = 0.06$; ○ – $x = 0.2$; ● – $x = 0.4$.

it results from Fig. 10:

$$\ln k_{ef} = 17.05 - 9.48 \times 10^3 \frac{1}{T}, \tag{15}$$

from which it results: $E_{ef} = 78.87 \times 10^3$ J/mol and $A_{ef} = 2.53 \times 10^7$.

The same result is obtained by estimating the energy of activation from the straight line slope in the $\ln v_p$ vs. $1/T$ coordinates (Fig. 11) according to the relationship:

$$\ln v_p = \ln\left[A_p\left(\frac{A_d}{A_t}\right)^{1/2}\right] + \ln(2f\mathrm{I}^{1/2}\mathrm{M}) - \frac{E}{RT}. \tag{16}$$

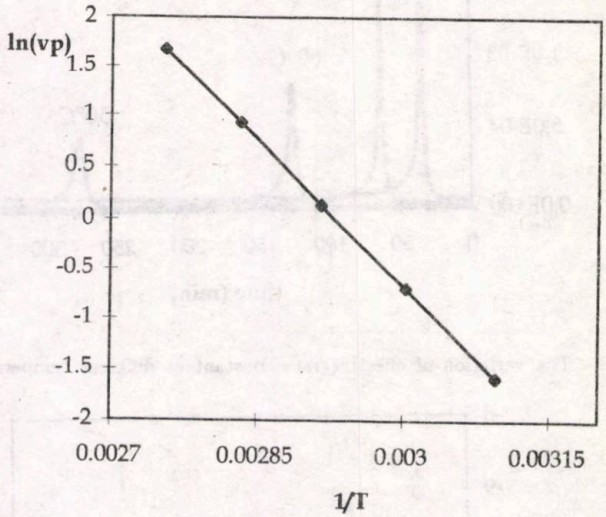

Fig. 11.– The linear dependence $\ln v_p$ vs. $1/T$.

The equation:

$$\ln v_p = 27.99 - 9.555 \times 10^3 \frac{1}{T} \tag{17}$$

corresponds to the straight line in Fig. 11 and it leads to $E_{ef} = 79.38 \times 10^3$ J/mol.

The influence of temperature on the polymerization degree was made evident in Fig. 7. The temperature increase favours low polymerization degrees.

The DP_n vs. T dependence is clearly illustrated in Fig. 12 according to the relationship:

$$\ln(\mathrm{DP}_n) = \ln\left(\frac{A_p}{A_t^{1/2}A_i^{1/2}}\right) + \ln\left(\frac{M}{\mathrm{I}^{1/2}}\right) + \frac{E_i/2 + E_t/2 - E_p}{RT}. \tag{18}$$

The equation of the straight line in Fig. 12 is:

$$\ln(\mathrm{DP}_n) = -9.70 + 5.81 \times 10^3 \frac{1}{T} \tag{19}$$

and, from the slope, the overall activation energy for obtaining a polymer of the DP_n polymerization degree is estimated, $E_{\mathrm{GP}_n} = 48.33$ J/mol.

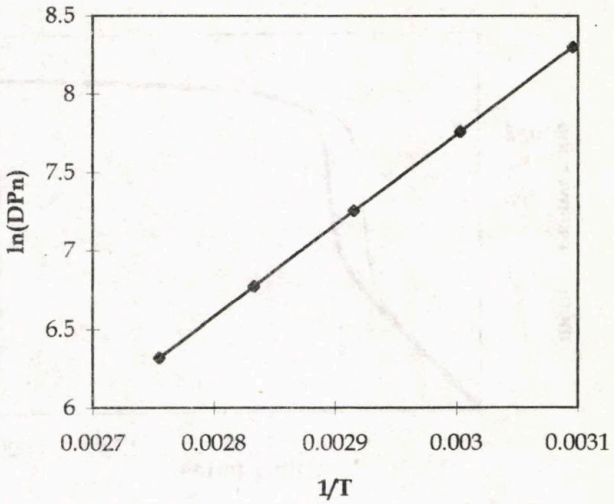

Fig. 12.– The linear dependence $\ln(\mathrm{DP}_n)$ vs. $1/T$.

5. Influence of the Volume Contraction

For many monomer/polymer systems a linear correlation was found for the volume contraction in function of the monomer conversion:

$$V = V_0(1 + \varepsilon x), \tag{20}$$

$$\varepsilon = \frac{V_{x=1} - V_{x=0}}{V_{x=0}}. \tag{21}$$

Consequently, the monomer and initiator concentrations and the reaction rate are the following:

$$M = M_0 \frac{1 - x}{1 + \varepsilon x}, \tag{22}$$

$$\mathrm{I} = \mathrm{I}_0 \frac{\exp(-k_d t)}{1 + \varepsilon x}, \tag{23}$$

$$v_p = \frac{M_0}{1 + \varepsilon x} \cdot \frac{\mathrm{d}x}{\mathrm{d}t}. \tag{24}$$

By assuming $\varepsilon = 0$ in the used model, several simulations are made on the model thus obtained under the same conditions as in previous runs in order to make possible the comparison of the two models.

The influence of the volume change on the monomer conversion and on the polymerization degree is depicted in Figs. 13 and 14 for the MMA polymerization at 70°C and $\mathrm{I}_0 = 25.8$ mol/m^3. The approximation of a constant volume results in a reaction time shorter and a polymerization degree higher than the actual ones.

From these points of view the effects of the volume contraction at low conversions (30% for the conditions under consideration) may be neglected.

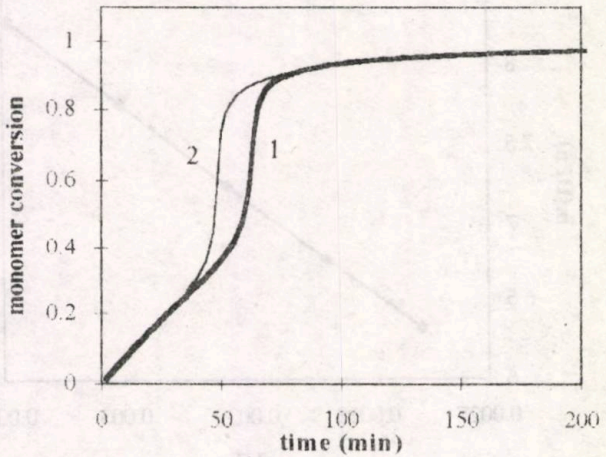

Fig. 13.– The influence of volume change on monomer conversion: *1* – variable volume; *2* – constant volume.

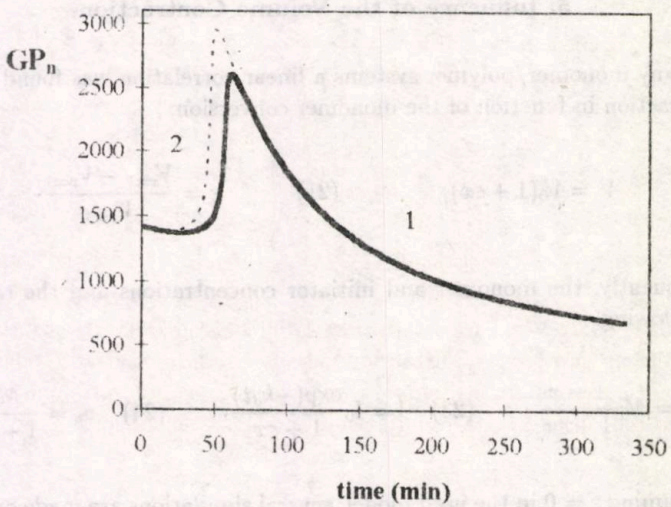

Fig. 14.– The influence of volume change on number average polymerization degree: *1* – variable volume; *2* – constant volume.

6. Conclusions

The influence of different parameters in the MMA batch bulk polymerization is studied by means of the model simulation in the following two purposes: a) to check the model by comparison the simulation results with the literature data; b) to reveal

a direction of the model using in order to obtain additional information concerning the MMA polymerization.

The initial conditions (the initial concentration of the monomer and of the initiator) influence the polymerization process as follows:

a) The increase of the initial monomer concentration results in the increase of the polymer molecular weight.

b) The increase of the initial initiator concentration accelerates the polymerization process and decreases the polymerization degree.

The temperature increase determines: a) the polymerization rate increase; b) the decrease of the polymer molecular weight; c) the increase of the maximum conversion.

The relationships which correlate the temperature, polymerization rate, polymerization degree and conversion permit the estimation of some kinetic amounts of the process, such as the kinetic constants and the energies of activation.

The volume variation in the radical polymerization can be neglected for the low conversions (till the critical conversion characteristic of the gel effect). Above this limit the approximation of a constant volume results in a reaction time and polymerization degree lower than the actual ones.

Notations

A, B, C_1, C_2 – terms in diffusion equations for propagation and termination rate constants;

A_d, A_i, A_p, A_t – preexponential factors for rate constants of initiator dissociation, initiation, propagation and termination;

D_n – dead polymer molecule with n units of monomer;

DP_n – number average degree of polymerization;

DP_w – gravimetric average degree of polymerization;

E_d, E_p, E_t – activation energies of initiation, propagation and termination, [J/mol];

E_{ef} – effective activation energy, [J/mol];

$E_{\theta p}, E_{\theta t}$ – activation energies for θ_p and θ_t, [J/mol];

f – initiator efficiency;

I – initiator concentration;

k_d – rate constant for initiation, [s^{-1}];

k_i – propagation rate constant for primary radical, [m^3/(mol s)];

k_p, k_t – rate constants for propagation and termination in the presence of gel effect, [m^3/(mol s)];

k_{ef} – effective rate constant, [m^3/(mol s)];

k_{p0}, k_{t0} – rate constants for propagation and termination in the absence of gel and glass effects, [m^3/(mol s)];

$k_d^0, k_{p0}^0, k_{t0}^0$ – frequency factors for rate constant of initiation, propagation and termination in the absence of gel and glass effects, [m^3/(mol s)];

M – monomer concentration, [mol/m^3];

P_n^* – macroradical with n units of monomer;

R^* – primary radical;

R – universal gas constant, [J/(mol K)];

T – temperature, [K];

T_{gp} – glass transition temperature of the polymer, [K];

t – time, [s];

v_p – polymerization rate, [mol/(m^3 s)];

V – reaction volume, [m^3];

x – monomer conversion;

θ_t, θ_p – characteristic migration times, [s];

θ_t^0, θ_p^0 – pre-exponential factors for θ_t, [(mol s)/m^3], and θ_p, [s];

ε – volume correction factor;

μ_k – k-th moment of all dead polymer species, [mol/m^3];
Φ_m – volume fraction of monomer;
λ_k – k-th moment of all polymer radicals, [mol/m^3].

Subscripts

0 – inlet value or value in absence of gel and glass effects.

Superscripts

0 – pre-exponential value.

Received, October 18, 1997

Technical University "Gh. Asachi", Jassy,
Department of Macromolecules

REFERENCES

1. Petrovan S., Curteanu S., Hung. J. Ind. Chem. (in press).
2. Curteanu S., Constantinescu M., Hung. J. Ind. Chem. (in press).
3. Curteanu S., Bulacovschi V., Hung. J. Ind. Chem. (in press).
4. Chiu W.Y., Carrat G.M., Soong D.S., Macromolecules, **16**, 34 (1983).

INFLUENŢA UNOR PARAMETRI ÎN POLIMERIZAREA RADICALICĂ DISCONTINUĂ ÎN MASĂ A METACRILATULUI DE METIL

(Rezumat)

Se studiază influenţa diferiţilor factori în polimerizarea radicalică discontinuă în masă a metacrilatului de metil (MMA) prin simulare pe model. Modelul utilizat foloseşte o schemă cinetică ce conţine descompunerea unui iniţiator, propagarea şi terminarea prin disproporţionare, precum şi relaţii ce cuantifică efectele de gel şi vitrifiere. Numeroase rezultate de simulare şi confruntarea cu date experimentale au fost analizate în studii anterioare [1],...,[3]. În acest articol se urmăresc influenţele condiţiilor iniţiale, a temperaturii şi a contracţiei volumului asupra conversiei, masei moleculare şi vitezei de reacţie. Rezultatele obţinute prin simulare reprezintă o etapă în verificarea modelului şi o modalitate de a obţine uşor informaţii suplimentare despre procesul de polimerizare studiat.

BULETINUL INSTITUTULUI POLITEHNIC DIN IAŞI
Tomul XLIV (XLVIII), Fasc. 1–2, 1998
Secţia II
CHIMIE şi INGINERIE CHIMICĂ

D.C. 678.744.422; 66.095.6

OBTENTION AND CHARACTERIZATION OF SOME POLY(VINYL ACETALS)

II. SYNTHESIS OF POLY(VINYL FORMAL) IN A MIXTURE OF WATER–ACETIC ACID AND IN ACETIC ACID

BY

M. RUSU and VERONICA MUNTEANU

A study of the poly(vinyl formal) synthesis by the acetalization of the poly(vinyl alcohol) and formaldehyde in a water–acetic acid medium and in an acetic acid medium is presented. The obtained results reveal that the use of a water–acetic acid medium allows an acetalization degree of about 80%, in the presence of 1.5% of chlorhydric acid. The introduction of 7% of zinc chloride into the reaction medium increases the acetalization degree up to 89%.

In the case of an acetic acid medium the acetalization degree is about 86% but this procedure involves the disadvantage of requiring polymer separation through precipitation and the organic solvent recovery too.

1. Introduction

Although it may be employed as a plastic material, as well, poly(vinyl formal)'s main usage is in the wire enamel and structural adhesives [1], [2]. In view of such applications, poly(vinyl formal) should have a certain chemical composition, which can be attained only through its synthesis, starting from poly(vinyl alcohol) and acetalization in an aqueous medium [1],[3],[4]. Nevertheless, acetalization in an aqueous medium, developing in the presence of chlorhydric acid as a catalyst, permits to obtain a poly(vinyl formal) with an 80% maximum degree of acetalization [5], which is not always sufficient for assuming the characteristics expected from such a polymer.

The present paper discusses the results of a study regarding the possible synthesis and characteristics of some poly(vinyl formals) obtained through the acetalization of poly(vinyl alcohol) with formic aldehyde, in a medium consisting of water–acetic acid mixture and, respectively, of acetic acid.

The study focused on the increasing the acetalization degree of poly(vinyl formal) over its limit value of 80%, obtained through acetalization in an aqueous medium.

2. Experimental

The following materials have been employed for the study:

a) poly(vinyl alcohol) (30 – 80 type ARACET APV, produced by S.C. ROMACRIL S.A., Râşnov) index of saponification 137 mg KOH/g, degree of polymerization 300...500, content of acetylic group 12.1%;

b) formic aldehyde, 37% aqueous solution (STAS 77-72) produced by S.C. NITRAMONIA S.A., Făgăraş;

c) technical grade chlorhydric acid (STAS 339-66);

d) aqueous solutions (48%) of zinc chloride (STAS 2262-88);

e) M-type sodium hydroxide (STAS 98-76);

f) natrium laurylsulfate (N.I. 7205-78, S.C. DETERGENTUL S.A., Timişoara);

g) demineralized water.

The synthesis was carried out in an 1 L four-neck flask, provided with perforated blade-type stirrer (120 rpm), an ascending refrigerator and two dripping funnels. The temperature required for the synthesis was attained by means of an electrically heated thermostated water bath. The components of the reaction system have been calculated so that the reaction mass should occupy only half of the volume of the flask.

3. Results and Discussion

The first reactions of acetalization were performed by the application of some working method and under the same conditions as when employing water as a reaction medium [5], the only difference being that water was substituted with water – acetic acid mixtures, in volumetric ratio of 90/10, 80/20, 75/25 and 70/30. The analyses performed on the poly(vinyl formal) obtained evidenced that, under as considered optimum conditions for the reaction medium made of water, the acetalization degree is not sensibly modified (remaining within the 79...81.5% limits), when the reaction medium was changed (Table 1).

Table 1

Influence of the Reaction Medium Nature on the Acetalization Degree

Sample	Reaction medium	Acetalization degree, [% mol]
41	water	78.8
46	water – acetic acid 90/10	79.1
47	water – acetic acid 80/20	79.8
48	water – acetic acid 75/25	80.4
49	water – acetic acid 70/30	81.5

A slight increase of the acetalization degree, observed with the increase of acetic acid from reaction medium, does not justify, from economical point of view, changing of the reaction medium, if considering the losses of organic solvent and the necessity of its recovery.

The obvious advantage conferred, nevertheless, by utilizing, as a reaction medium, of the water – acetic acid mixture, comes from the possibility of reducing the amount

of chlorhydric acid in the system (from 10.5% with water as a reaction medium, up to 1.5% when the reaction medium used is water – acetic acid, in a 70/30 ratio).

The above observations, correlated with certain literature indications [5], lead to the conclusion that the composition of the reaction mixture should be modified by the introduction of zinc chloride into the system, as well as the conditions of synthesis are modified (increase of the reaction temperature at 60°C, and reduction of the reaction's duration at 8 hours).

Such modifications imposed changes in the working method, as well, as follows. In the reaction vessel it was first introduced the solution of poly(vinyl alcohol) and then, successively, the solutions of formic aldehyde, zinc chloride and emulgator. Maintained under stirring, the reaction mass was heated at 60°C, when the chlorhydric acid was introduced.

The first synthesis of this group have been employed with a 75/25 water – acetic acid mixture as a reaction medium, the only variable taken into consideration being the ratio of zinc chloride. The obtained results (Table 2) evidenced that the presence of zinc chloride in the system induces a significant increase of the acetalization degree. At the beginning this parameter increases with the increase of zinc chloride concentration (up to 6.3...6.9%), after which the increase of the ratio of this component in the system has no influence at all, on the acetalization degree.

Table 2

Influence of Zinc Chloride Concentration on the Acetalization Degree

Sample	$ZnCl_2$ conc., [%]	Acetalization degree, [% mol]	Observation
50	5.30	74	High solubility of polymer
51	5.51	76	High solubility of polymer
52	5.60	80	High solubility of polymer
53	6.90	88	High solubility of polymer
54	16.60	88.8	High solubility of polymer

Considering this synthesis, the conclusion was reached that, when using as a reaction medium the mixture formed water (75 parts) and acetic acid (25 parts), a zinc chloride concentration of about 7% is sufficient for achieving an acetalization degree of 88%.

In order to reduce the losses of organic solvent, the above mentioned synthesis have been repeated, the used reaction medium being a mixture of water – acetic acid (83/17 ratio); from here, the conclusion was drawn that, for such a reaction medium, fulfilment of 88...89% acetalization degree is possible only by a 13...15% increase of zinc chloride's concentration in the system.

When using the acetic acid as reaction medium, the working method has been different from the former synthesis, which is mainly due to the poly(vinyl alcohol) insolubility in acetic acid and to the poly(vinyl formal) solubility in this solvent.

In such a case, in the reaction vessel it was introduced first the dissolving agent, followed, under stirring, by the chlorhydric acid, poly(vinyl alcohol) and the solution of formic aldehyde. The content of the reaction vessel was heated at 70°C, the temperature being maintained for three hours – a condition for occurrence of the acetalization reaction; in the end the reaction mass was cooled at 20°C.

The molar carbonylic/hydroxylic groups ratio applied was of 0.7, the solvent/poly (vinyl alcohol) ratio being calculated so that the content of dry matter in the obtained solution should be of 4±0.2% (viscosity 18.5 cP).

Polymer's separation was carried out through precipitation, the solution of poly (vinyl formal) being injected (at a pressure of 0.4 MPa) in a mixing vessel containing water, under stirring (with 3,000 rpm stirrer).

The precipitated polymer was separated through filtration, washed repeatedly with water (both before and after neutralization with sodium hydroxide), and dried under vacuum (60°C, 1.0 Pa residual pressure).

The study followed exclusively the influence of concentration in chlorhydric acid on the polymer's characteristics, the obtained results being presented in Table 3.

Table 3

Influence of the Chlorhydric Acid Concentration on the Poly(vinyl formal) Chemical Composition

Sample	HCl conc. %	Content of functional groups, [% mol]		
		acetalic	acetylic	hydroxylic
55	0.9	78.0	10.8	11.2
56	0.8	83.5	12.3	4.4
57	1.0	84.0	11.2	4.8
58	1.5	85.8	10.5	3.2

All this results show that the highest degree of acetalization is obtained when the chlorhydric acid concentration in the system is 1.5%.

4. Conclusions

The present study, devoted to the synthesis of poly(vinyl formal) through acetalization of poly(vinyl alcohol) with formic aldehyde, in a water – acetic acid mixture and acetic acid, put into evidence the following aspects:

1. When using a mixture of water – acetic acid as a medium, the maximum degree of acetalization achieved is around 80%, sensibly equal to that recorded when the reaction medium is water. The method has the advantage of reducing to 1.5% (comparatively with 10%, when water constitutes the reaction medium) chlorhydric acid's concentration in the system, but also the disadvantage of involving the organic solvent's recovery from the system, introduction, into the water – acetic acid reaction medium, of 7% zinc chloride permits to increase the acetalization degree up to about 89%.

2. When acetic acid is used as a reaction medium, poly(vinyl formal) with around 86% degree of acetalization is obtained, the method having the disadvantage of requiring polymer separation through precipitation and the recovery of the organic solvent too.

Received, May 28, 1997

Technical University "Gh.Asachi", Jassy, Department of Macromolecules

REFERENCES

1. U š a k o v S.N., *Polivinilovyi spirt i ego proizvodnye.* Vol.**1** a. **2**, Izd. AN SSSR, Moskva, 1960.
2. N i k o l a e v A.F., *Sintetičeskie polimery i plastističeskie massy na ikh osnove.* Izd. Khimia, Leningrad, 1966.
3. M a r k H., *Encyclopedia of Polymer Science and Technology.* Vol.**14**, John Wiley, New York, 1971, 149-239.
4. R o z e n b e r g M.E., *Polimery na osnove polivinilatzetata.* Izd. Khimia, Leningrad, 1983.
5. M u n t e a n u V., C h i f o r A., B i r o M., D u m i t r a ş c u V., R u s u M., Materiale Plastice, **34**, *3-4*, 233 (1997).

OBŢINEREA ŞI CARACTERIZAREA UNOR POLIVINIL ACETALI

II. Sinteza polivinil formalului în mediu de amestec apă–acid acetic şi în acid acetic

(Rezumat)

S-a studiat sinteza polivinil formalului prin acetalizarea polialcoolului vinilic cu aldehidă formică în mediu de amestec apă–acid acetic şi acid acetic. Rezultatele obţinute au evidenţiat faptul că, în cazul folosirii ca mediu de reacţie a amestecului apă–acid acetic gradul de acetalizare realizat este de aproximativ 80%, în condiţiile unei concentraţii în acid clorhidric de 1,5%. Introducerea în acest mediu de reacţie a 7% clorură de zinc permite creşterea gradului de acetalizare la 89%.

Pentru mediu de reacţie acid acetic, gradul de acetalizare realizat este 86%, procedeul implicând însă dezavantajul că impune separarea polimerului prin precipitare şi necesită recuperarea dizolvantului organic.

BULETINUL INSTITUTULUI POLITEHNIC DIN IAŞI
Tomul XLIV (XLVIII), Fasc. 1–2, 1998
Secţia II
CHIMIE şi INGINERIE CHIMICĂ

D.C. 678-13

RHEOLOGICAL BEHAVIOUR OF SOME SOLUTIONS OF TERNARY COPOLYMER ACRYLONITRILE–VINYLACETATE–α-METHYL-STYRENE

BY

M. NICU, CARMEN ZAHARIA, *FLORIN MOŢOC, **MAGDALENA-DUMITRIŢA VICOL, CONSTANŢA IBĂNESCU and MARIA LUNGU

It was analysed the rheological shear properties of some ternary copolymer solutions, acrylonitrile–vinylacetate–α-methyl-styrene (PAN), with different concentrations, in two kind of solvents and at different temperatures, for the obtaining of the values of rheological parameters specific to the behaviour of the Ostwald–de Waele model and it was proposed a method of linearization the flow curves using as independent variable a reduced shear rate.

1. Introduction

The use of tubular threads of membrane type in different separation techniques applied into industry and medicine have imposed the development of some large research fields tied, on the one hand, by the study of systems used with this end of view [1] and, on the other hand, by the analysis of the permeability and selectivity properties of the prepared membrane [2].

The use of acrylonitrile–vinylacetate–α-methyl-styrene (PAN) ternary copolymer of MELANA type for the preparation of tubular membrane, supposes the preparation of some spinning solutions in ethylene carbonate with the addition of pores calibration agent [3]. The knowledge of the behaviour in the flow of some kind of solutions is an essential condition for the characterization of systems used and for the design of its necessary processing equipments.

The paper proposes the study of rheological characteristics of PAN copolymer solutions at different temperatures and the estimation of the effects produced by the additions of potassium iodine as pores calibration agent.

2. Results and Discussion

It were used solutions of acrylonitrile–vinylacetate–α-methyl-styrene ternary copolymer (PAN) made at FIBREX, Săvineşti, using as solvent an aqueous solution

of ethylene carbonate 87% (weight) (CE), with and without the addition of 5% potassium iodine (KI) as pores calibration agent. The concentrations of solution were 5, 10, 15 and 20% (weight), but the experimental temperatures were 40°, 50°, 60°, 70° and 80°C.

The rheological measurements of studied solutions were made on a rheoviscosimeter Rheotest 2 type, with coaxial cylinders; with them it was designed the flow curves and was determined the apparent viscosity values.

The flow curves of PAN copolymer solutions in ethylene carbonate (Figs. 1,...,4) and of copolymer in ethylene carbonate with addition of potassium iodine (Figs. 5,..., 8) at different temperatures and at concentrations of 5, 10, 15 and, respectively, 20% (weight), certify the non-Newtonian behaviour of these liquids. Excepting the 5% PAN solution in CE (Fig. 1) and 5% PAN solution in CE+KI, at temperatures over 50°C (Fig. 2), the other studied liquids present complete flow curves with typical shape of "S" in which are distinguished the three fields: the first Newtonian field according to slight shear rates, the non-Newtonian intermediate and the second Newtonian field, at high shear rates.

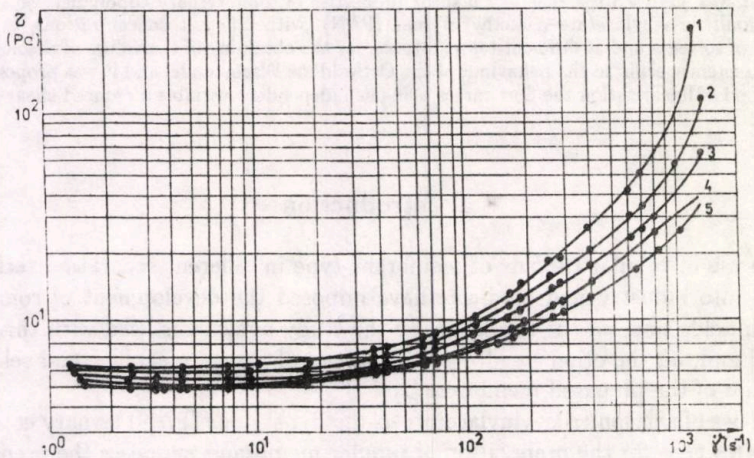

Fig. 1.– The flow curves of 5% PAN solution in CE at various temperatures: *1* – 40°C; *2* – 50°C; *3* – 60°C; *4* – 70°C; *5* – 80°C.

The increasing of solution concentration determines the shift of the non-Newtonian field to more and more slight shear rates, so that, for the first set of solutions (Figs. 1,...,4), the passing from a solution to an other with a concentration increased with 5% determines the decreasing with a unit of a critical shear rate ($\dot{\gamma}$) at which the shear stress (τ) variation with the shear rate is increasing. The same observation can be done in the case of the second set of solutions (Figs. 5,...,8), noting that the passing way from the 10% solution to 15% one is marked by modification of Newtonian field from 8...50 s^{-1} to 30...100 s^{-1}.

The same shift of the viscosity anomaly to smaller $\dot{\gamma}$ is also determined by decreasing the temperature of solution studied; the fact is compliant through the decreased

influence of brownian movement on the displacing the flow elements of the liquids comparing with the shear effect in the system.

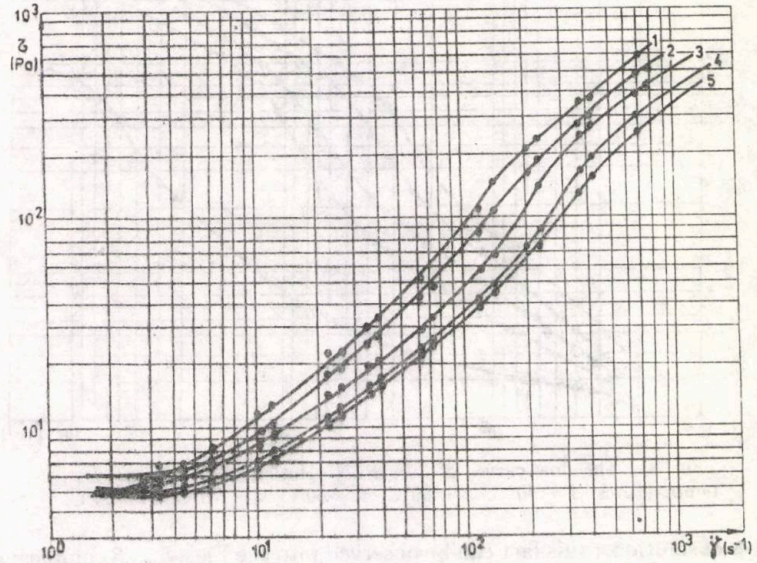

Fig. 2.– The flow curves of 10% PAN solution in CE at various temperatures: *1* – 40°C; *2* – 50°C; *3* – 60°C; *4* – 70°C; *5* – 80°C.

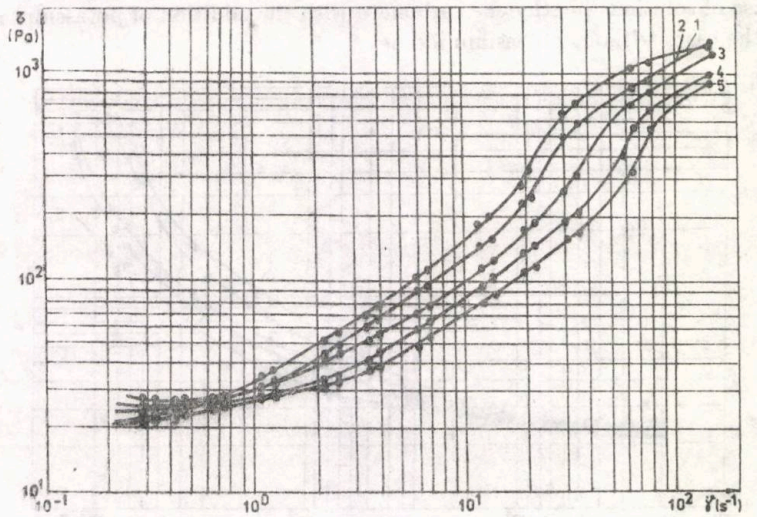

Fig. 3.– The flow curves of 15% PAN solution in CE at various temperatures: *1* – 40°C; *2* – 50°C; *3* – 60°C; *4* – 70°C; *5* – 80°C.

An interesting influence on the flowing properties is exerted by the presence in the solvent of potassium iodine which determines modifications on the shape of the

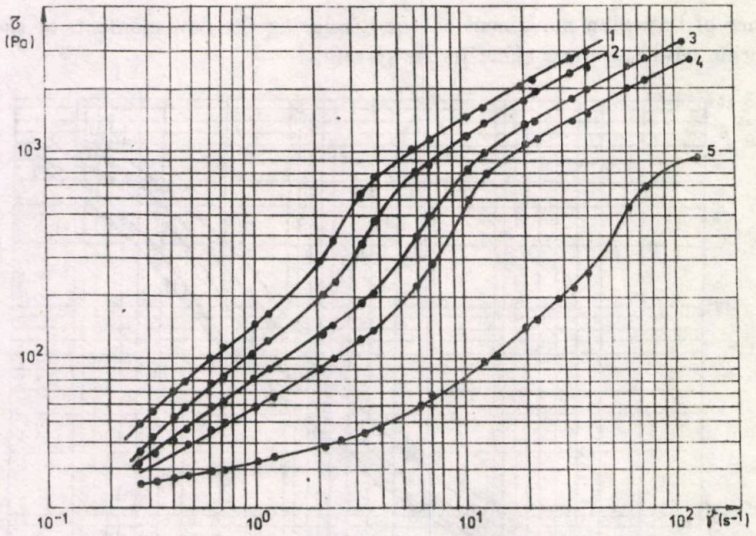

Fig. 4.– The flow curves of 20% PAN solution in CE at various temperatures: *1* – 40°C; *2* – 50°C; *3* – 60°C; *4* – 70°C; *5* – 80°C.

flow curves of solutions; this fact can be observed into the Figs. 5,...,8 comparing with the Figs. 1,...,4. Thus, the observed difference between the two Newtonian fields, so that the field of shear stresses according to the viscosity anomaly is much restricted in the case of solutions in ethylene carbonate with the addition of potassium iodine than in the cases without potassium iodine.

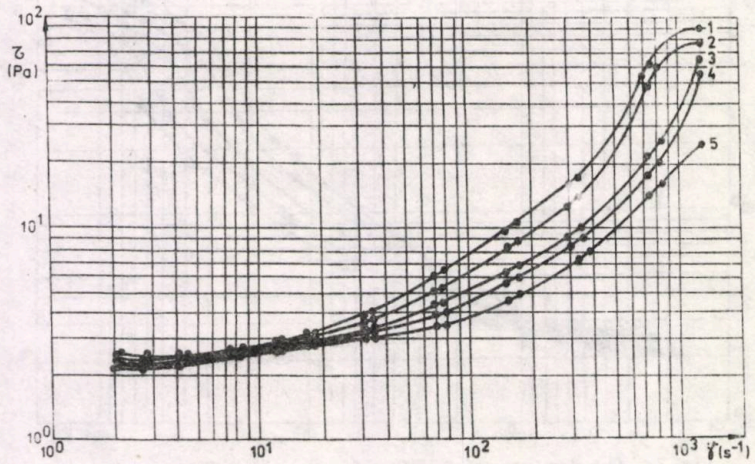

Fig. 5.– The flow curves of 5% PAN solution in CE+KI at various temperatures: *1* – 40°C; *2* – 50°C; *3* – 60°C; *4* – 70°C; *5* – 80°C.

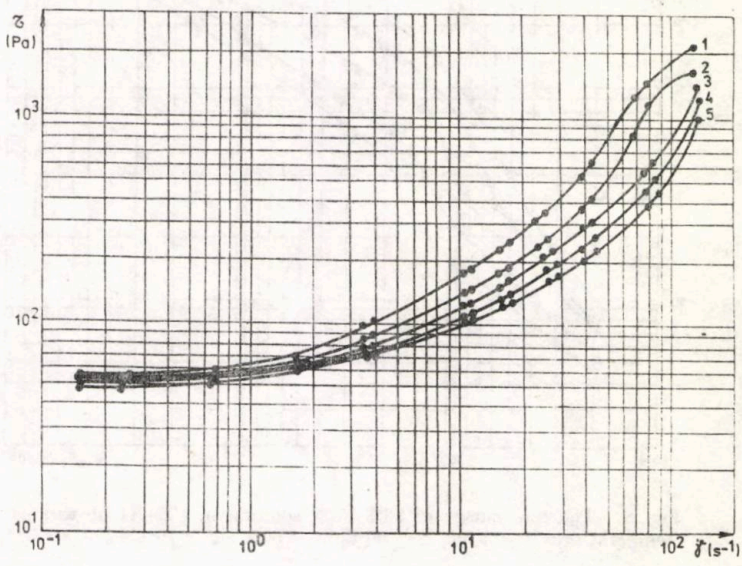

Fig. 6.– The flow curves of 10% PAN solution in CE+KI at various temperatures: *1* – 40°C; *2* – 50°C; *3* – 60°C; *4* – 70°C; *5* – 80°C.

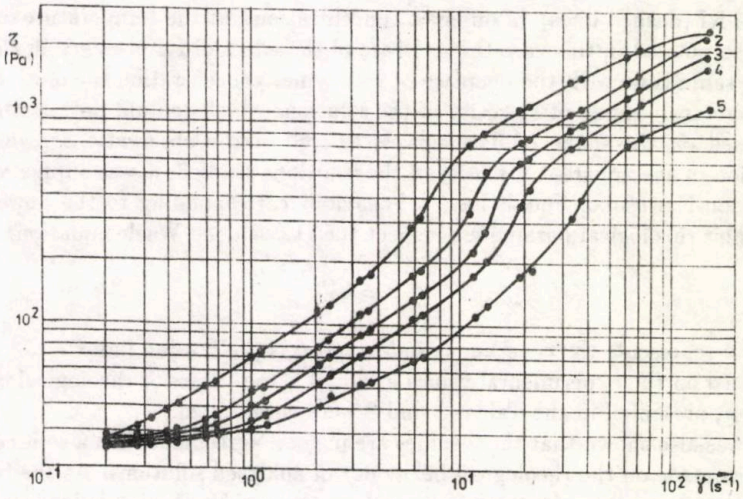

Fig. 7.– The flow curves of 15% PAN solution in CE+KI at various temperatures: *1* – 40°C; *2* – 50°C; *3* – 60°C; *4* – 70°C; *5* – 80°C.

The calculation of apparent viscosity of solutions, $\eta_a = \tau/\dot{\gamma}$, permitted the following of this variation versus the shear rate. It was found, in this case, that, in general, the viscosity of solutions decreases with the increase of $\dot{\gamma}$, specific property

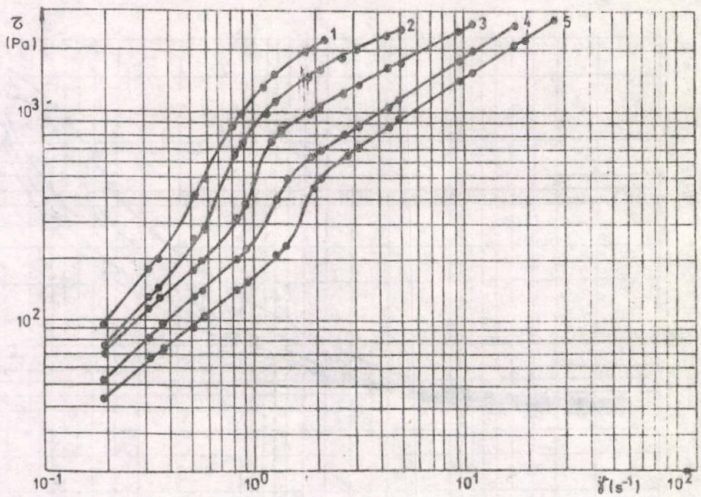

Fig. 8.– The flow curves of 20% PAN solution in CE+KI at various temperatures: *1* – 40°C; *2* – 50°C; *3* – 60°C; *4* – 70°C; *5* – 80°C.

of pseudoplastic fluids. This decrease of viscosity is more unexpected for the solutions of low concentration. In Fig. 9 were represented the variation of apparent viscosity with the shear rate for PAN solution in CE (solid lines) and PAN solutions in CE+KI (dashed lines), of different concentrations, at the temperature of 60°C. It was also noticed in this case the decrease of the effect of KI presence in the system at the same time with the decrease of copolymer concentration in solution, as well the increase of apparent viscosity of the solutions which contain potassium iodine.

Based on the shape of flow curves, as well of the observations regarding the variation of the apparent viscosity of the solutions studied, it was supposed that all these non-Newtonian liquids have a behaviour corresponding to the power law, so that their rheological parameters respect the Ostwald-de Waele equation:

$$\tau = k\dot{\gamma}^n, \tag{1}$$

where k represents the consistency index and n is the flowing index.

Based on the experimental values of τ and $\dot{\gamma}$ the values of rheological constants, k and n, presented in the Tables 1 and 2 were determined.

It was also shown that these values are in good agreement with a series of considerations made on the rheological behaviour of analysed solutions. At the beginning, the sub-unitar values of flowing index reflects the non-Newtonian behaviour (pseudoplastic) of all solutions. Also, the non-Newtonian character (lower and lower values of n) is increasing together with the decrease of concentration and increase of solution temperature.

As was expected, the values of consistency index, k, increases with the increase of solution concentration and the decrease of experimental temperature.

Table 1

The k and n Values for PAN Solutions in Ethylene Carbonate

Temperature,[°C]	40		50		60		70		80	
Concentration,[%weight]	k	n	k	n	k	n	k	n	k	n
5	3.009	0.28	2.676	0.37	2.730	0.34	3.201	0.25	3.378	0.22
10	2.173	0.78	2.078	0.80	1.959	0.75	1.752	0.73	1.720	0.72
15	42.217	0.69	36.752	0.67	36.528	0.60	32.88	0.56	30.900	0.52
20	163.49	0.84	119.89	0.88	94.527	0.85	76.19	0.81	63.84	0.78

Table 2

The k and n Values for PAN Solutions in Ethylene Carbonate with Potassium Iodine

Temperature,[°C]	40		50		60		70		80	
Concentration,[%weight]	k	n	k	n	k	n	k	n	k	n
5	1.92	0.55	2.15	0.49	2.35	0.43	2.42	0.39	2.62	0.36
10	31.41	0.55	30.26	0.50	28.72	0.41	26.82	0.38	26.60	0.31
15	81.79	0.77	57.12	0.77	49.60	0.73	2.49	0.70	36.02	0.61
20	1,047.10	0.99	594.20	0.98	412.20	0.96	278.00	0.89	210.5	0.88

The influence of potassium iodine addition in ethylene carbonate, in which is solved the copolymer, appears also very clearly in the Tables 1 and 2, with the observation that, in general, the values of flowing index are higher in solutions with KI, but the values of consistency index are considerably superior at these solutions, for those without KI. Exception is the solution of 5% concentration at which the effect of KI presence is much low; this fact can be shown in the Fig. 9.

The modification of the rheological properties made in solutions by the presence in the ethylene carbonate of potassium iodine can be explained through some modifications in the structure of flowing elements determined by the modifications in the solvent affinity towards the polymer. It seems that the presence of KI have as effect the increase of polymer–solvent interactions comparatively with the polymer–polymer ones, effect completed by increasing of solution concentration, so that the 20% PAN solutions in CE+KI will have the flowing index very close to unit, corresponding to the Newtonian behaviour.

Supposing an exponential dependence of consistency index, with the form [4]:

$$k = k_0 \exp\left[-\frac{k_1(T - T_0)}{T_0}\right], \tag{2}$$

where k_0 is the value of consistency index at the reference temperature, T_0, the values of coefficient k_1 were determined as the average of obtained values at five current temperatures, considering $T_0 = 313$ K and the k_0 values according to this temperature (Table 3). It is shown that the influence of temperature on the consistency index is strongly manifested in the case of solutions with higher concentrations for which the k values are higher.

This influence is also increased in the case of solutions containing potassium iodine.

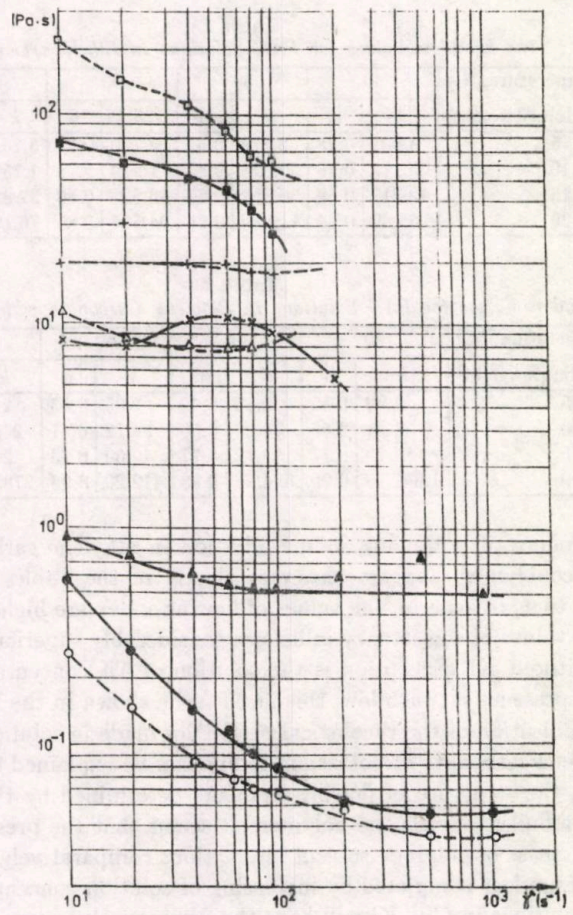

Fig. 9.– The variation of apparent viscosity with the shear rate for PAN solutions in CE (solid lines) and PAN solutions in CE+KI (dashed lines) at different concentrations at 60°C: •, ○ – 5%; ▲, △ – 10%; ×, + – 15%; ■, □ – 20%.

Calculating again the values of consistency index with Eq.(2), using data of Table 3, are obtained results very close to the data presented into the Tables 1 and 2, the total average error being $\varepsilon_1 = -1.81\%$. Therefore it can be considered that the rheological data of Tables 1 and 2 respect the Eq.(2) of exponential variation vs. temperature.

In the same manner is verified the law of linear variation with temperature of the flowing index of the studied solutions, having the expresion:

$$n = n_0 - k_2 \frac{T - T_0}{T_0}, \tag{3}$$

where n_0 is the value of flowing index at the reference temperature, T_0. It seems

that a good agreement with theoretical relation exists, k_2 constant having the values shown in Table 3. The recalculated values for the flowing index in these conditions correspond satisfactorily with the experimental data, the total average error being $\varepsilon_2 = +0.35\%$.

Table 3

The Values of k_1 and k_2 Coefficients in Equations (2) and (3)

Concentration of solution, [% weight]		5	10	15	20
PAN sol. in CE	k_1	0.541	1.634	2.916	8.079
	k_2	-0.494	1.460	1.180	0.282
PAN sol. in CE+KI	k_1	-2.860	1.285	7.508	13.980
	k_2	1.682	1.844	0.996	0.867

With the aim to obtain some generalized flow curves we suppose that the model of shear flow valid for the suspensions of solid particules in liquid medium [5] can be applied to the polymeric concentrate solutions, too.

In the case of the two classes of studied solutions, supposing the reference solution is a 5% PAN one, c_r, the method shown in the Fig. 10 was applied for the determination of the B factors which permits to obtain the reduced shear rate. Thus, after the plotting of flow curves families of PAN solutions in CE and, respectively, PAN solutions in CE+KI, was chosen the value $\tau_r = 100$ Pa, which corresponds to the values of $\dot{\gamma}$ presented in Table 4. The distances measured on the graph $\log \tau = f(\log \dot{\gamma})$ represent the decreasing factors of internal shear rates, $\dot{\gamma}_i$, w.r.t. $\dot{\gamma}_r$ for reference solution:

$$B = \frac{\dot{\gamma}_r}{\dot{\gamma}_i}. \tag{4}$$

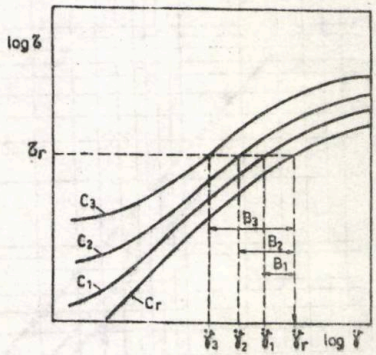

Fig. 10.– Method of determination of increasing factor of shear rate [5].

Table 4

The Values of Shear Rate, $\dot{\gamma}$, Corresponding to $\tau = 100$ Pa.s and the Values of Shear Rate Variation Factors B

Sol. conc., [% weight] Solvent		10	15	20
CE	$\dot{\gamma}$, [s^{-1}]	180	14	4.3×10^{-2}
($\dot{\gamma}_r = 1.900\ s^{-1}$)	$B = \dot{\gamma}_r/\dot{\gamma}$	10.55	135.71	44.186
CE+KI	$\dot{\gamma}$, [s^{-1}]	7	5.5	0.14
($\dot{\gamma}_r = 2.700\ s^{-1}$)	$B = \dot{\gamma}_r/\dot{\gamma}$	385	490	19.285

In the Fig. 11 was represented the variation of shear stress, τ, as a function of reduced shear rate ($B\dot{\gamma}$) for the solutions with 10, 15 and 20% concentrations in CE and, respectively, in CE+KI, at 60°C. It is shown that, in general, straight lines

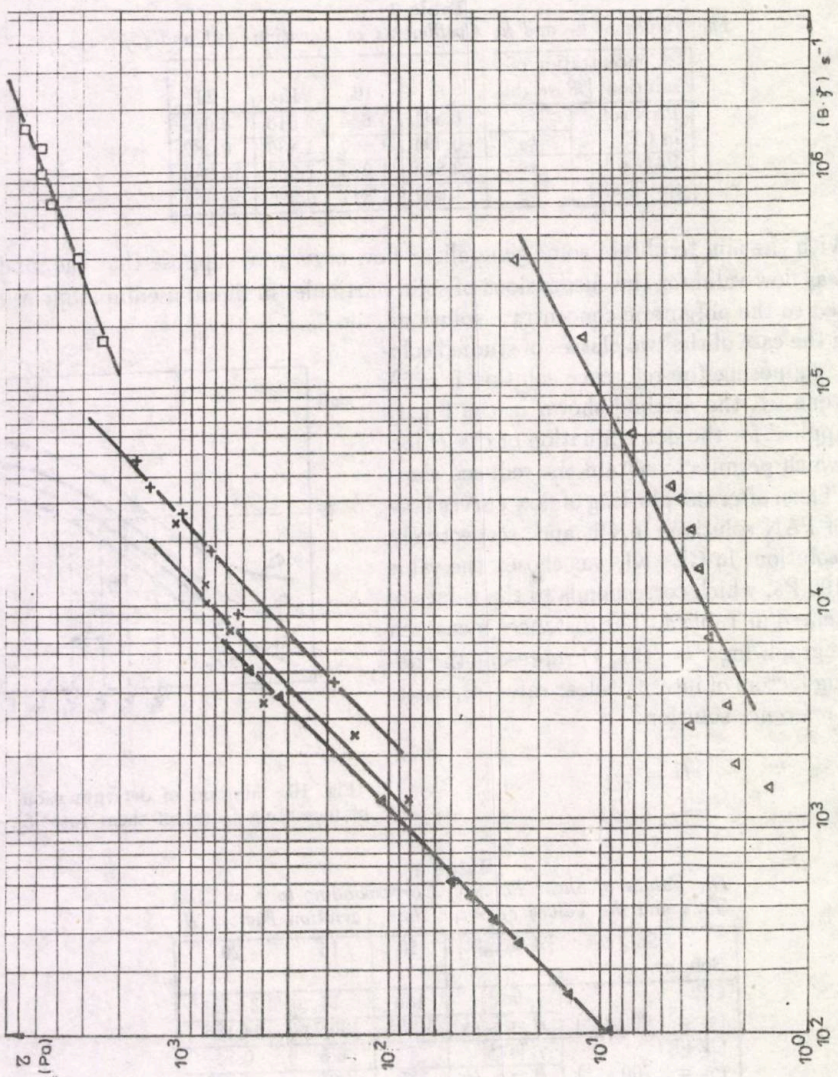

Fig. 11.- The variation of shear stress as a function of reduced shear rate for solutions: ▲,△ – 10%; ×,+ – 15%; ■,□ – 20% in CE and, respectively, CE+KI, at 60°C.

are obtained, a part of them being very close and with slopes equal with an unit, excepting only the solutions with KI of 10 and 20% concentrations. Therefore, the only advantage of these representations is the obtaining of a linear form of flow curves, but the invariance with the concentration is not concludent.

3. Conclusions

The rheological properties of some ternary copolymer solutions of MELANA type, in ethylene carbonate, with and without potassium iodine as pores calibration agent, which will be used for the preparing of tubular membrane, are studied.

The studied solutions have non-Newtonian behaviour of pseudoplastic type, the increase of copolymer concentration in solution determined the change of place of appearance of viscosity anomaly to lower values of shear rate. The same effect on the flow curves, and so, on the solutions viscosity, had the decrease of temperature, too.

The presence in solvent of potassium iodine determines modifications of the rheological behaviour of solutions, important being the decrease of the field of shear stress which correspond to the viscosity anomaly and the increase of the effect of potassium iodine presence, when the copolymer concentration in solution increases. The apparent viscosity of solutions which contain potassium iodine is higher than of solutions without this addition.

Supposing that the studied solutions respect the power law, were determined the rheological parameters k and n and were proposed equations of their variation with temperature, which were in good agreement with the experimental results.

The representation of flow curves as functions of reduced shear rate using an increasing factor of shear rate with concentration leads, in general, to some straight lines, a part of them being very close and having slopes equal with unit. Exceptions represent the systems with potassium iodine; in these cases the straight lines are very different ones from the others, so that, these lines cannot be included into a possible master curve, independent with respect to concentration. Therefore, the advantage of the applied method is, in principal, the linearization of the flow curves.

Received, October 8, 1997

Technical University "Gh.Asachi", Jassy,
Department of Environmental Engineering
and
Department of Macromolecules,
**"A.T. Laurian" High School, Agnita*
and
***S.C. Polirom S.A., Roman*

REFERENCES

1. Simionescu Cr.I., Asandei N., Nicu M., Patent RO *84683* (1984).
2. Nicu M., Nicu V., Lupei V., Constantin N., Asandei N., Patent RO *93638* (1987).
3. Nicu M., Nicu V., Asandei N., Materiale plastice, **29**, *1*, 64 (1992).

4. Tudose R.Z., Asandei N., Volintiru T., Lungu M., Merică E., Ivan Gh., *Reologia compuşilor macromoleculari*. Vol.2, Ed. Tehnică, Bucureşti, 1983.
5. Gleissle W., Baloch M.K., *Praktische Rheologie der Kunststoffe und Elastomere*, von Pahl M.St., Laum H.M., Gleissle W., VDI-K-Seminar, Baden-Baden, Sept. 19-21, 1989.

COMPORTAREA REOLOGICĂ A SOLUŢIILOR DE COPOLIMER TERNAR ACRILONITRIL-ACETAT DE VINIL-α-METILSTIREN

(Rezumat)

S-au studiat proprietăţile reologice ale unor soluţii de copolimer ternar acrilonitril-acetat de vinil-α-metilstiren de două concentraţii, în două tipuri de solvenţi şi la diferite temperaturi, obţinându-se valorile parametrilor reologici caracteristici comportării conform modelului Ostwald-de Waele şi s-a propus o metodă de generalizare a curbelor de curgere prin utilizarea ca variabilă independentă a vitezei de forfecare reduse.

BULETINUL INSTITUTULUI POLITEHNIC DIN IAŞI
Tomul XLIV (XLVIII), Fasc. 1–2, 1998
Secţia II
CHIMIE şi INGINERIE CHIMICĂ

D.C. 676.16; 577; 15

CONTRIBUTIONS TO THE STUDY OF ENZYMATIC TRANSFORMATIONS OF HIGH-YIELD PULPS

BY

***IULIANA SPIRIDON and VALENTIN I. POPA**

The beechwood high-yield pulp was treated with two commercial enzyme preparations differing between them by the enzymes existing in the mixture. The obtained data evidenced that the enzymatic treatments influenced both pulp behaviour in the beating process and their paper properties. The transformations having taken place agree with the enzyme components and their dose.

1. Introduction

The strength and morphology of the wood fiber strongly influence the papermaking process and the quality of the finished paper. Understanding the nature of these influences is essential in designing effective process configurations and developing optimal operating strategies.

Pretreatment of pulp or semichemical pulps with xylanolytic enzymes can reduce bleach chemicals consumption and improve overall brightening [1]. Thus, increased sweeling of the fiber cell walls as a result of a part of xylan removal [2], and cleavage of lignin-carbohydrate bonds have been proposed as mechanisms of enhanced pulp bleachability by xylanase treatment. At the same time it is expected that the enzymatic treatment should influence the chemical and structural composition of the fibers, and paper characteristics could be thus affected.

That is why, in the present paper, a comparative study is perfomed to follow the effects of the enzymatic treatments using two commercial preparations in the case of high-yield pulps.

2. Experimental

In this study, high-yield pulp from beech, obtained by neutral sodium-sulphite cooking (NSSC) process, was used.

Enzymatic treatment was performed with two enzymatic preparations, Carthazyme HS (produced by Sandoz Ltd.) and Pulpzyme HB (by Novo).

Treatment with *Carthazyme HS* was performed at a consistency of 10%, temperature 45°C, pH = 4.5...5 (by addition of 1N H_2SO_4), time 120 min., with an addition

of enzymes of 5 and 10 IU/g (oven dry basis).

The treatment with *Pulpzyme HB* was made at 10% pulp consistency. The pulp slurry was adjusted to a pH = 7.5 (by addition of phosphate buffer). Enzyme was added at a dose of 0.5 and 1.0 IU/g (oven dry basis). Throughout the entire 120 min. reaction, pulp temperature was maintained at 60°C.

Beating was realised in a Yokro mill, for 5, 10, 15 and 20 min., respectively.

Analysis. Cellulose, hemicelluloses and lignin have been determined by standard methods of wood chemistry [3],...,[5]. The handsheets were prepared on a Rapid-Kothen apparatus and strength properties were established in standard conditions.

3. Results and Discussion

Semichemical pulping is a two-stage process that requires a mild chemical treatment of the chips to weaken the intercellular bonding by partial removal of hemicellulose and lignin, followed by mechanical treatment to separate the individual fibers. This process converts wood to a pulp with little breaking or splitting of the fibers. In contrast to fully cooked pulps, which contain only minor amounts of lignin, semichemical pulp may contain more than half of the 20% to 25% lignin found in many hardwood species [6]. Pulps in the lower semichemical yield range and those that require only moderate mechanical treatment for fiberization are frequently referred to as high-yield pulps, particularly if cooked by a sulphite or kraft process. These processes have been introduced as a result of their adaptability to low-cost abundant hardwood to produce high-yield pulps for corrugating board and other products having outstanding properties. The beechwood chips were cooked with a solution of sodium sulphite in an industrial plant.

Hardwood NSSC pulp contains more pentosans than pulps cooked by any other common process.

Although the dissolution of lignin is described as a two-stage process – i.e., sulphonation followed by hydrolysis – solubilization begins quite soon since some of the lignin molecules are small enough to dissolve immediately on sulphonation, in contrast to the large molecules which must hydrolyse before they can pass into solution.

Thus, as seen in Fig. 1, almost all components (hemicelluloses and lignin) remain unmodified.

On the other hand, the enzymatic treatment could influence fibers chemical composition and structure, both as a function of their initial state of modification and the composition of the enzyme mixture.

Since the high-yield pulps have a high content of lignin it is expected that hydrolytic enzymes should have a limited access to the polysaccharides existing in the substrate and, as a consequence, to produce only a surface external modification of the fibers.

From the data presented in Table 1, some modifications in the chemical composition of fibers can be observed, determined by the nature and dose of the used preparations.

In the case of Pulpzyme HB, a lower releasing capacity of carbohydrates from

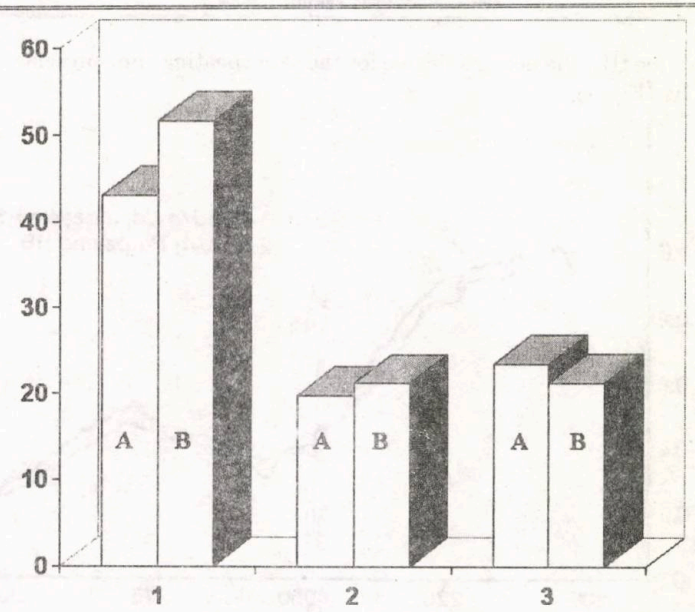

Fig. 1.– Modifications of chemical composition of beechwood by NSSC process: *1* – cellulose, [%]; *2* – hemicellulose, [%]; *3* – lignin, [%]; *A* – beechwood; *B* – high-yield pulp.

Table 1
Chemical Composition of Pulps after Enzymatic Treatment

Pulp treated with	Cellulose, [%]	Hemicellulose, [%]	Lignin, [%]
5 IU/g Carthazyme HS	52.8	21.4	20.8
10 IU/g Carthazyme HS	58.2	21.9	19.6
0.5 IU/g Pulpzyme HB	53.4	22.8	20.6
1 IU/g Pulpzyme HB	54.6	23.4	19.1
untreated	51.6	21.2	21.3

pulp is observed if the results are compared with the transformations determined by Carthazyme HS. This fact may be explained by the composition of Carthazyme HS, which is presented by Sandoz Co. as a cocktail of hemicellulase and cellulase enzymes, being thus more active towards the polysaccharides from the substrate. Xylanase treatment may produce swelling of fibers and a fragmentation of xylan, allowing the diffusion of lignin fragments released after hydrolytic reactions in the lignin–carbohydrates complex.

This process is confirmed by the UV spectra of filtrates resulted after enzymatic treatments of high-yield pulps (Fig. 2) The maximum at 280 nm evidences the action of enzymes on the lignin–carbohydrates complex. Further, the effect of enzymatic treatments on pulps behaviour in the paper manufacture was investigated. Thus, in the beating operation, the treatment of pulps with Carthazyme HS determines decreasing of the beating degree with four units by increasing of enzyme dose from 5 to 10 IU/g, for a beating time of 20 min. (Fig. 3) while, in the case of pulps treated

with Pulpzyme HB, the beating degree for the same beating time presents an increase of four units (Fig. 4)

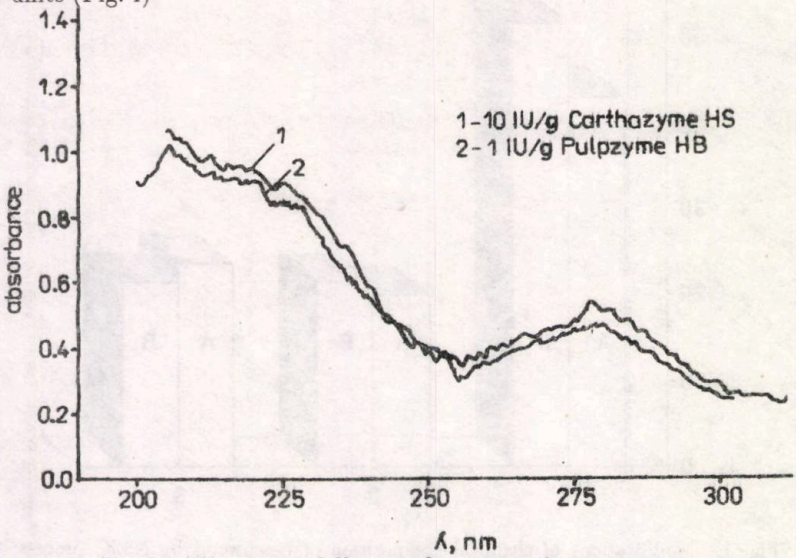

Fig. 2.– UV spectra of filtrates after enzymatic treatments.

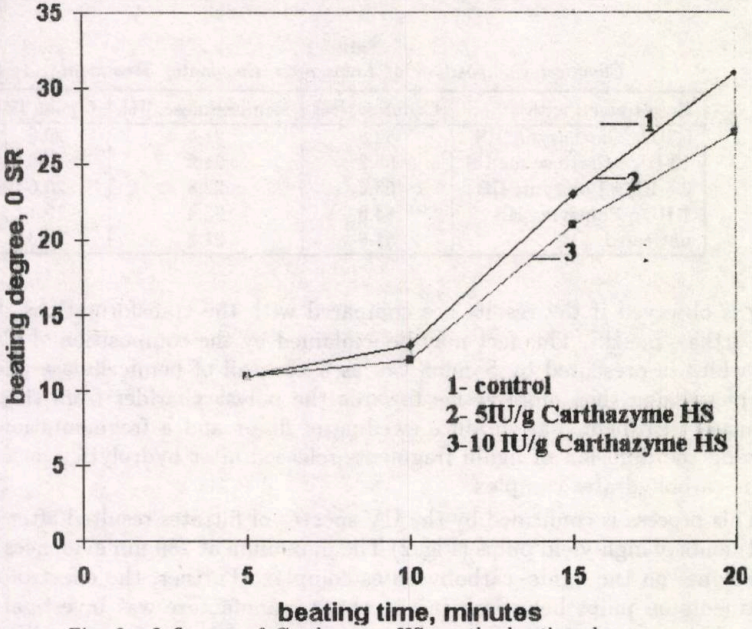

Fig. 3.– Influence of Carthazyme HS on the beating degree.

These differences may be explained by peculiarities of fibers transformation in the enzymatic treatment. It seems that by increasing the enzyme dose, a "desinte-

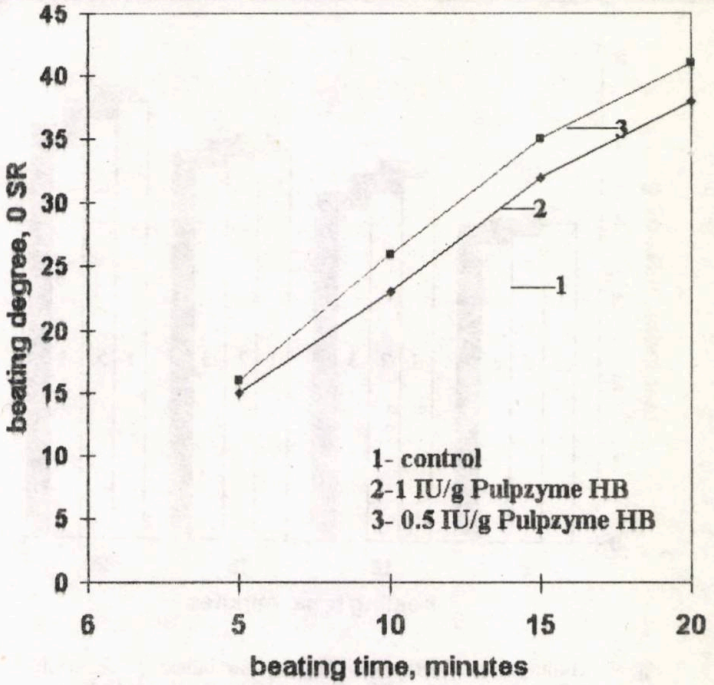

Fig. 4.– Influence of Pulpzyme HB on the beating degree.

gration" of the fibers and elimination of fibrils attached to fibers are produced [7]. This process is characteristic to the cellulase component present in Carthazyme HS preparation, which explains the decrease of the beating degree of pulps treated with this enzyme.

At the same time, complex transformations, such as fibrillation of the long fibers and modification of the fines' content following the action of enzyme could influence the drainage process and sheet formation.

Because fine fibers are more numerous after the enzymatic treatment, more fiber–fiber contacts per unit area are formed and therefore long wet webs and resistant dry sheets are obtained. The sheet formation is also improved, since the fine fibers have a greater mobility and a lower tendency to flocculate.

On the other hand, the fines fraction is more accessible to enzymatic attack due to an increased accessible surface. In other words, improving of high-yield pulp drainage is determined by the degradation of the amorphous regions from pulp. Also, cleavage of some elements of the fine fraction may contribute to interfiber bonding, which affects the tear index; this decrease with the increase of beating degree is probably due to the decrease of individual fiber strength and shipping of the fibers a flattened surface after enzymatic treatments. Figs. 5 and 6 show the relationship between the beating degree and tear index of high-yield pulps treated with different enzyme doses.

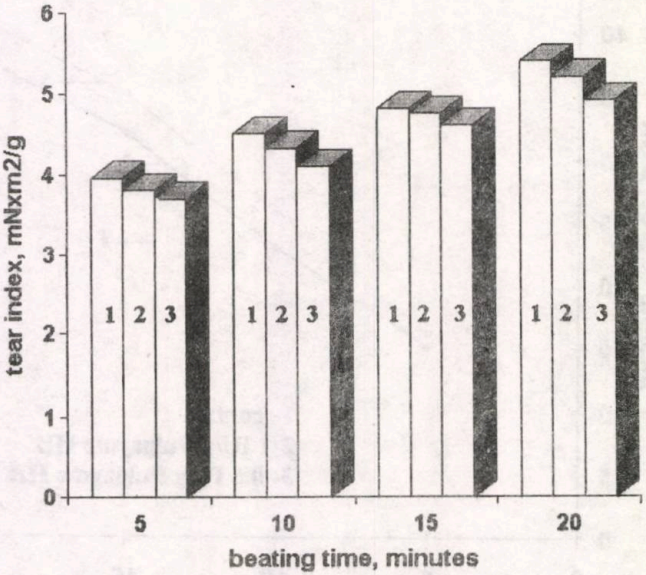

Fig. 5.– Influence of Carthazyme HS on tear index: *1* – control; *2* – 5 IU/g Carthazyme HS; *3* – 10 IU/g Carthazyme HS.

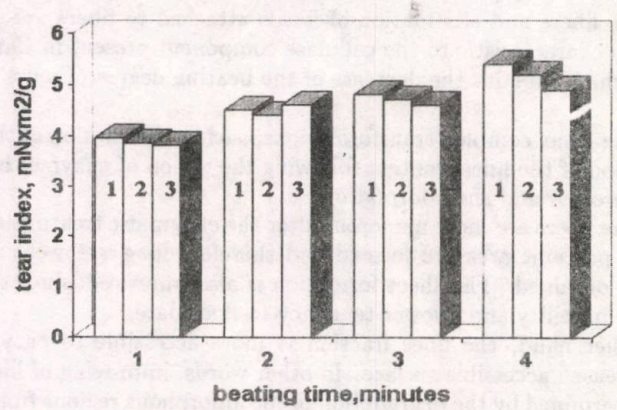

Fig. 6.– Influence of Pulpzyme HB on the tear index: *1* – control; *2* – 0.5 IU/g Pulpzyme HB; *3* – 1 IU/g Pulpzyme HB.

If for both enzymatic preparation, the tear index of pulps decreases with the increase of enzyme dose, the values of breaking length for pulps treated with Pulpzyme HB are better than of those treated with Carthazyme HS.

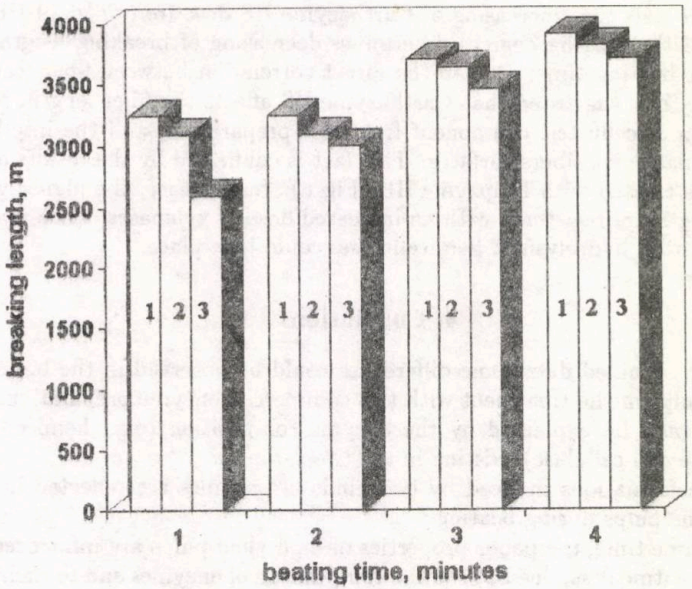

Fig. 7.– Influence of Carthazyme HS on breaking length: *1* – control; *2* – 5 IU/g Carthazyme HS; *3* – 10 IU/g Carthazyme HS.

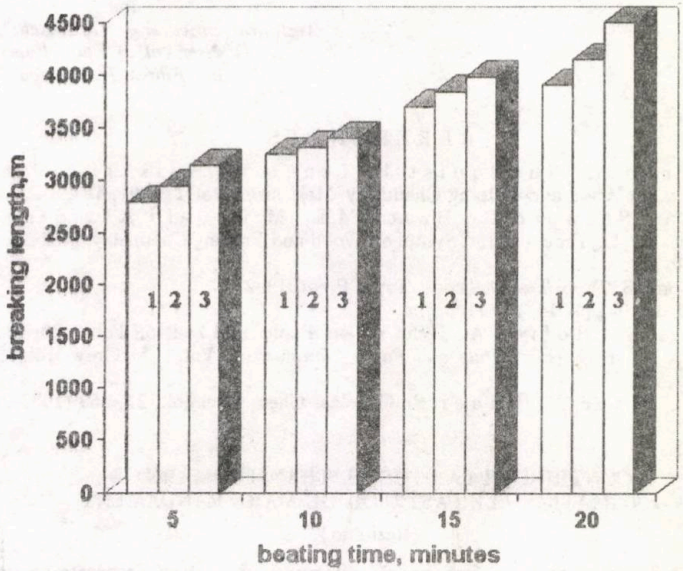

Fig. 8.– Influence of Pulpzyme HB on the breaking length: *1* – control; *2* – 0.5 IU/g Pulpzyme HB; *3* – 1 IU/g Pulpzyme HB.

Thus, Fig. 7, showing the dependence between the beating degree and break-

ing length, reveals that increasing of Carthazyme HS dose from 5 to 10 UI/g (and decreasing of the beating degree) determines decreasing of breaking length, for all values of the beating time. Due to the direct correlation between fiber length and breaking one, it is suggested that Carthazyme HS affects the fiber length, probably by the action of cellulasic component from this preparation, and the interbonding capacity by flattening fibers surfaces. This fact is confirmed by the results obtained for the pulps treated with Pulpzyme HB (Fig. 8). In this case, the higher values of breaking length are registered with an increased dose of xylanases, when swelling of fibers and partial hydrolysis of hemicelluloses could take place.

4. Conclusions

From the obtained data some differences could be observed in the behaviour of high-yield pulps in the treatment with two commercial enzyme preparations. These differences could be explained by the enzyme composition (e.g., hemicellulase or hemicellulase and cellulase) existing in the two samples.

The transformations induced by two kinds of enzymes are reflected in the behaviour of the pulps during beating.

At the same time, the paper properties of high-yield pulps are influenced by the enzymatic treatment as, due both to the composition of enzymes and to their applied doses.

Received, December 9, 1997

*"P.Poni" Institute of Macromolecular Chemistry, Jassy
and
Technical University "Gh.Asachi", Jassy, Department of Pulp, Paper and Fibres Technology*

REFERENCES

1. Kantelinen A., Sundquist J., Linko M., Viikari L., Proc. 6th Int. Symp. on Wood and Pulping Chemistry, Melbourne, vol. 1, 1991, 493.
2. Clark T.A., Steward D., Bruce M.E., McDonald A.E., Single A.P., Senior D., Proc. 6th Int. Symp. on Wood and Pulping Chemistry, Melbourne, vol. 1, 1991, 193.
3. * * T 222 om-88, Tappi Test Methods, Tappi Press, 1992.
4. Leopold B., Tappi, **44**, 230 (1961).
5. Kurchner K., Hoffer A., Techn. Chem. Papier und Zellstoff Fabr., **26**, 125 (1963).
6. Mac Donald R.G. (Ed.), *Pulp and Paper Manufacture*. Vol. 1, McGraw-Hill, New York, 1969, 226.
7. Oltus E., Mato J., Bauer S., Cellulose Chem. Technol., **21**, 663 (1987).

CONTRIBUŢII LA STUDIUL TRANSFORMĂRILOR ENZIMATICE ALE PASTELOR DE MARE RANDAMENT

(Rezumat)

Semiceluloza din lemn de fag a fost supusă tratamentului cu două preparate enzimatice comerciale care diferă prin compoziţia enzimelor prezente în amestec. Datele obţinute au evidenţiat că tratamentele enzimatice influenţează comportarea pastelor în procesul de măcinare şi proprietăţile lor papetare. Transformările produse sunt în concordanţă cu natura enzimelor prezente în sistem şi cu doza folosită.

BULETINUL INSTITUTULUI POLITEHNIC DIN IAŞI
Tomul XLIV (XLVIII), Fasc. 1–2, 1998
Secţia II
CHIMIE şi INGINERIE CHIMICĂ

RECENZII BOOK REVIEWS

SPELLMAN F.R., *Wastewater Biosolids to Compost.* Technomic Publishing AG, Basel, Switzerland, 1996, 245 pp., ISBN 1-56676-461-0.

Wastewater solids have traditionally been grouped under the title of sewage sludge or sludge. The most recent trend is to use the term biosolids in place of sludge, "changing an ugly-four letter word into something more fitting". This reflects the fact that a significant portion of wastewater solids is composed of biomass, which can be put to beneficial use.

"Composting biosolids is not a money-making enterprise. Instead, it is a viable option that can be used to reuse biosolids in an earth-friendly manner. Isn't this what waste disposal should be all about?" So states Frank S p e l l m a n, in his latest book, *Wastewater Biosolids to Compost*, which describes, explaines and evaluates a successful biosolids-to-compost option.

Dr. S p e l l m a n is the Environmental Health and Safety Manager for the Hampton Roads Sanitation District in Virginia Beach, Virginia. He is also the author of *Stream Ecology and Self-Purification, Safe Work Practices*, and *Microbiology for Water/Wastewater Operators* (Technomic Publishing, 1996, and 1997).

The text is designed to provide the decision-maker, site manager, site engineer, as well as local public administrators with a user-friendly guide-book to wastewater composting-from building the facility to processing the waste solids.

The author warns that in order for biosolids to become a viable waste disposal alternative, key players must work together. If biosolids composting is rushed into careful planning, it can lead to problems and unnecessary expense because the technology is still new. However, with 201 biosolids composting facilities on line and over 100 more under development, time and experience will help to fine-tune this important waste disposal/reuse process.

Chapters titles include: Capacity & Design Criteria. ASP Model Composting Facility. Bulking Material. Receiving, Mixing and Material Handling Requirements. Composting: Aerated Static Pile. Curing & Drying. Screening. Distribution & Marketing. Sampling & Testing. Odor Control. Health & Safety Control. Health & Safety Concerns. Economics of Biosolids Composting.

SCHIK J.-P. (Hrsg.), *Korrosionsschutz mit wässrigen Lacksystemen.* Expert Verlag, Renningen, Germany, 1997, 192 S., ISBN 3-8169-1462-4.

Das Buch stellt einen Beitrag zur Gesamtreduzierung von Emissionen dar. Hier geht es um den Ersatz von Lösemitteln durch Wasser.

Eine umfangreiche Zusammenstellung der derzeitigen, ausgereiften, wäßrigen Lacksysteme wird angeboten. Sie haben Eingang bei verschiedenen Anwendungen und jetzt immer mehr auf dem Beschichtungssektor und beim Korrosionsschutz gefunden. Vorurteile gegen „Wasser" in diesem Zusammenhang werden abgebaut.

Die Entwicklung der wäßrigen Lacksysteme für den Korrosionsschutz, die Verarbeitung und ihr unterschiedliches Eigenschaftsbild auch im Vergleich zu konventionellen Lacken, werden ausführlich beschrieben. Einen breiten Rahmen nehmen Hinweise auf die Lackzusammensetzung, Berichte über Praxiserfahrungen und Vorschläge für Problemlösungen ein.

I n h a l t: Die naßchemische Vorbehandlung von Metallen vor der Lackierung – Grundlagen wäßrige 2K-Systeme – Wäßrige 1K-Systeme für den Korrosionsschutz – Spezielle Hinweise zu wasserverdünnbaren 2K-Epoxidsystemen für den Korrosionsschutz-Aktive Korrosionsschutzpigmente auf Basis von Phosphaten – Die Eigenschaften von Füllstoffen in wäßrigen Beschichtungssystemen – Zum Einsatz von Lackadditiven in wäßrigen Korrosionsschutz-Systemen – Wasserverdünnbare Beschichtungsstoffe für den Korrosionsschutz-Praxisfahrungen mit wäßrigen 1K- und 2K-Lackierungen im Industriebereich – Applikationstechnik für Wasserlacke.

THILOW A. (federführend), *Entgrat-Technik. Entwicklungsstand und Problemlösungen.* Expert Verlag, Renningen, Germany, 1992, 240 S., ISBN 3-8169-0796-2.

Dieser Themenband zeigt den aktuellen Stand der Entgrattechnik auf. Er vermittelt zu dem Hinweise, welche Gratdaten als Entscheidungskriterien herangezogen werden können, wie sie beeinflußbar sind und welche Entgratverfahren sich im konkreten Fall eigenen. So ist zum Beispiel der Einfluß auf die Gratausbildung durch die Auswahl der Fertigungsparameter und der Fertigungsfolge mitentscheidend für den nachträglichen Entgrataufwand bzw. für das anzuwendende Entgratverfahren.

Es werden die Entgratverfahren vorgestellt, und Anwendungsbereich wie Einsatzgrenzen werden durch Eckdaten aufgezeigt. Ausserdem erhält der Leser Angaben zu den Kosten und zur Wirtschaftlichkeit. Abgerundet wird das Thema durch die Darstellung der sogenannten „Exoten" unter den Entgratverfahren wie Druckfließläppen, magnetabrasive Feinstbearbeitung und Hochdruckwasserstrahlen.

I n h a l t: Grundlagen zur Lösung von Entgratproblemen – Gleitschleifen, ein klassisches Verfahren mit modernster Technologie – Elektrotechnisches und chemisches Entgraten von Oberflächen – Elektrochemisches Formentgraten und Konturbearbeiten – Entgraten mit Bürsten, Fräsern und ähnlichen Werkzeugen und mögliche Anlagenkonzepte – Modulares Roboter-Entgratsystem – Thermische Entgratmethode – Entgraten mit Industrierobotern – Nichtkonventionelle Entgratverfahren.

* * * *Encyclopedia of Environmental Biology.* 1995, Academic Press, San Diego, London; vol. I, 157 pp., ISBN 0-12-226731, vol. II, 641 pp., ISBN 0-12-226732-8, vol. III, 687 pp., ISBN 0-12-226733; Editor-in-Chief, William A. N i e r e n b e r g.

The *Encyclopedia of Environmental Biology* is intended for use by both students and research professionals. Articles have been chosen to reflect important areas in the study of the environment, topics of public and research interest, and coverage of environmental issues vital to lawyers. Each article provides a comprehensive overview of the selected topic to satisfy readers from students tc professionals.

The *Encyclopedia* is designed with the following features to allow maximum accessibility. Articles are arranged in alphabetical order by subject. A complete table of contents appears in the front, matter of each volume. This list of titles represents topics carefully selected by editorial board. Here, such generaltopics as "Acid Rain" and "Speciation" are listed.

A 10,000 entry Subject Index is located at the end of Volume 3. The index is the most direct way to access the *Encyclopedia* to find specific information. Although the article "Evolution and Extinction" is thorough and complete, additional text on evolution can be found in articles such as "Galápagos Islands" and "Bird Communities". Subjects in the index are listed alphabetically and indicate the volume and page number where corresponding information can be found.

The Index of Related Titles appears in Volume 3 following the Subject Index. This index presents an alphabetical list of the articles as they appear in the *Encyclopedia.* Following each article title is a group of related articles that appear in the *Encyclopedia.*

Articles contain an outline, a glossary, cross-references, and a bibliography. The outline allows a quick scan of the major areas discussed within the article. The glossary contains terms that may be unfamiliar to the reader, with each term defined in the *context of its use in that particular article.* Thus, a term may appear in the glossary for another article defined in a slighly different manner or with a subtle nuance specific to that article. For clarity, we have allowed these differences in definition to remain so that the terms are defined relative to the context of each article.

Each article contains cross-references to order *Encyclopedia* articles. Cross-reference are found at the end of the paragraph containing the first mention of a subject covered more fully elsewhere in

the *Encyclopedia*. By using the cross-references, the reader gains the opportunity to find additional information on a given topic.

The bibliography lists recent secondary sources to aid the reader in locating more detailed or technical information. Review articles and research articles that are considered of primary importance to the understanding of a given subject area are also listed. Bibliographies are not intended to provide a full reference listing of all material covered in the context of a given article, but are provided as guides to further reading.

SPELLMAN F.R., *A Guide to Compliance for Process Safety Management/Risk Management Planning (PSM/RMP)*. Technomic Publishing AG, Basel, Switzerland, 1997, 186 pp., ISBN 1-56676-533-1.

Establishing, maintaining and refining a comprehensive Process Safety Management (PSM) and Risk Management Program (RMP) is a daunting task. The regulations are complicated and unclear. The resources available to manage a program are limited.

Now published, *A Guide to Compliance for Process Safety Management/Risk Management Planning (PSM/RMP)* explains and demonstrates a tested and proven methodology for installation of complete safety and risk programs.

This book provides the public administrator, plant manager, plant engineer, and organization safety professionals with the tool needed to ensure full compliance with the requirements of both regulations. Those with interests in HazMat Response and mitigation procedures will also find it of use.

The author, Frank R. S p e l l m a n, Ph.D., CSP, CHMM, is the Environmental Health and Safety Manager for the Hampton Roads Sanitation District in Virginia Beach, Virginia. He is also the author of *Stream Ecology and Self-Purification, Safe Work Practices, Microbiology for Water/Wastewater Operators, Wastewater Biosolids to Compost, Dewatering Biosolids, and Incinerating Biosolids* (Technomic Publishing 1996, 1997).

According to the author, this guidebook is designed to enable the water wastewater, and general industry person who has been assigned the task of complying with these new rules to accomplish this compliance effort in the easiest accurate manner possible. More than anything else, this guidebook really is a "template". It provides a pattern that can be used to devise a compliance package that is accurate. Like the standard template, this guidebook can provide the foundation and the framework from which any covered organization's PSM and RMP effort can be brought into proper compliance. The user simply "plugs-in" site specific information into the model presented in this guidebook.

The book is divided into three parts: Introduction, Process Safety Management, and Risk Management Planning (RMP).

Chapter titles include: Employee Participation In PSM. Process Safety Information. Process Hazard Analysis. Updating Standard Operating Procedures (SOPS). PSM. Training Requirement. Contractors and PSM. Pre-Startup Safety Review. Mechanical Integrity. Hot Work Permit. Management of Change. Incident Investigation. Emergency Planning & Response. Compliance Audits. Trade Secrets. Risk Management Program. Hazard Assessment: Offsite Consequence Analysis. Risk Management Plan.

TAKEO MITSUI (Ed.), *New Cosmetic Science*. Elsevier Science, Amsterdam, The Netherlands, 1997, 499 pp., ISBN 0-444-82654-8.

Cosmetic science covers the fields from natural sciences to human and social sciences, and is an important interdisciplinary element in various scientific disciplines.

New Cosmetic Science is a completely updated comprehensive review of its 35 years old counterpart Cosmetic Science.

New Cosmetic Science has been written to give as many people as possible a better understanding of the subject, from scientists and technologists specializing in cosmetic research and manufacturing, to students of cosmetic science, and people with a wide range of interests concerning cosmetics. The relationship between the various disciplines comprising cosmetic science, and cosmetics, is described in Part I. In addition to discussing the safety of cosmetic, the "Usefulness of Cosmetics", rapidly becoming an important theme, is described using research examples. The latest findings on cosmetic stability are presented, as are databases, books and magazines, increasingly used by cosmetic scientists.

Part II deals with cosmetics from a usage viewpoint, including skin care cosmetics, makeup cosmetics, hair care cosmetics fragrances, body cosmetics, and oral care cosmetics. Oral care cosmetics and body cosmetics are presented with product performance, types, main components, prescriptions and manufacturing methods described for each item.

This excellent volume enlightens the reader not only on current cosmetics and usage, but indicates future progress enlarging the beneficial effects of cosmetics.

Products with better pharmaceutical properties (cosmeteuticals), working both physically and psychologically, are also highlighted.

C o n t e n t s: (Chapter headings) Introduction to Cosmetic Science. 1. Purpose of cosmetics. 2. Meaning of cosmetics. 3. Classification. 4. Quality characteristics and quality assurance. 5. Development process of cosmetics. 6. Scientific background, technology and its future.

Part I. 1. Cosmetics and skin. 2. Cosmetics and hair and nails. 3. Colour and cosmetic colour materials. 4. Cosmetics and fragrances. 5. Raw materials of cosmetics. 6. Cosmetics and pharmaceutical agents. 7. Cosmetics and physical chemistry. 8. Stability of cosmetics. 9. Preservation of cosmetics. 10. Safety of cosmetics. 11. Usefulness of cosmetics. 12. Cosmetics and containers. 13. Aerosol technology in cosmetics. 14. Analytical chemistry of cosmetics. 15. Cosmetic manufacturing equipment. 16. Regulations on cosmetics. 17. Cosmetics and information.

Part II. 1. Skin care cosmetics. 2. Make-up cosmetics. 3. Hair care cosmetics. 4. Fragrance products. 5. Body cosmetics. 6. Oral care cosmetics. Index.

FEY-OTTE, *Wörterbuch der Kosmetik*. Wissenschaftliche Verlagsgesellschaft, Stuttgart, Germany, 1997, 311 S., ISBN 3-8047-1464-1.

In dem Buch geben über 3000 Stichwörter Aufschluß über Begriffe aus der dekorativen, pflegenden und erhaltenden Kosmetik, zu Aufbau und Funktion der Haut und ihrer Anfangsgebilde sowie über die chemische Konstitution von Grundlagen, Hilfs- und Wirkstoffen, die für die Herstellung kosmetischer Mittel verwendet werden. Dieses Wörterbuch bietet, auch im Hinblick auf die bevorstehende Kennzeichnungspflicht der Inhaltsstoffe von Kosmetika, den Apothekern, Dermatologen, Kosmetikern, Drogisten und allen interessierten Verbrauchern eine Vielzahl von Informationen über die Zusammensetzung kosmetischer Präparate und ihre Wirkung.

Data apariţiei: noiembrie 1998, Comanda: 218,
Coli tipar: 8, Tiraj: 275 exemplare

UNIVERSITATEA TEHNICA „GH. ASACHI" IASI
TIPOGRAFIA

Str. Lascăr Catargi Nr. 38

ISSN 0254-7104